Workshop on Hyperon Physics, Huizhou, Apr 12-15, 2024

HIAF能区重离子碰撞中超子产生和超核物理研究

Zhao-Qing Feng (冯兆庆)

School of Physics and Optoelectronics, South China University

of Technology, Guangzhou

*Email: fengzhq@scut.edu.cn

Collaborators：Hui-Gan Cheng and Si-Na Wei

Outline

- Hyperon, cluster and hypernuclear cluster production via heavy-ion collision and hadron induced reactions-**overview**
- LQMD transport model and recognizing cluster
- Fragmentation reaction and hyperfragment production
- Summary and perspective

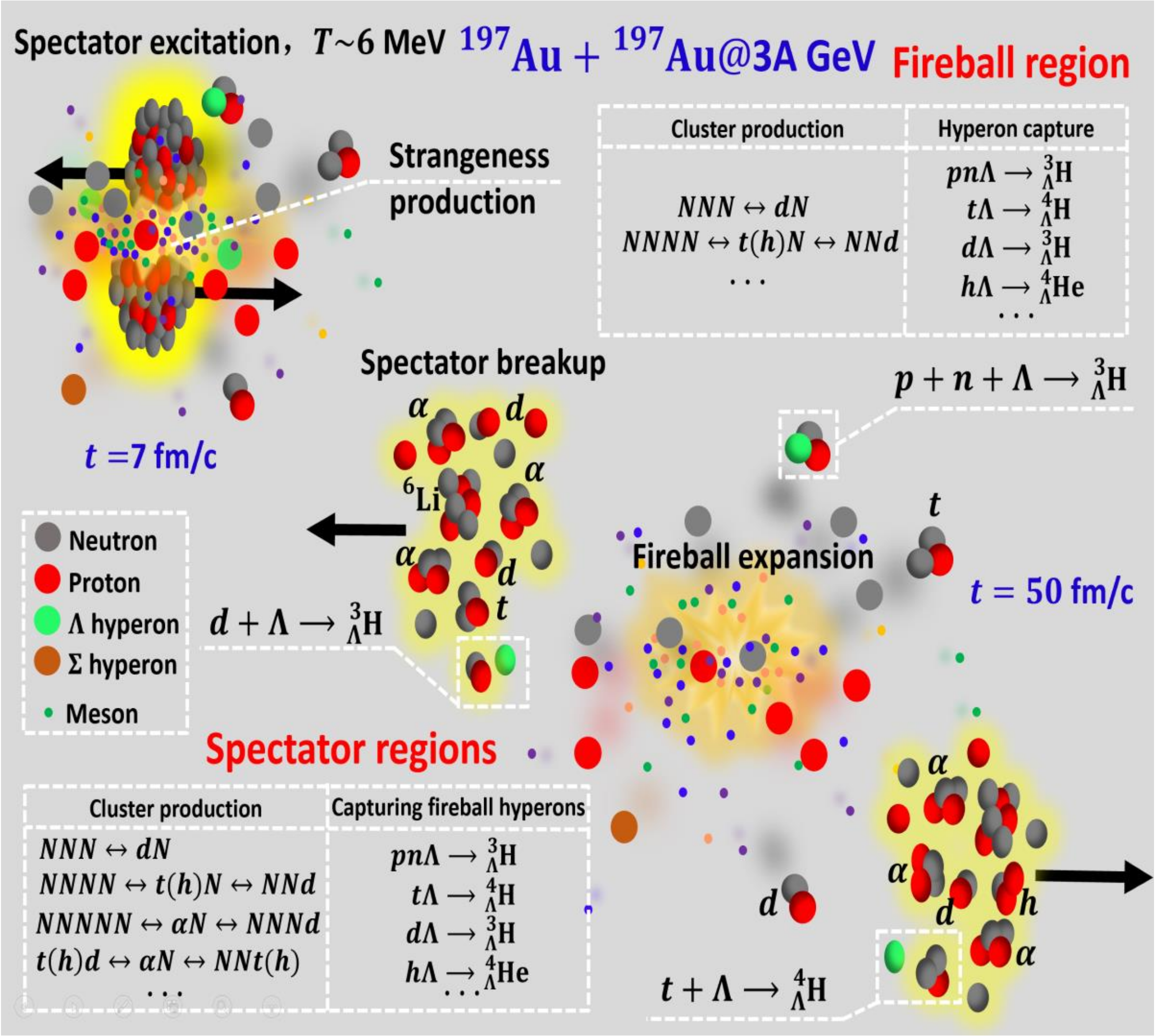

Strange particles production in hadron-hadron collisions

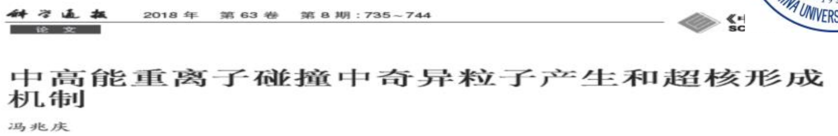

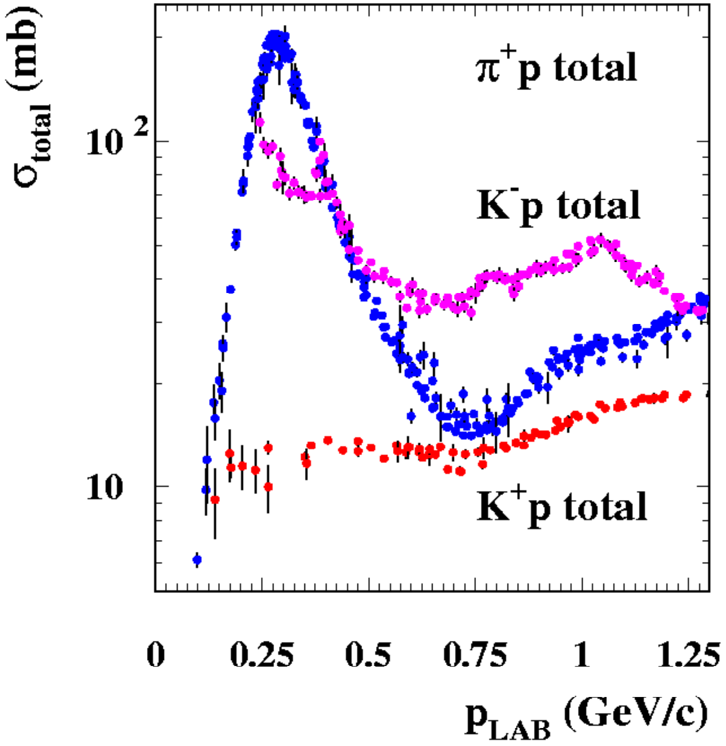

mean free path at ρ_0:

$\lambda(\pi) = 0.3$ fm

$\lambda(K^+) = 5$ fm

$\lambda(K^-) = 0.8$ fm

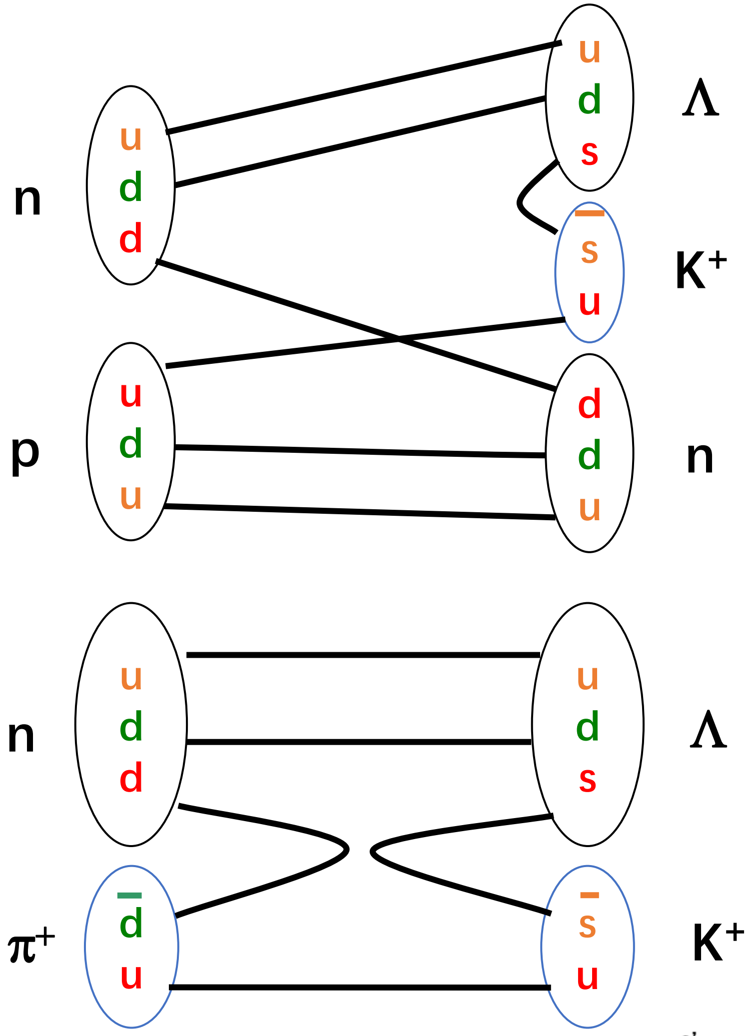

$e+p \rightarrow e' + K^+ + \Lambda$

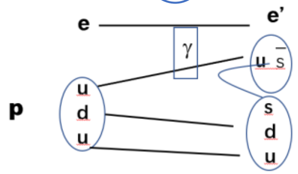

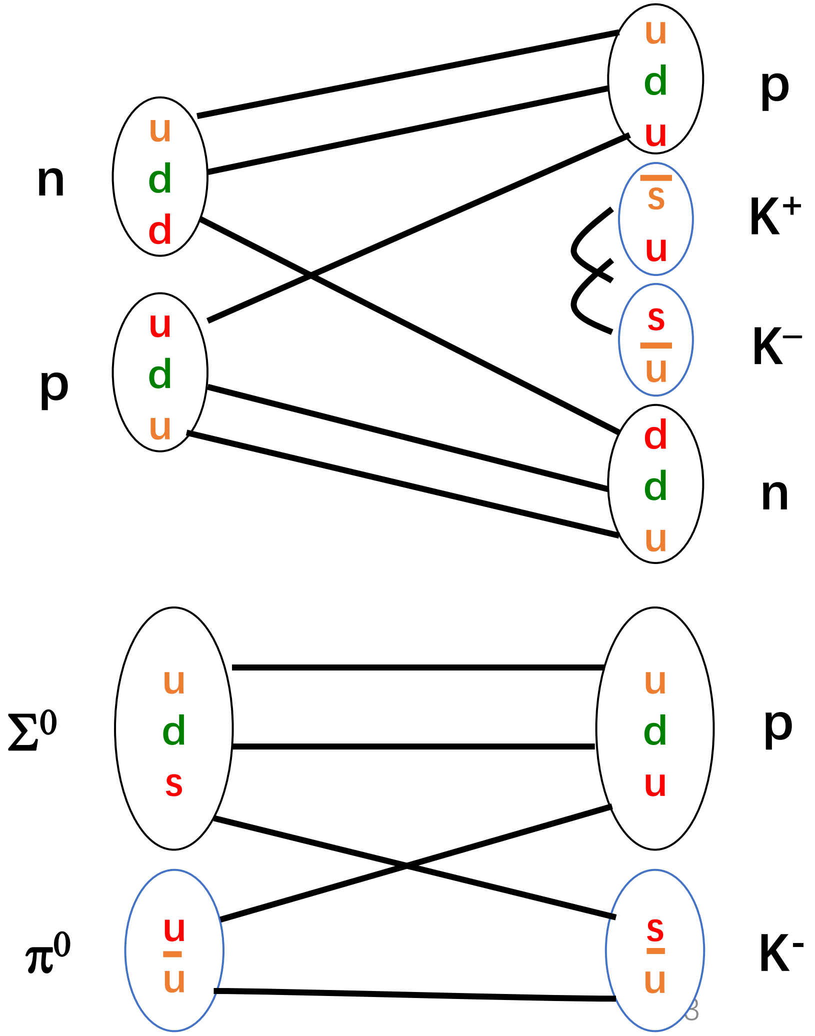

C. Hartnack et al. / Physics Reports 510 (2012) 119–200

K^+ production

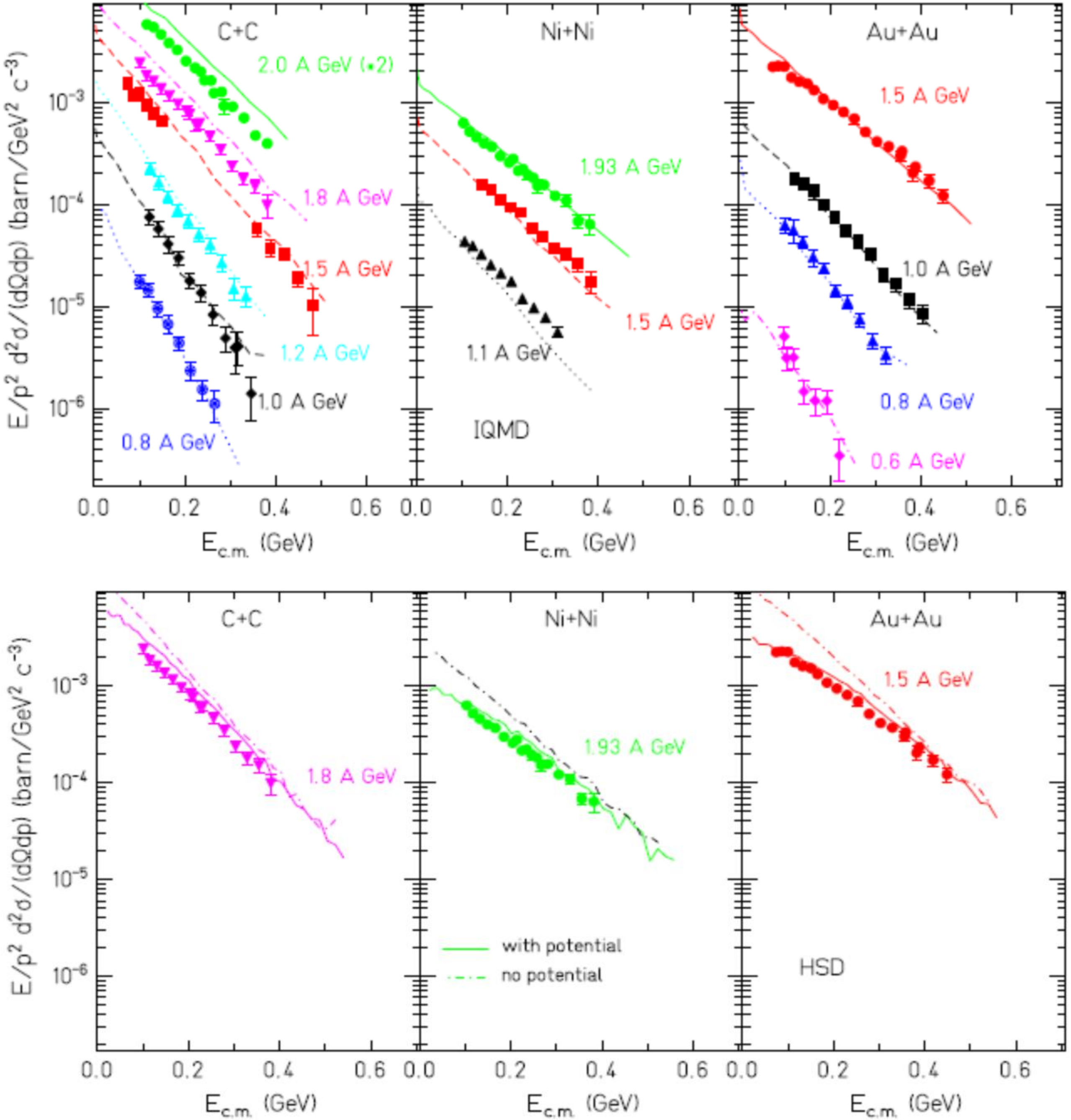

C. Hartnack et al. / Physics Reports 510 (2012) 119–200

Λ production

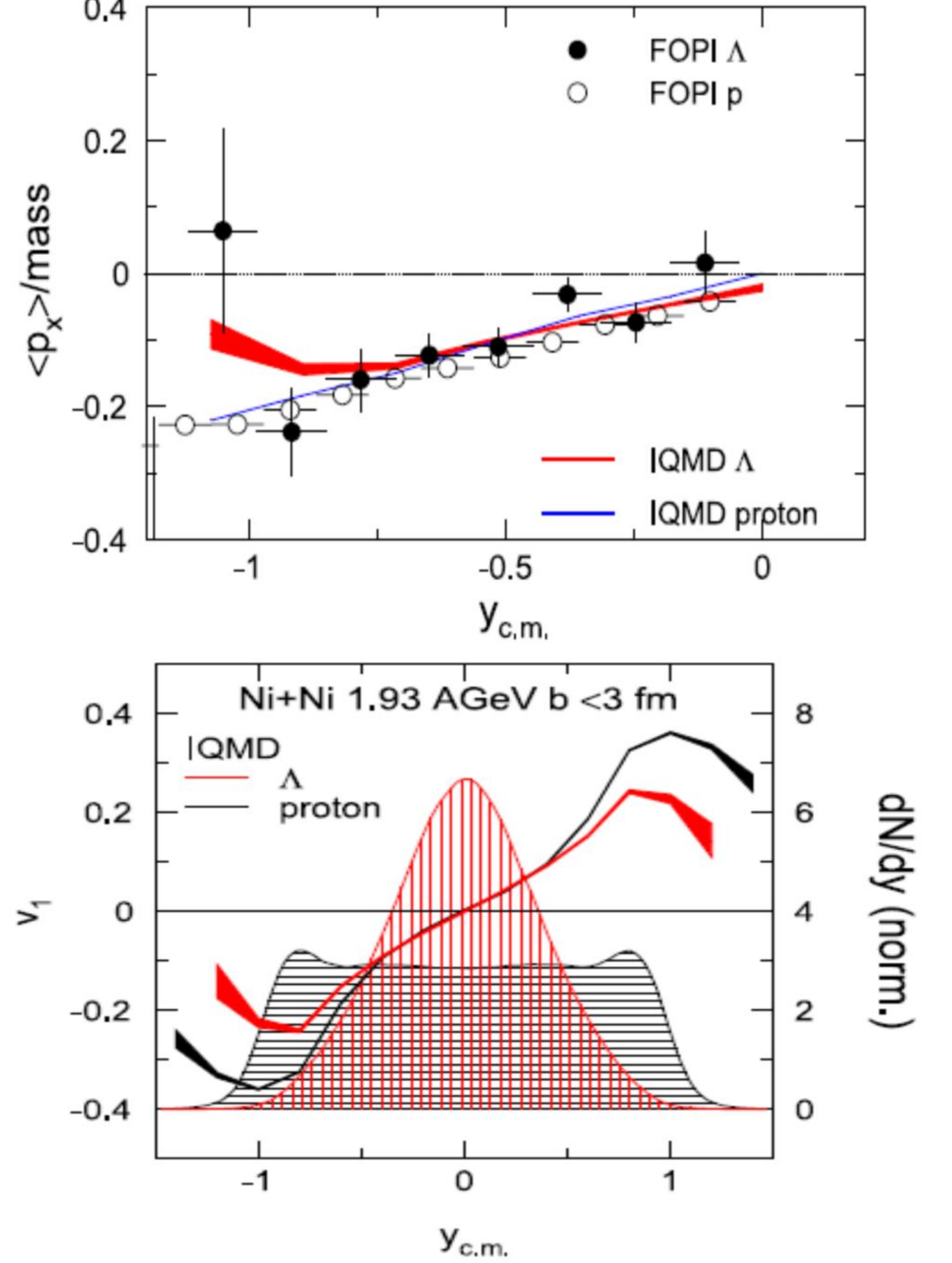

同位旋对称核物质状态方程

K^+介子探针：

- KN相互作用势
- Δ衰变宽度
- NΔ吸收截面

G.Q. Li, C. M. Ko, PLB349(1995)405. **BUU**

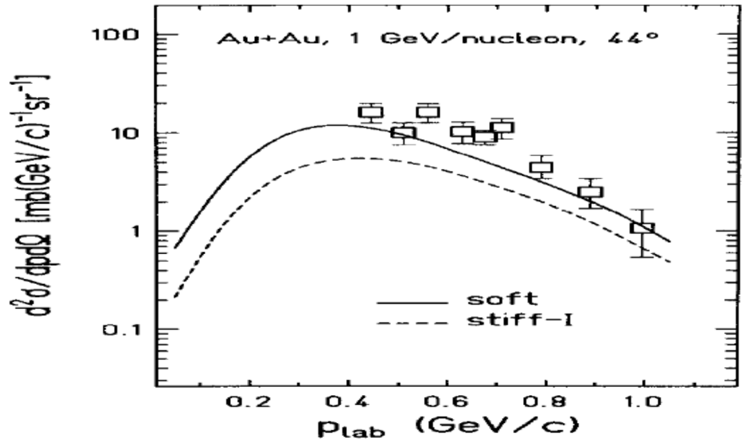

C. Fuchs et al., PRL86(2001)1974. **QMD**

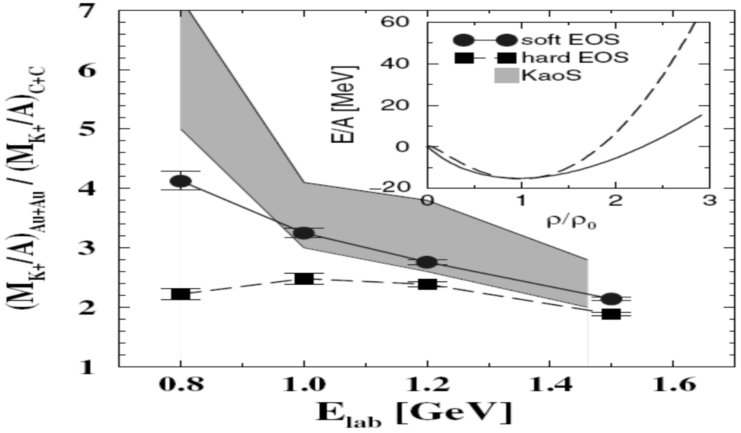

P. Danielewicz, R. Lacey and W.G. Lynch, Science 298, 1592 (2002)

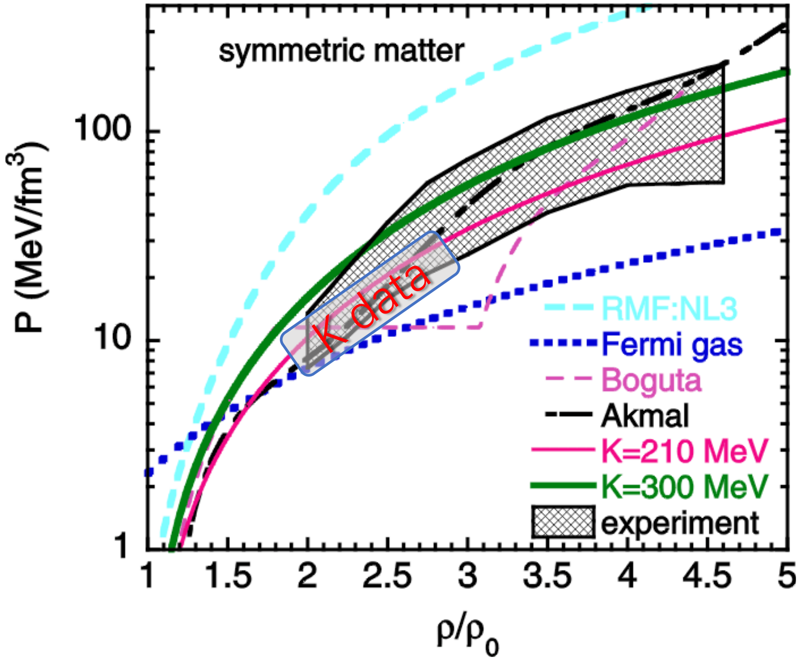

Ch. Hartnack et al., PRL96 (2006) 012302. **IQMD**

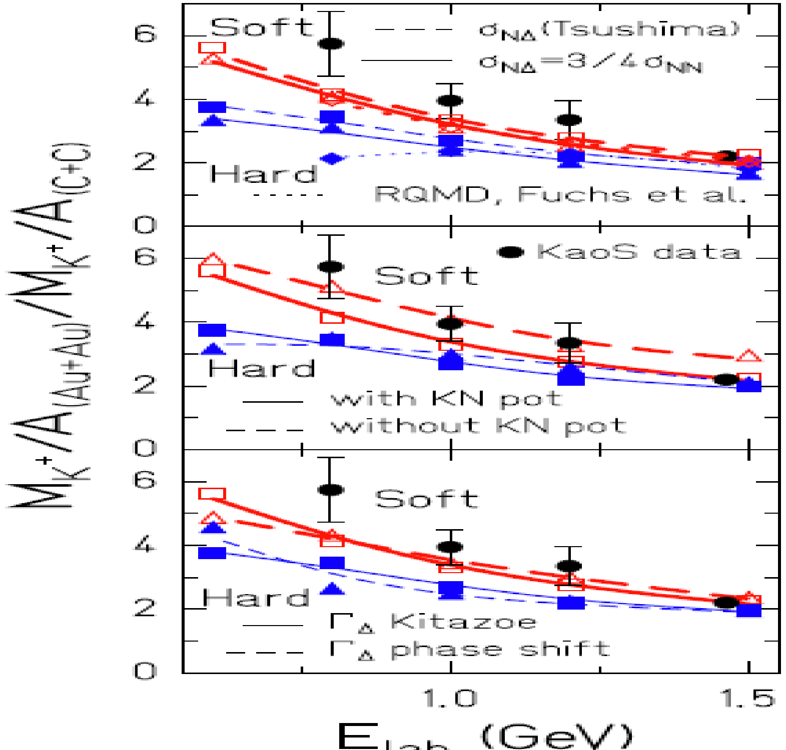

Z. Q. Feng, PRC 83 (2011) 067604. **LQMD**

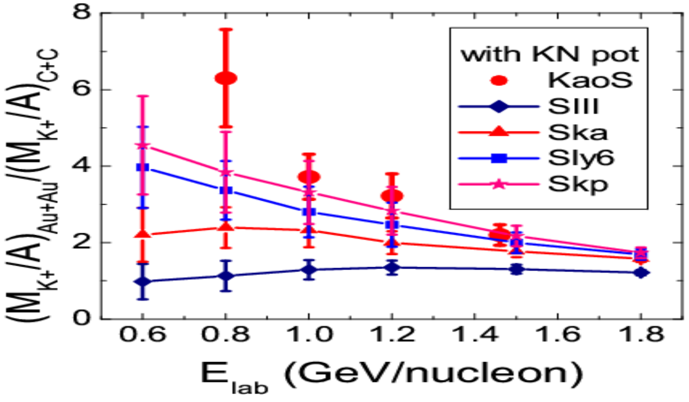

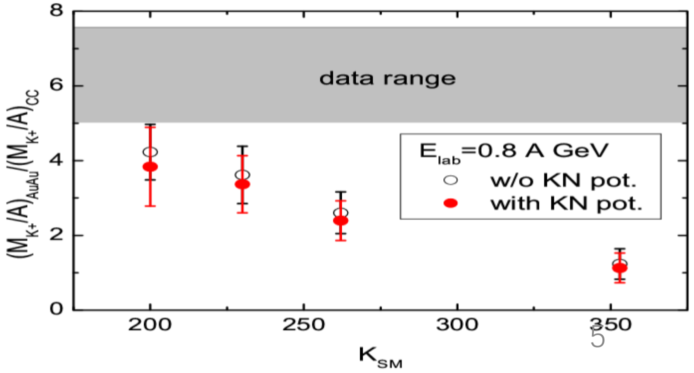

The ratio of K^-/K^+ as a function of transverse mass (kinetic energy) in collisions of $^{12}C + ^{12}C$ and protons on ^{12}C and ^{197}Au at the beam energies of 1.8*A* GeV and 2.5 GeV (Z. Q. Feng et al., Phys. Rev. C 90, 064604 (2014))

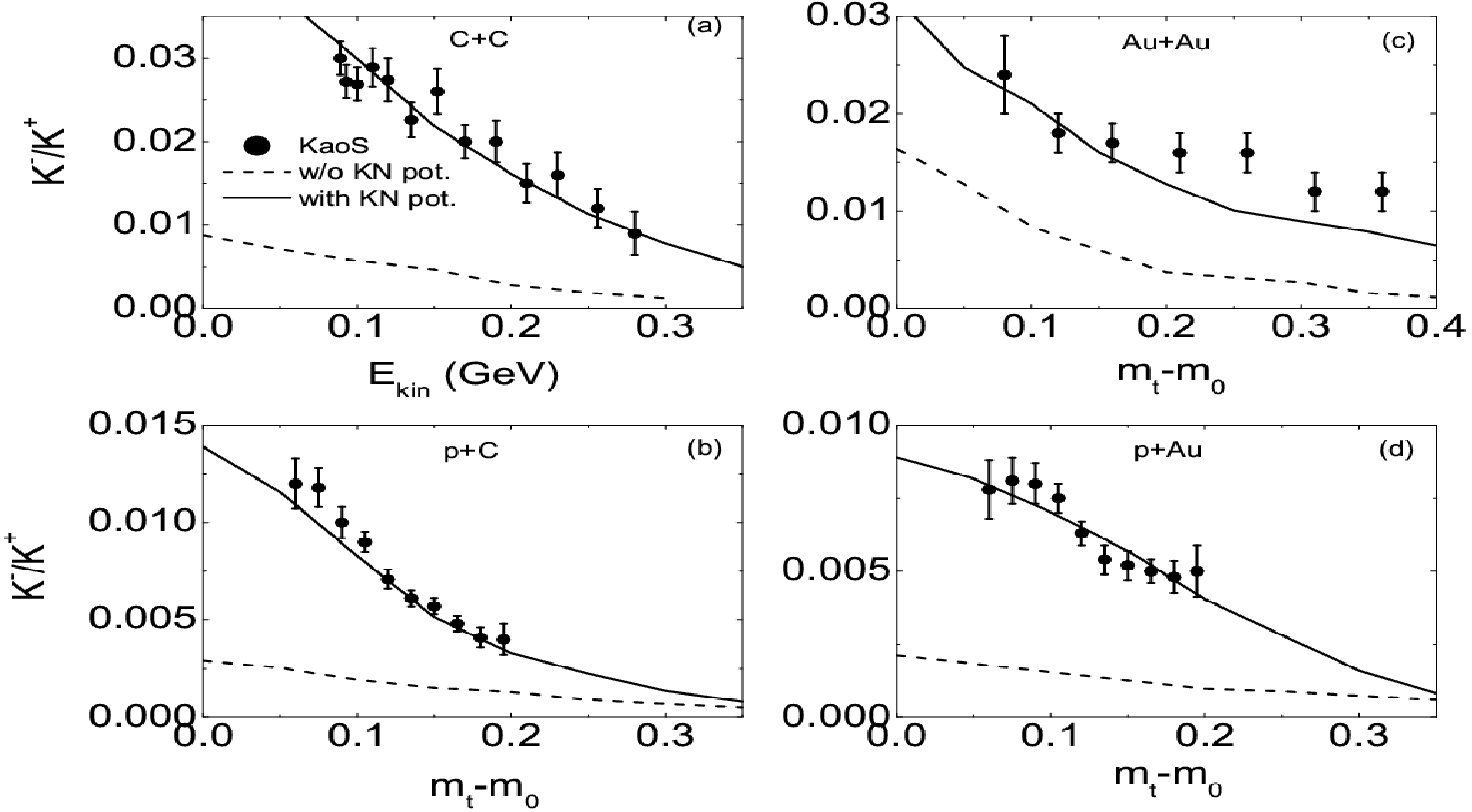

$V_{K+}(\rho_0)$= 28 MeV, $V_{K-}(\rho_0)$= -100 MeV

Hyperons in neutron stars (NS)

S. Weissenborn, D. Chatterjee, J. Schaffner-Bielich, Nucl. Phys. A 881, 62 (2012)
W. Z. Jiang, R. Y. Yang, and D. R. Zhang, Phys. Rev. C 87, 064314 (2013)
Diego Lonardoni, Alessandro Lovato, Stefano Gandolfi, and Francesco Pederiva, Phys. Rev. Lett. 114, 092301 (2015)

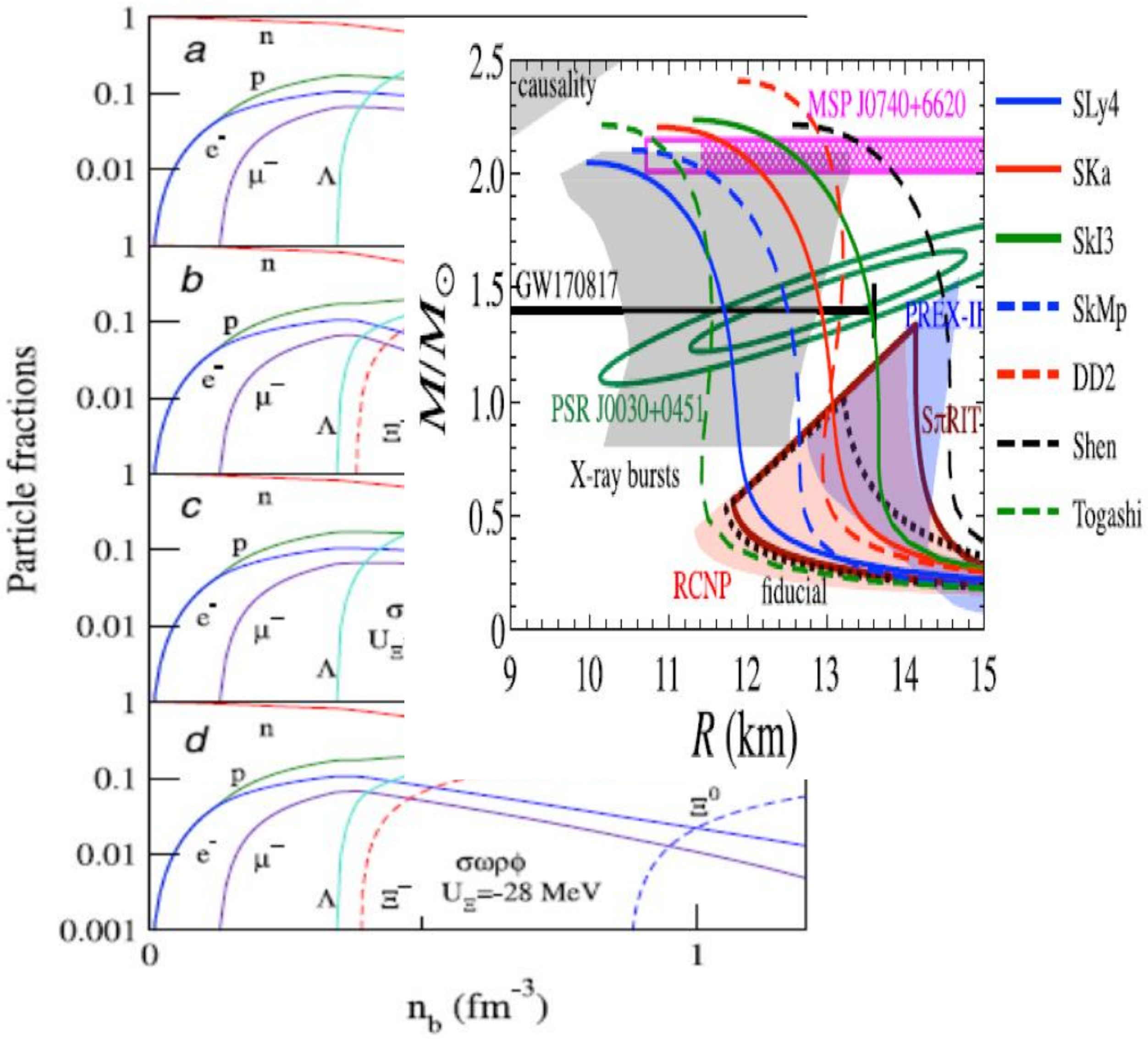

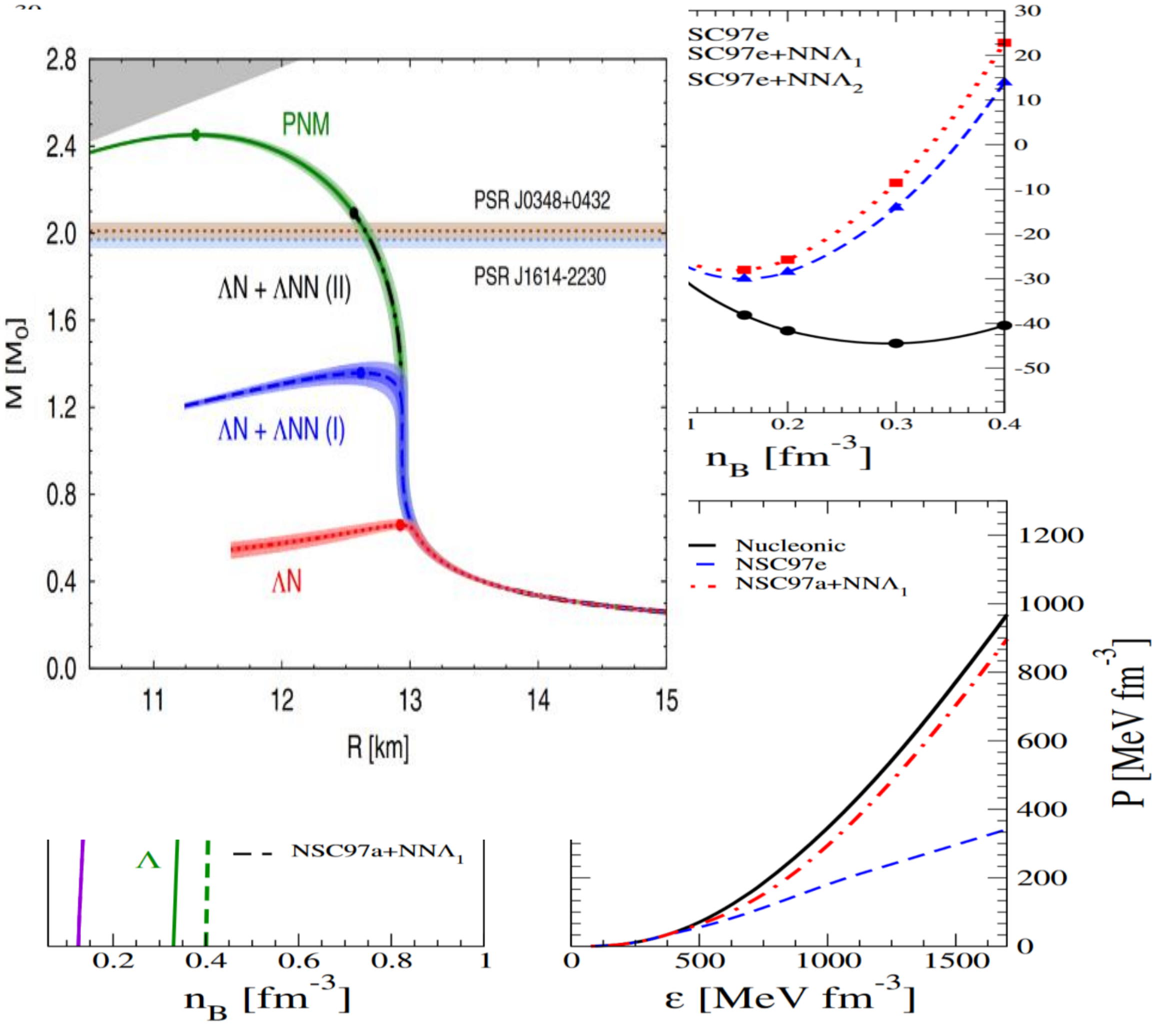

Cluster production in heavy-ion collisions

Experiments:
SSC and CSR(HIRFL), INDRA (GANIL), CHIMERA (LNS), NSCL (MSU), FOPI and HADES (GSI) …

P. Russotto *et al.*, PRC 91, 014610 (2015)

Temporal evolution of density profile

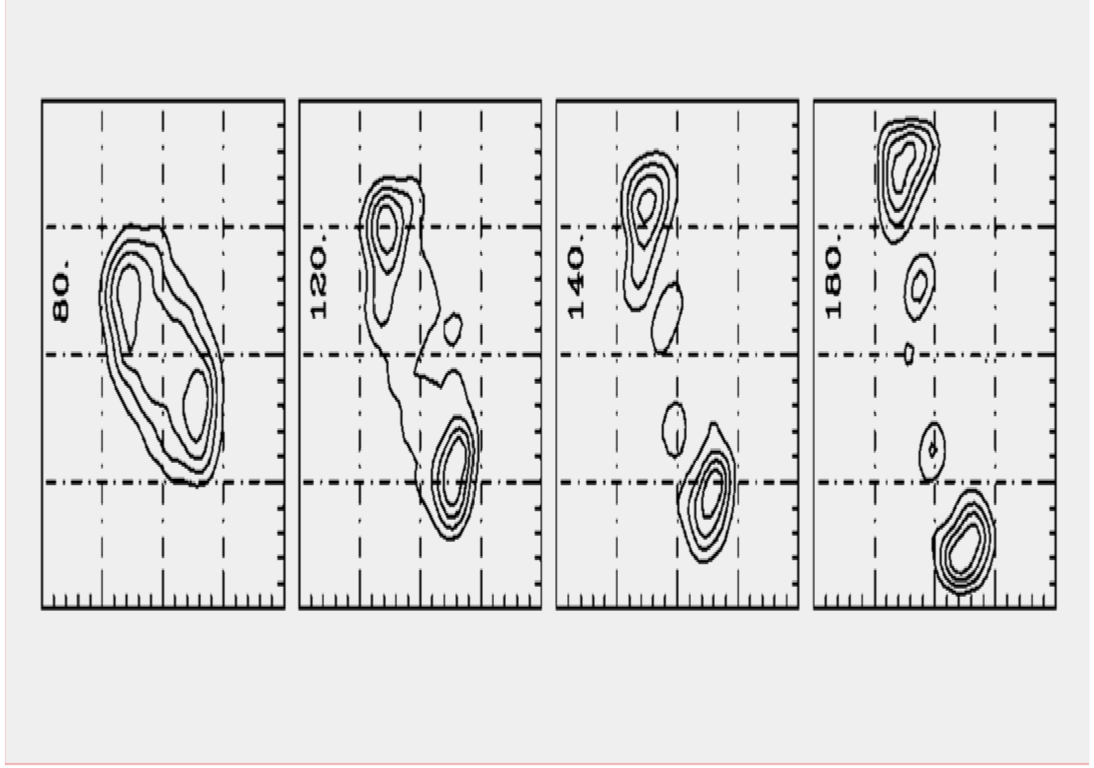

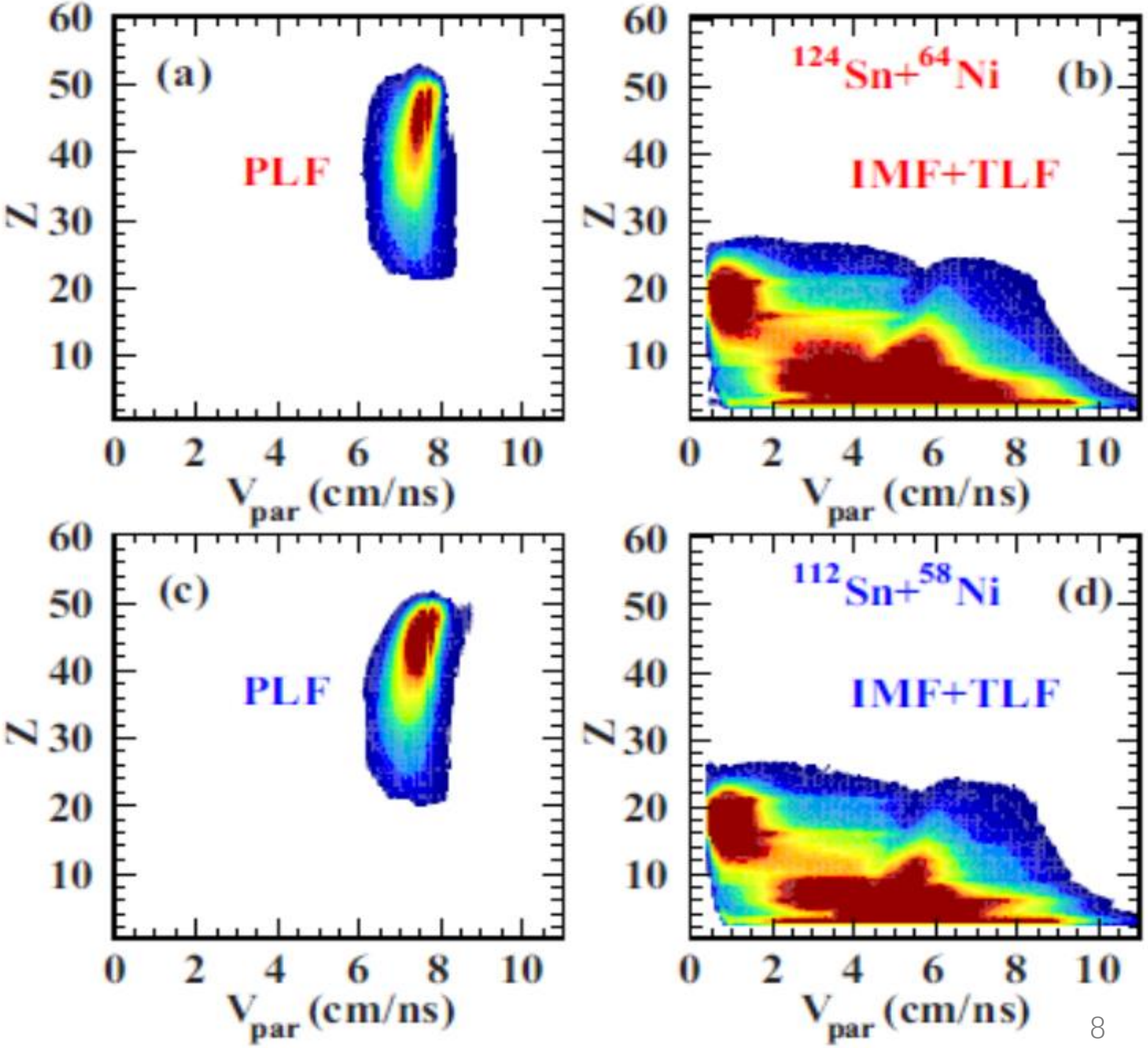

Cluster production measurement at FOPI

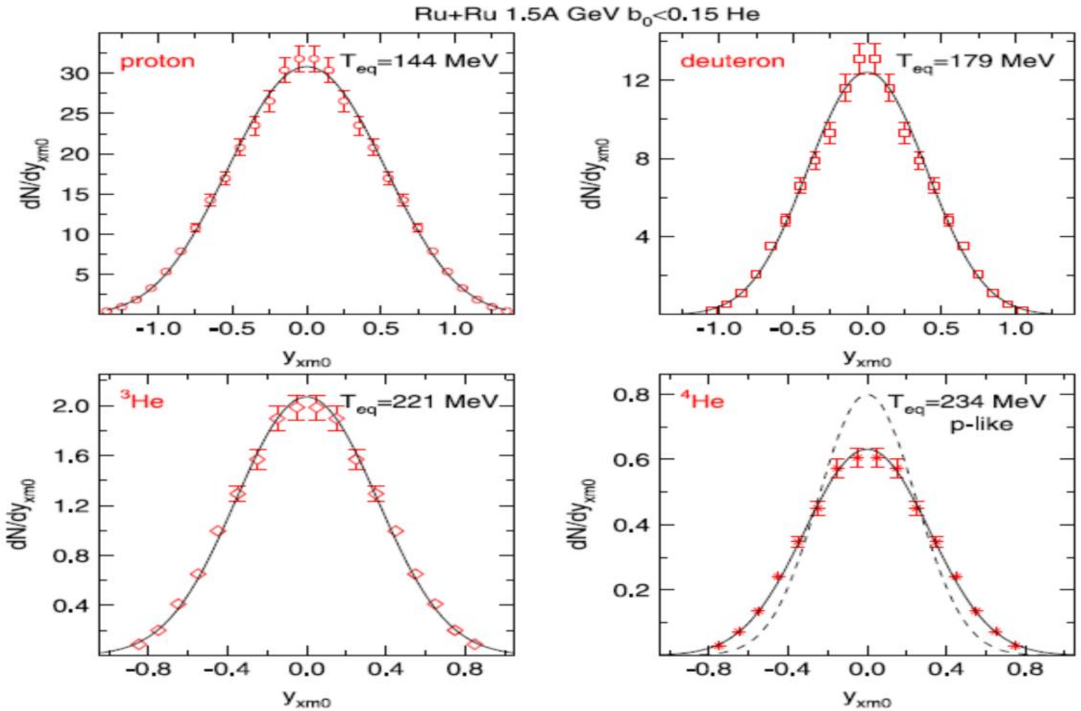

Multiplicities and charge balance for Au + Au at $E/A = 0.15$ GeV and $b_0 < 0.15$.

$Z = 1$	59.9 ± 3.0	p	24.1 ± 1.2	$Z = 2$	25.0 ± 1.8	^{3}He	8.4 ± 0.9
		d	20.4 ± 1.4			^{4}He	16.6 ± 1.7
		t	15.1 ± 1.5				
		Li	5.0 ± 0.5	Be	1.69 ± 0.17		
		B	1.44 ± 0.15	C	0.90 ± 0.09		
		N	0.50 ± 0.05	O	0.26 ± 0.03		

Multiplicities and charge balance for Ni + Ni at $E/A = 0.25$ GeV and $b_0 < 0.15$.

$Z = 1$	34.9 ± 1.8	p	19.2 ± 1.0	$Z = 2$	9.0 ± 0.7	^{3}He	3.24 ± 0.33
		d	10.5 ± 0.8			^{4}He	5.79 ± 0.58
		t	5.1 ± 0.5				
		Li	0.91 ± 0.09	Be	0.26 ± 0.03		
		B	0.10 ± 0.01				

ELSEVIER
Available online at www.sciencedirect.com
ScienceDirect
Nuclear Physics A 848 (2010) 366–427
NUCLEAR PHYSICS A
www.elsevier.com/locate/nuclphysa

Systematics of central heavy ion collisions in the 1A GeV regime

FOPI Collaboration

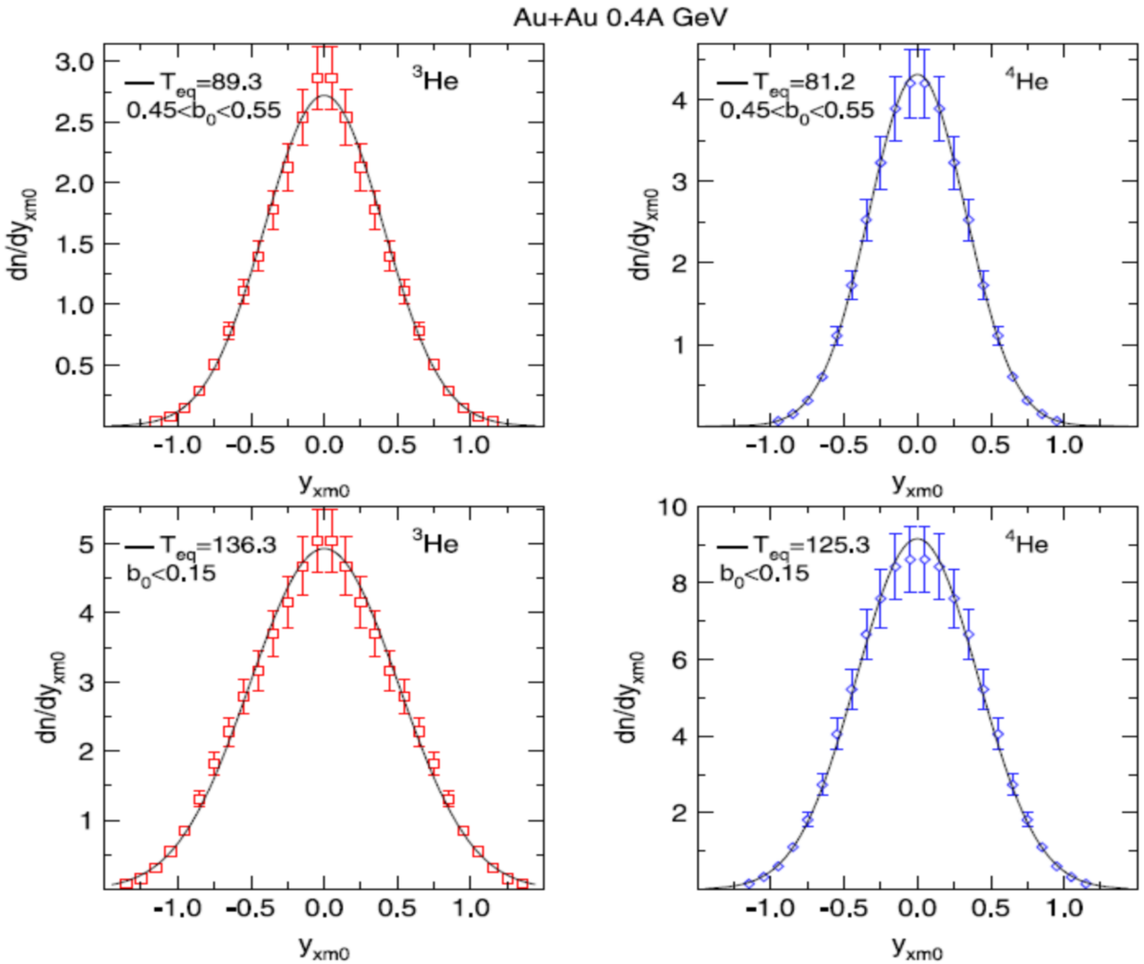

Cluster production measurement

at FOPI INDRA-FAZIA

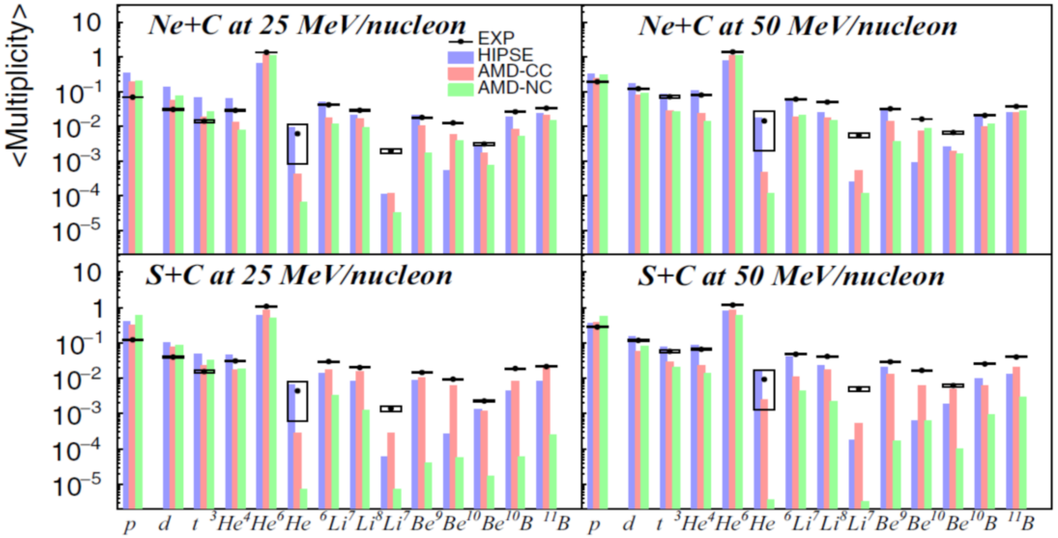

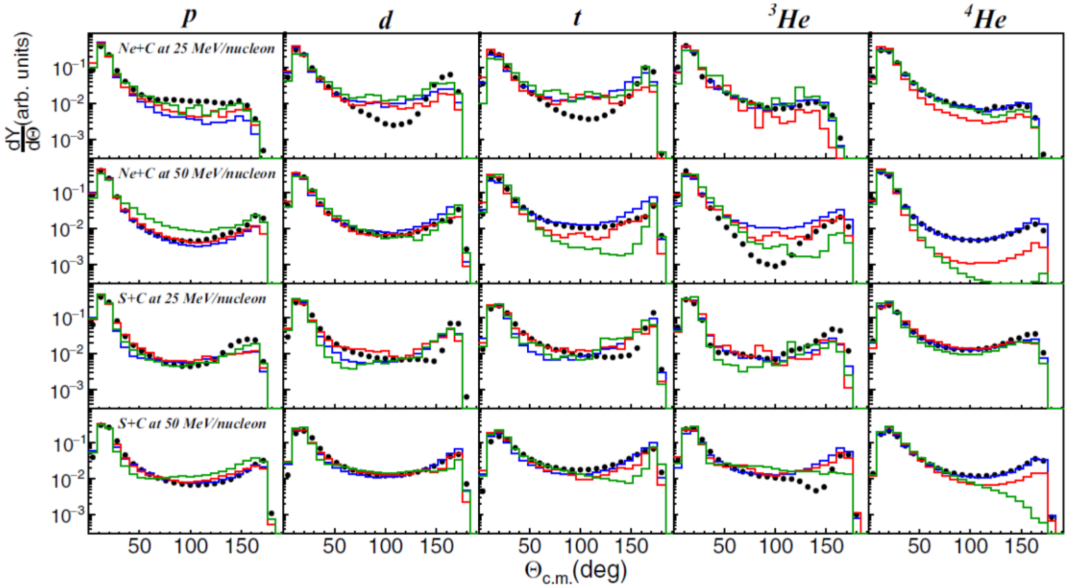

PHYSICAL REVIEW C **107**, 044614 (2023)

Featured in Physics

Examination of cluster production in excited light systems at Fermi energies from new experimental data and comparison with transport model calculations

C. Frosin,[1,2,*] S. Piantelli,[2] G. Casini,[2] A. Ono,[3] A. Camaiani,[4] L. Baldesi,[2] S. Barlini,[1,2] B. Borderie,[5] R. Bougault,[6] C. Ciampi,[1,2] M. Cicerchia,[7] A. Chbihi,[8] D. Dell'Aquila,[9,10] J. A. Dueñas,[11] D. Fabris,[12] Q. Fable,[13] J. D. Frankland,[8] T. Génard,[8] F. Gramegna,[7] D. Gruyer,[6] M. Henri,[8] B. Hong,[14,15] M. J. Kweon,[16] S. Kim,[17] A. Kordyasz,[18] T. Kozik,[19] I. Lombardo,[20,21] O. Lopez,[6] T. Marchi,[7] K. Mazurek,[22] S. H. Nam,[14,15] J. Lemarié,[8] N. LeNeindre,[6] P. Ottanelli,[2] M. Parlog,[6,23] J. Park,[14,15] G. Pasquali,[1,2] G. Poggi,[1,2] A. Rebillard-Soulié,[6] B. H. Sun,[24] A. A. Stefanini,[1,2] S. Terashima,[24] S. Upadhyaya,[19] S. Valdré,[2] G. Verde,[20,13] E. Vient,[6] and M. Vigilante[25,26]
(INDRA-FAZIA Collaboration)

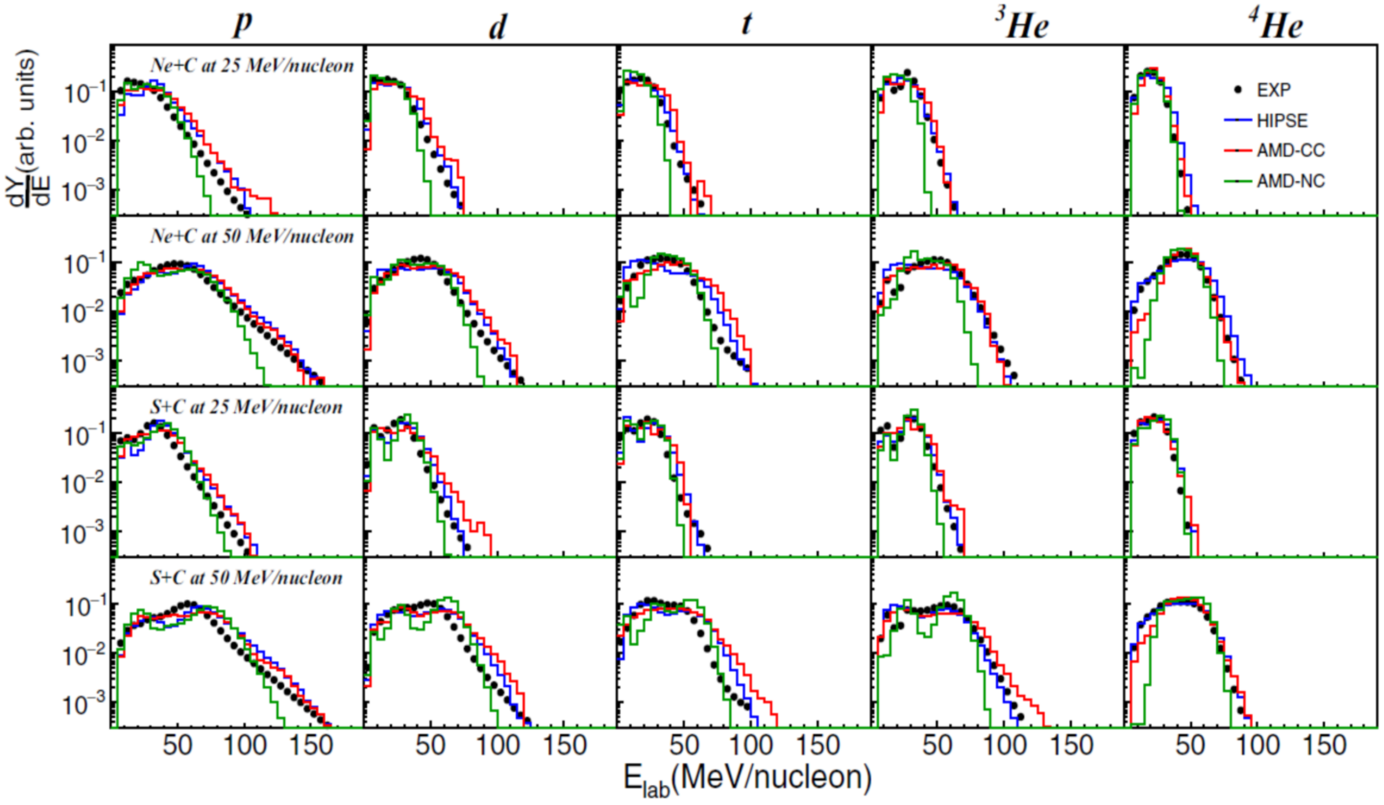

Advantage of HICs for HN production

1. Neutron-rich/proton-rich HN nuclei and spectroscopies
2. Multistrangeness HN (S=-2) $_{\Lambda\Lambda}X$和$_{\Xi}X$
3. Interaction potentials of NΛ, NΞ NNΛ, etc

H. Tamura, *Prog. Theor. Exp. Phys.* (2012) 02B012

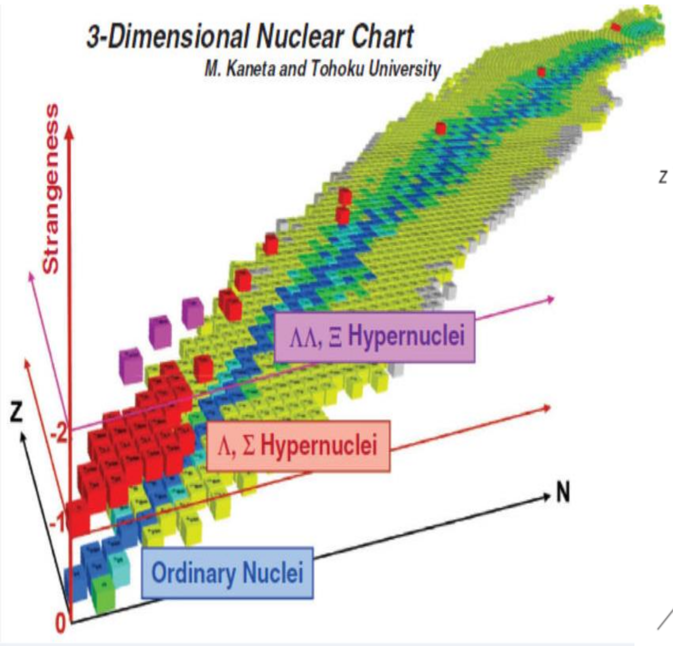

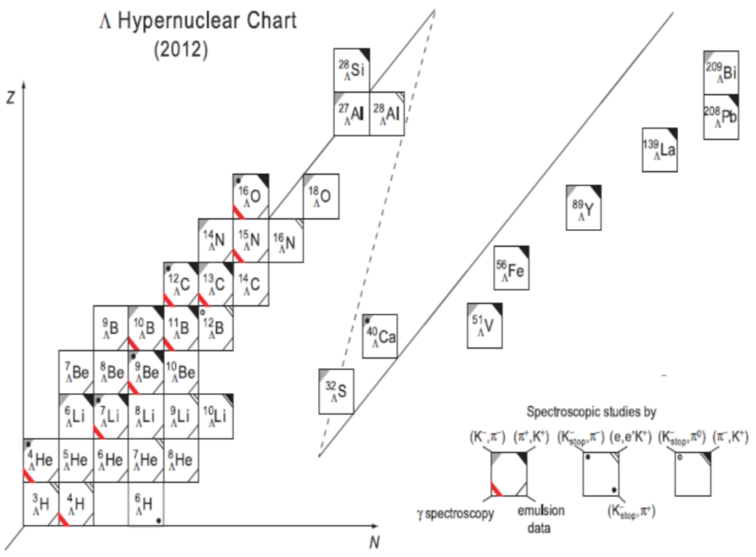

PHYSICAL REVIEW C **102**, 044002 (2020)

Observation of a $\overline{K}NN$ bound state in the ^{3}He(K^-, Λp)n reaction

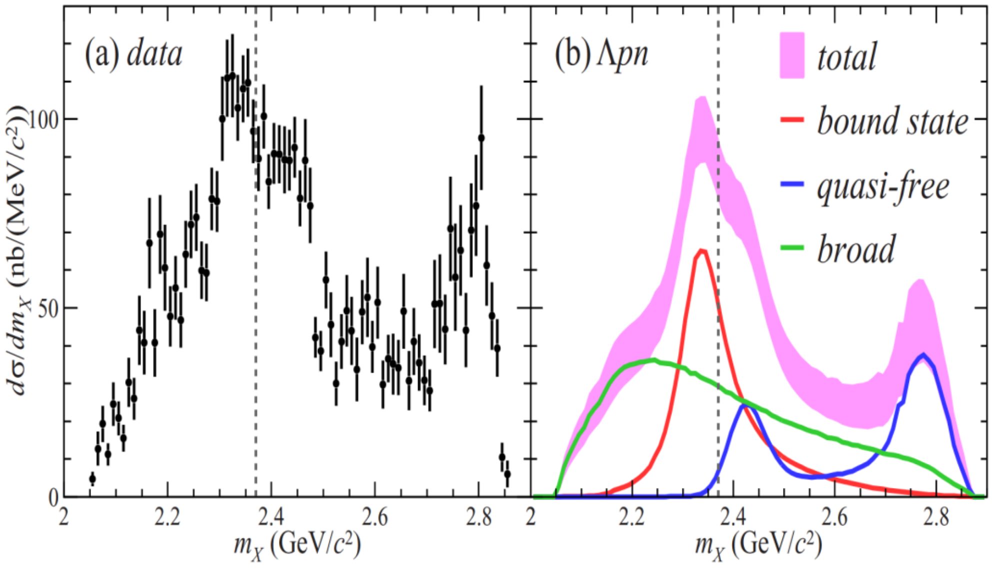

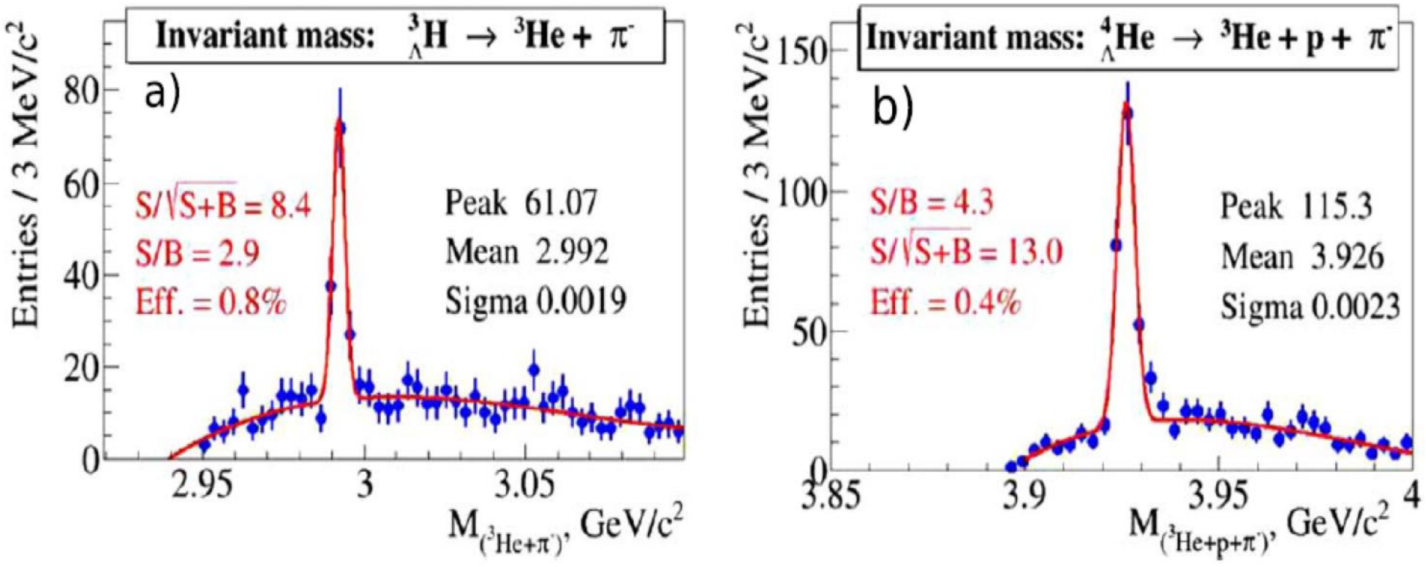

Estimation of proton-rich and neutron rich HN with GSI exotic beam

C. Rappold, J. López-Fidalgo, PRC 94, 044616 (2016)

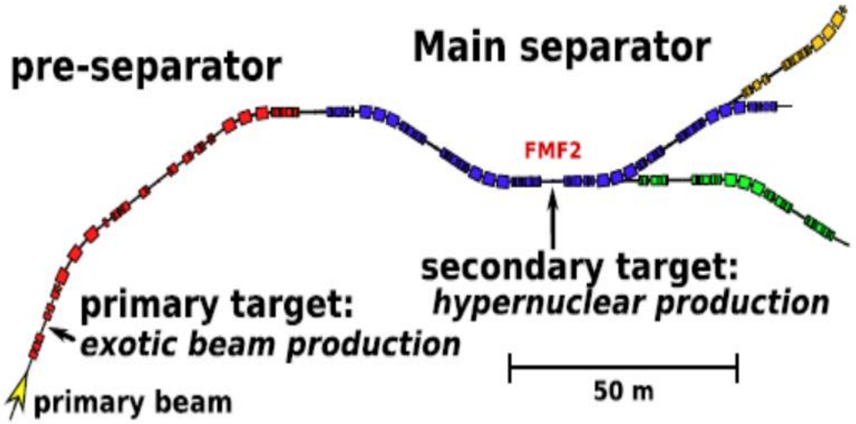

$^{8}_{\Lambda}Be$

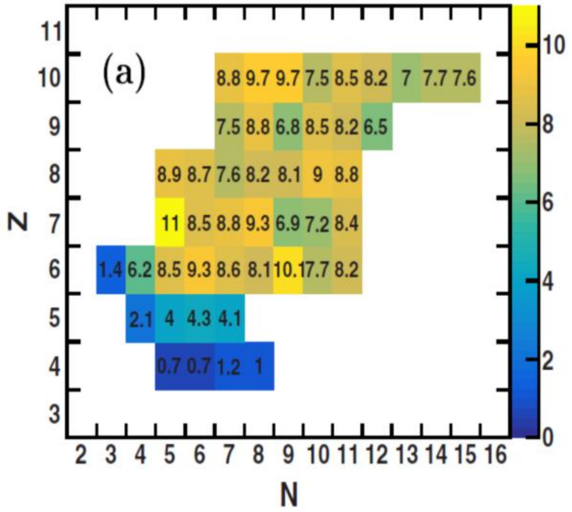

$^{11}_{\Lambda}Be$

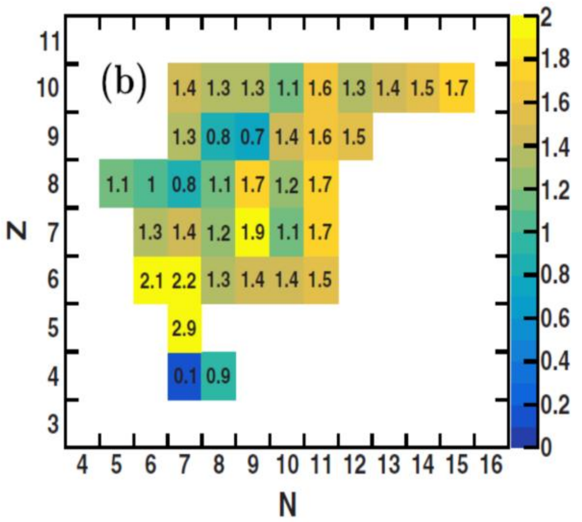

Λ-hypernuclei

μb

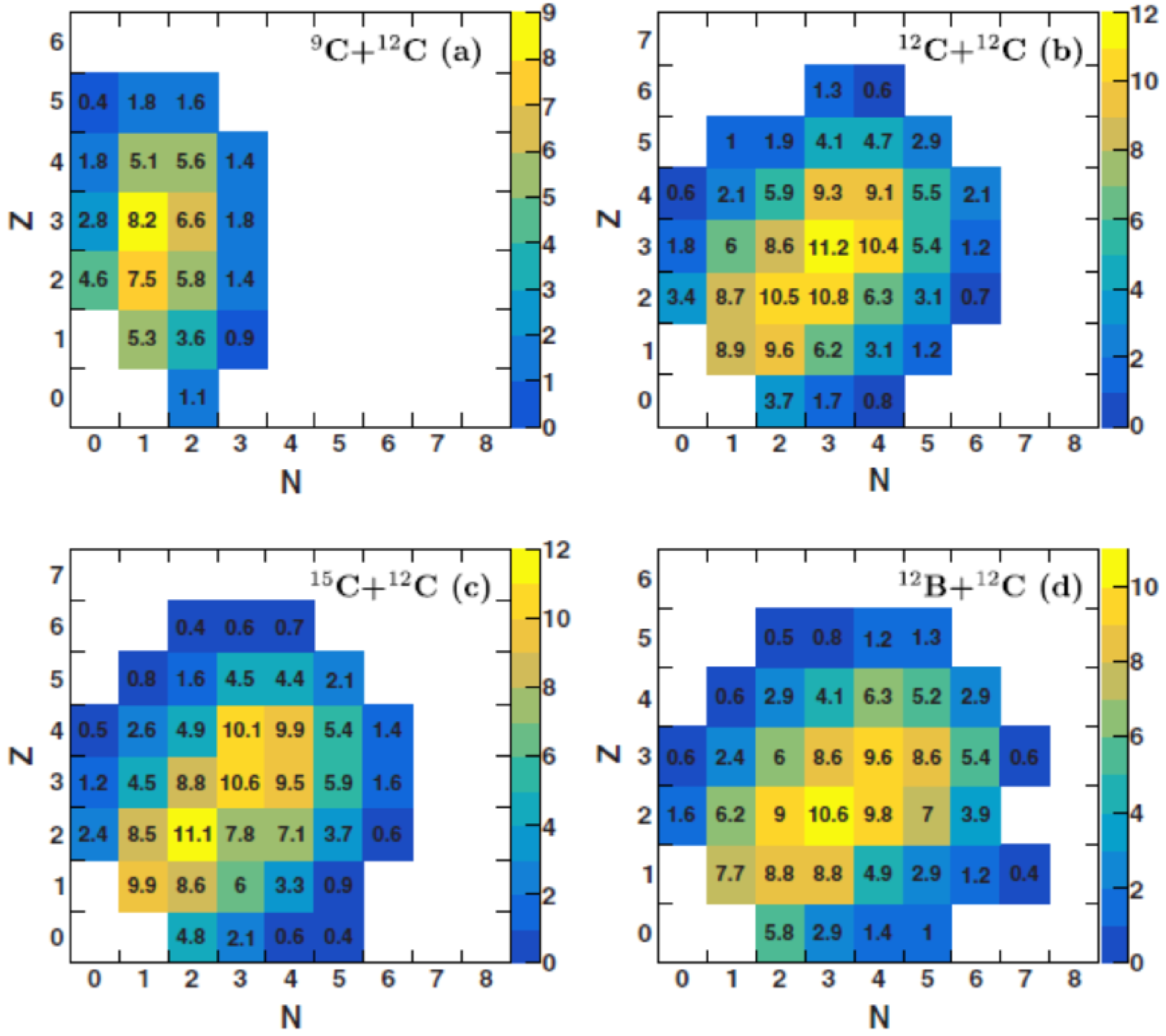

ALICE Collaboration, https://doi .org /10 .48550 /arxiv.2209 .07360

Radius and binding energy HN

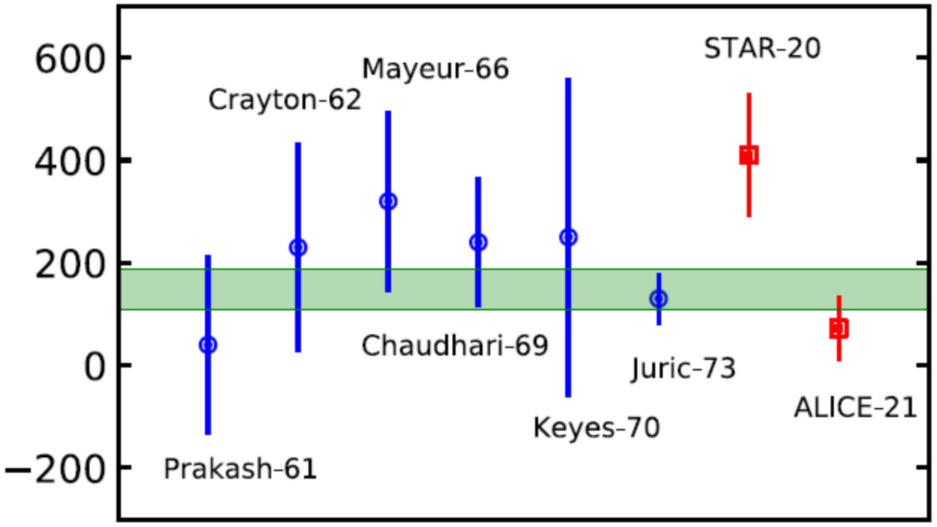

$B_\Lambda=72^{+63}_{-36}$ keV

R~10 fm

B_Λ= 148 ± 40 keV

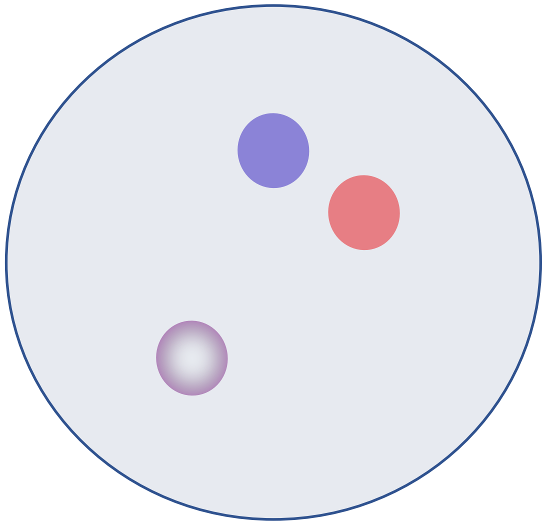

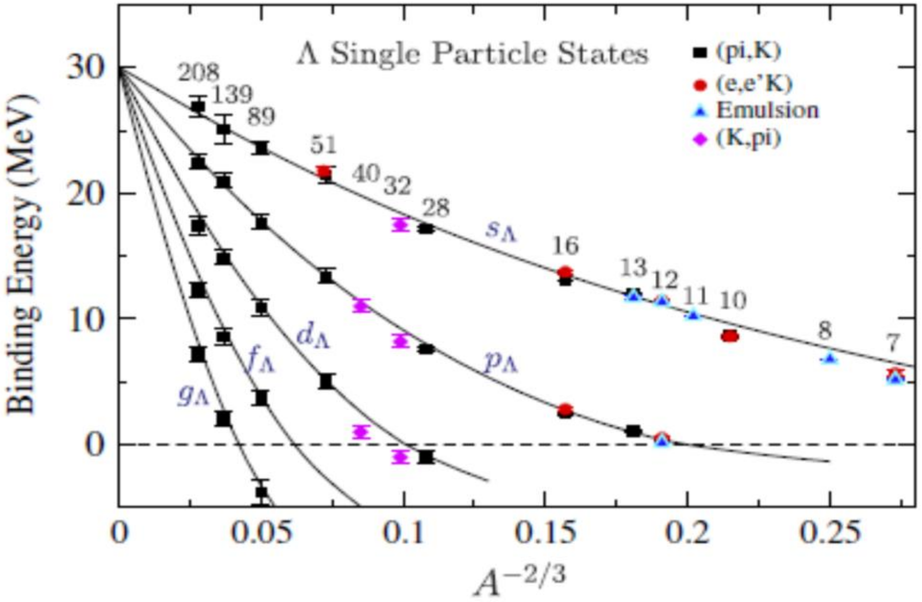

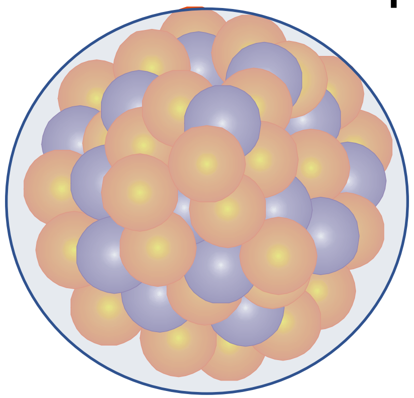

Millener, D. J., C. B. Dover, and A. Gal, 1988, Phys. Rev. C 38, 2700

(Hyper-)cluster production in HICs-statistical approach

A. Andronic, P. Braun-Munzinger, J. Stachel, H. Stöcker, Physics Letters B 697 (2011) 203–207

Pb+Pb

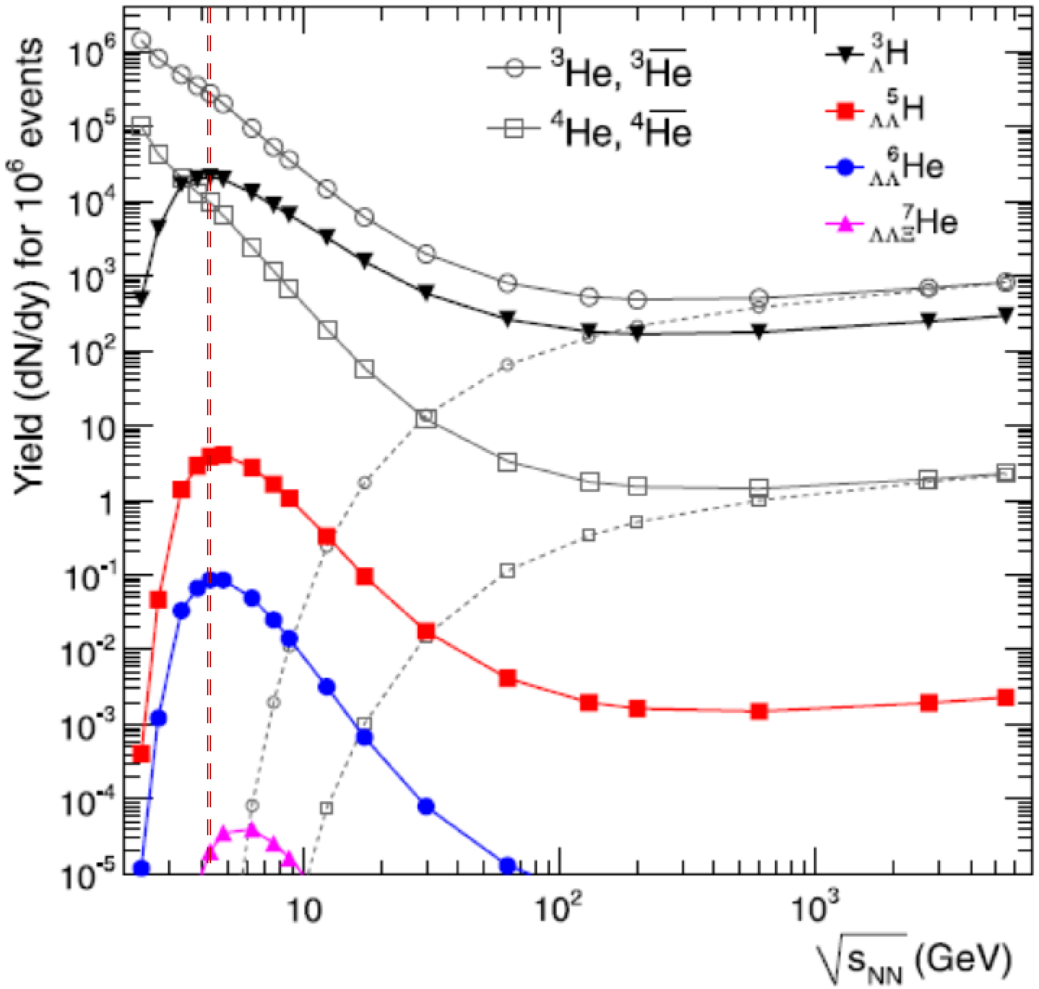

N. Buyukcizmeci, R. Ogul, A. S. Botvina, M. Bleicher, Phys. Scr. 95 075311 (2020)

Statistical multifragmentation model (SMM)

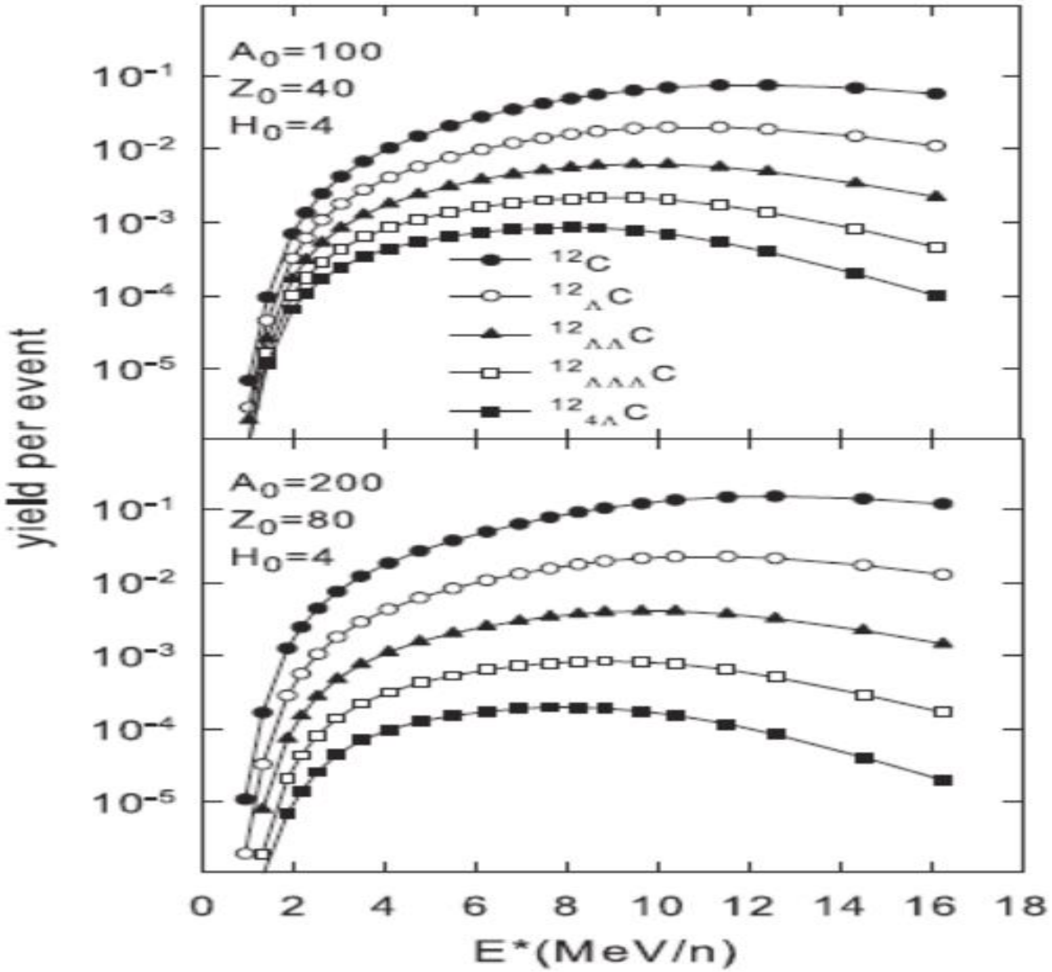

Transport model + coalescence approach

A.S. Botvina, J. Steinheimer, E.Bratkovskaya et al., Physics Letters B 742 (2015)7–14

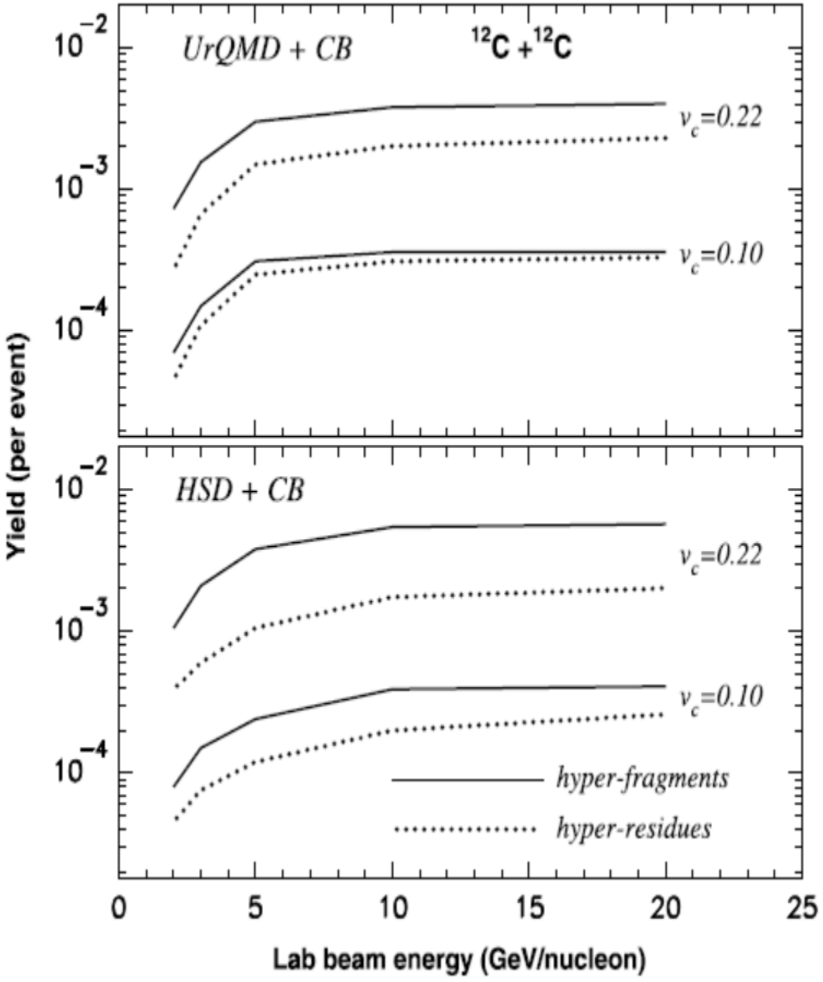

J. Aichelin, E. Bratkovskaya, A. Le Fèvre et al., Physical Review C 101, 044905 (2020)
A. Le Fèvre, J. Aichelin, C. Hartnack and Y. Leifels 100, Physical Review C 034904 (2019)

^{6}Li+^{12}C@2A GeV

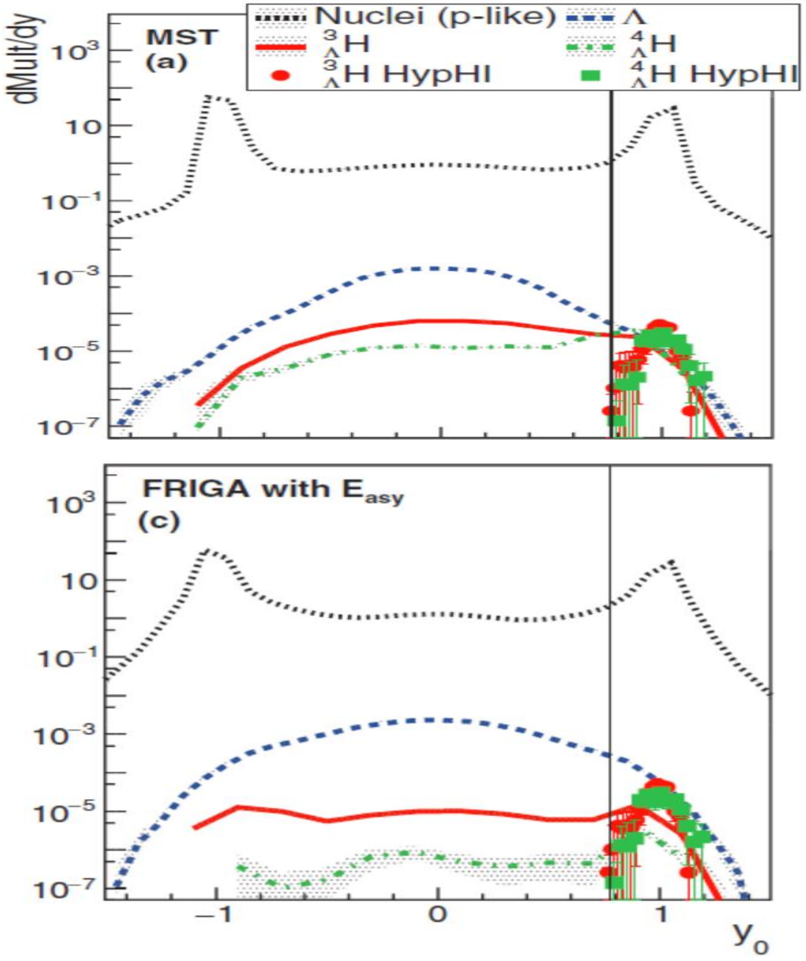

科学通报 2018 年 第 63 卷 第 8 期: 735~744
论 文
《中国科学》杂志社 SCIENCE CHINA PRESS

中高能重离子碰撞中奇异粒子产生和超核形成机制

冯兆庆
中国科学院近代物理研究所, 兰州 730000
E-mail: fengzhq@impcas.ac.cn

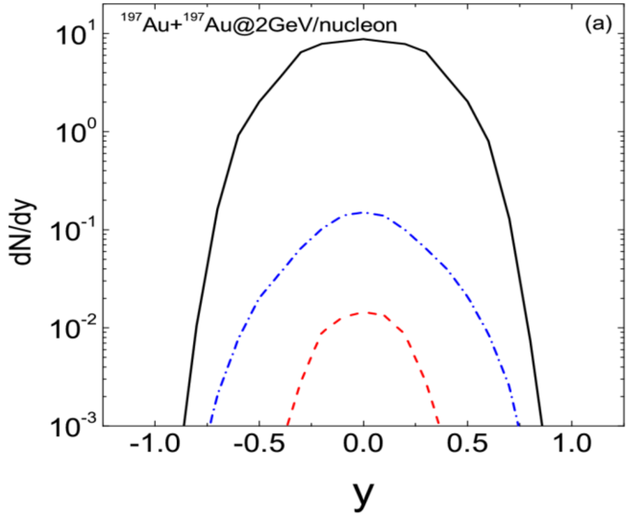

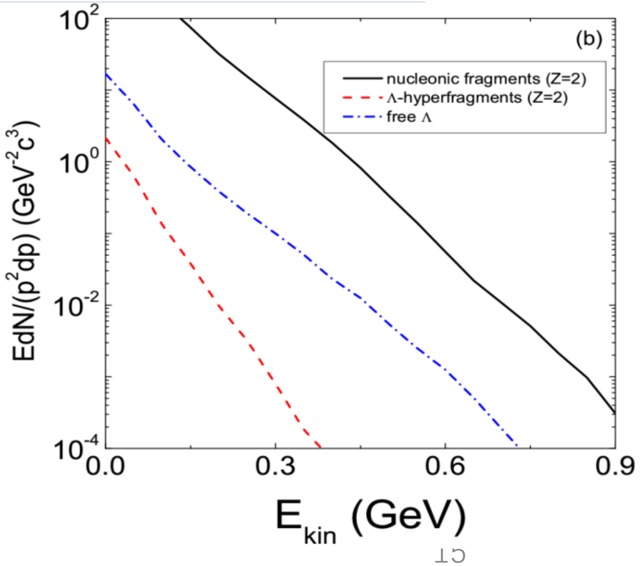

Recognizing a nuclear cluster or hypernuclear cluster

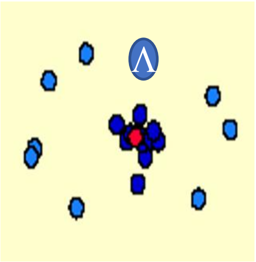

1) Classical coalescence approach in phase space for nuclides of Z>2 combined with the GEMINI decay code (minimum spanning tree (MST) procedure)

$|r_i - r_j| \leq 3$ fm, $|r_i - r_Y| \leq 4.5$ fm , $|p_i - p_j| \leq 0.3$ GeV/c

C. Samanta et al, J. Phys. G: Nucl. Part. Phys. 32 (2006) 363
Z. Q. Feng, Phys. Rev. C 102, 044604 (2020)

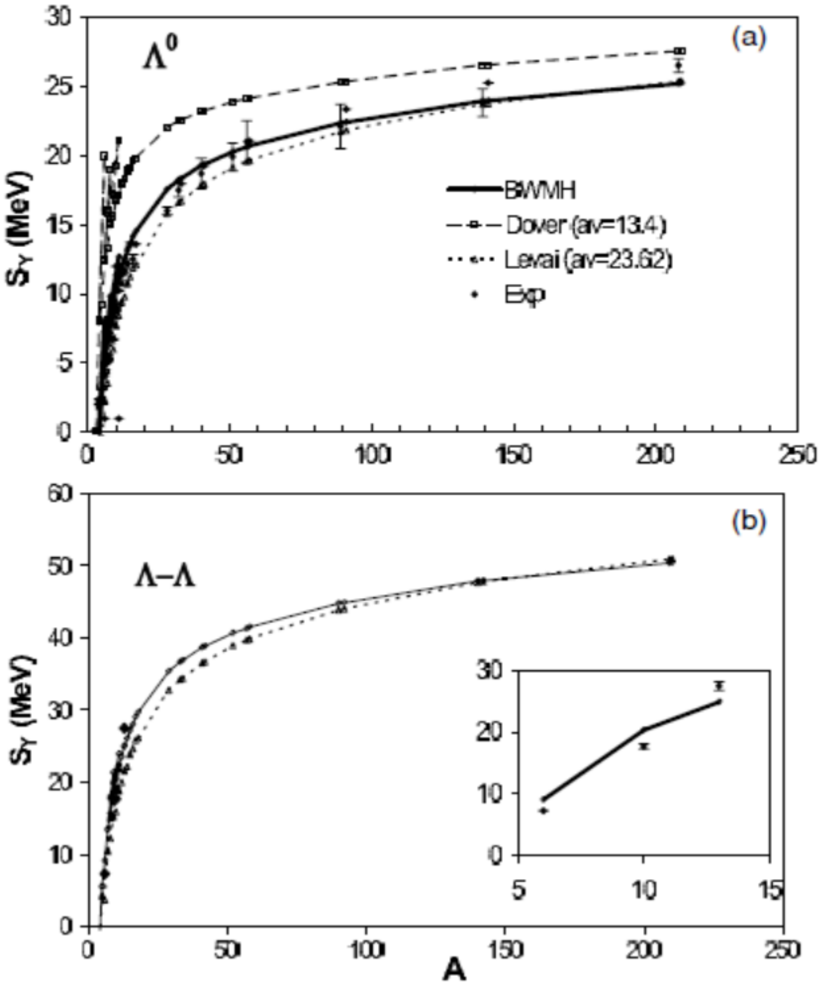

Binding energy:

$$E_B(Z_i, N_i) = \sum_j \sqrt{p_j^2 + m_j^2} - m_j + \frac{1}{2} \sum_{j,k,k\neq j} \int f_j(\mathbf{r}, \mathbf{p}, t) f_k(\mathbf{r}', \mathbf{p}', t) \times v(\mathbf{r}, \mathbf{r}', \mathbf{p}, \mathbf{p}') d\mathbf{r}\, d\mathbf{r}'\, d\mathbf{p}\, d\mathbf{p}' + \frac{1}{6} \sum_{j,k,l} \sum_{k\neq j, k\neq l, j\neq l} \int f_j(\mathbf{r}, \mathbf{p}, t) f_k(\mathbf{r}', \mathbf{p}', t) \times f_l(\mathbf{r}'', \mathbf{p}'', t) v(\mathbf{r}, \mathbf{r}', \mathbf{r}'', \mathbf{p}, \mathbf{p}', \mathbf{p}'') \times d\mathbf{r}\, d\mathbf{r}' d\mathbf{r}'' d\mathbf{p}\, d\mathbf{p}' d\mathbf{p}'',$$

Excitation energy $E^*(Z_i, N_i, nY)$

$= E_B(Z_i, N_i, nY) - E_{LD}(Z_i, N_i, nY)$

The decay of excited hypernucleus is described by the GEMINI code!

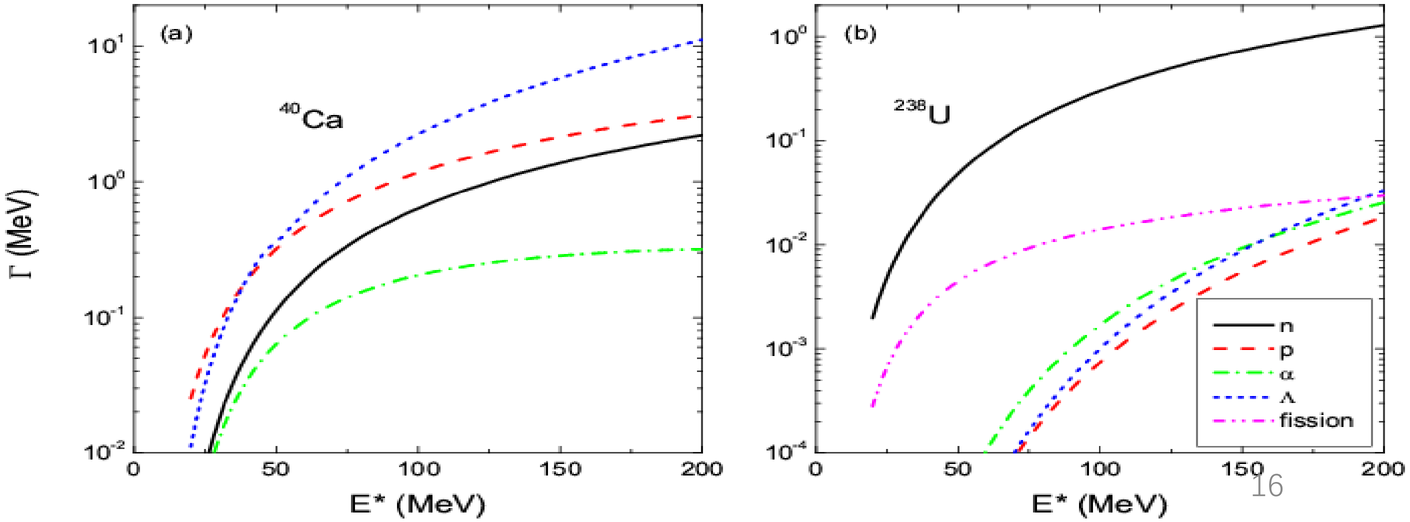

2) Wigner density approach for Z≤2

R. Mattiello et al., Phys. Rev. C 55, 1443 (1997)

$$\frac{dN_M}{d^3P} = G_M \binom{A}{M}\binom{M}{Z}\frac{1}{A^M}\int\prod_{i=1}^{Z} f_p(\mathbf{r}_i,\mathbf{p}_i)\prod_{i=Z+1}^{M} f_n(\mathbf{r}_i,\mathbf{p}_i)$$

$$\times\rho^W(\mathbf{r}_{k_1},\mathbf{p}_{k_1},...,\mathbf{r}_{k_{M-1}},\mathbf{p}_{k_{M-1}})$$

$$\delta(\mathbf{P}-(\mathbf{p}_1+...+\mathbf{p}_M))d\mathbf{r}_1 d\mathbf{p}_1 ... d\mathbf{r}_M d\mathbf{p}_M$$

$^3{}_\Lambda H$ via $^{197}Au+^{197}Au$

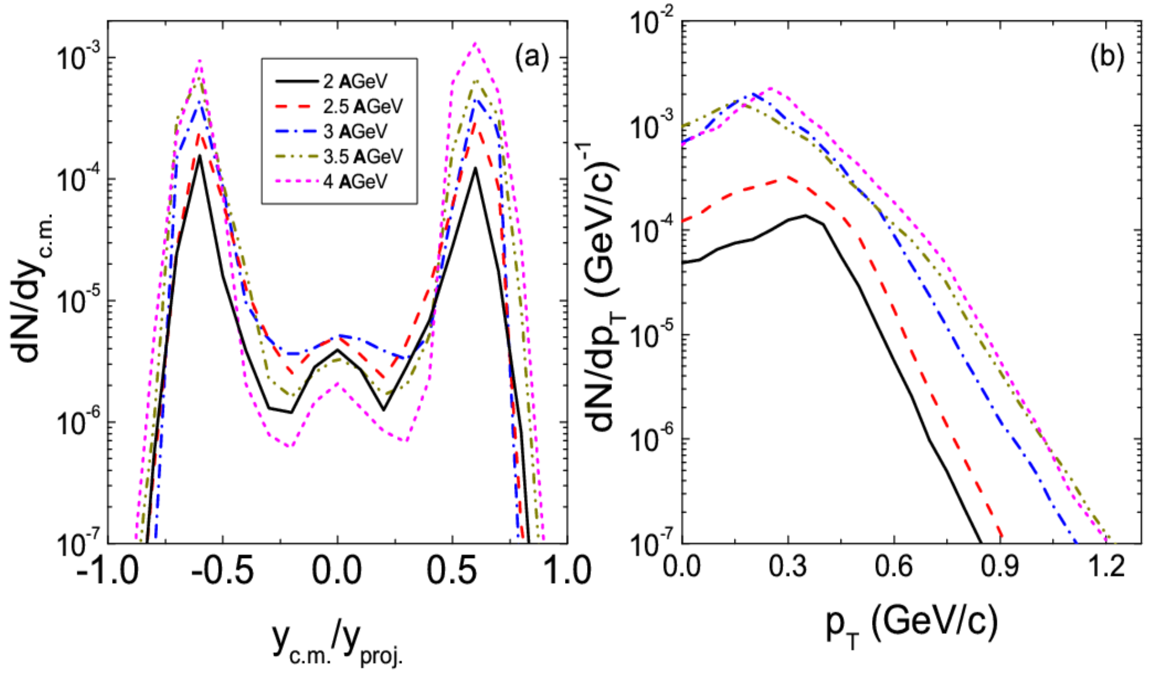

LQMD calculation: Eur. Phys. J. A, 57 (2021) 18; FOPI data from Nucl. Phys. A 876, 1 (2012)

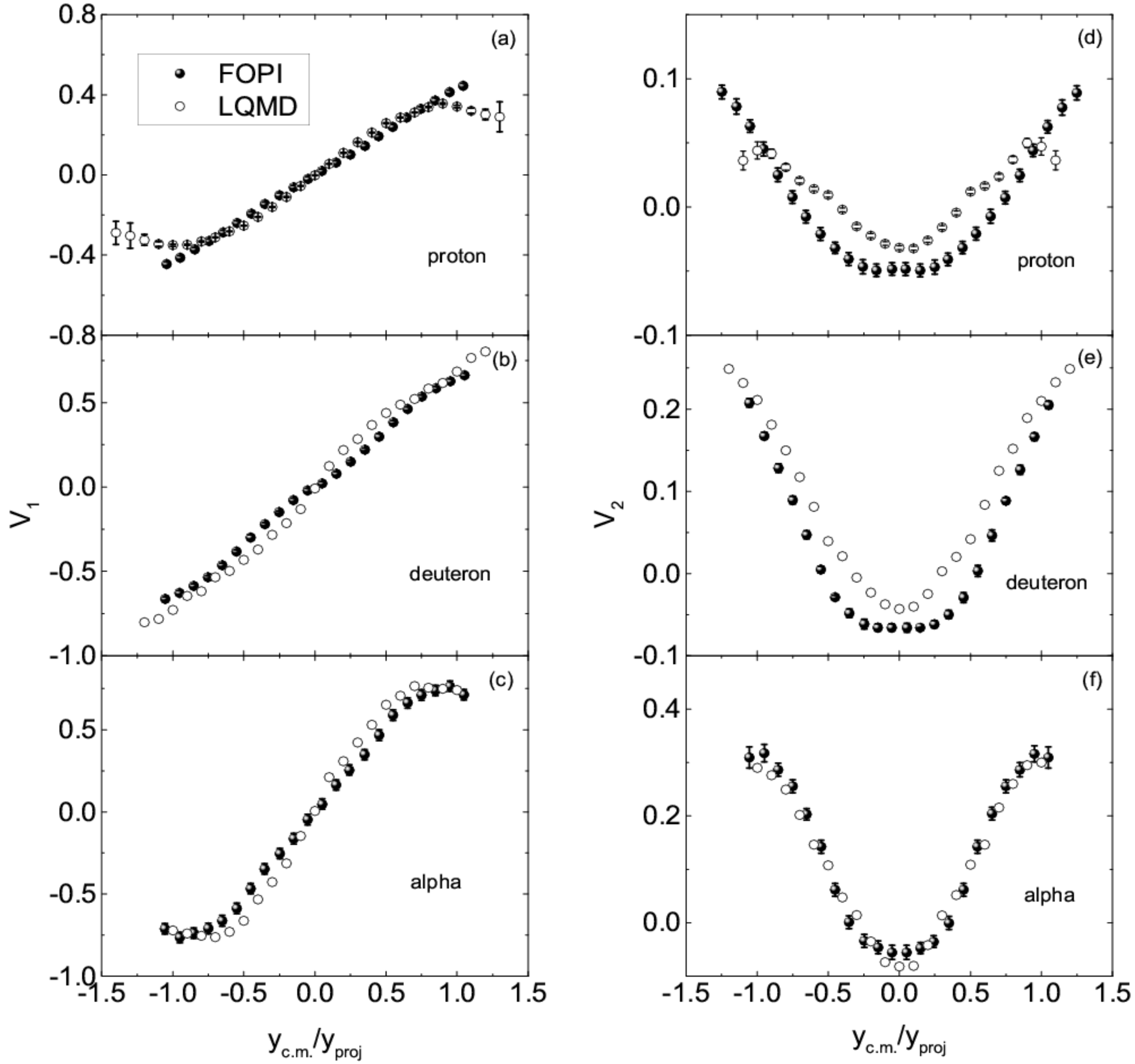

Zhao-Qing Feng, Eur. Phys. J. A, 57 (2021) 18, LQMD calculation

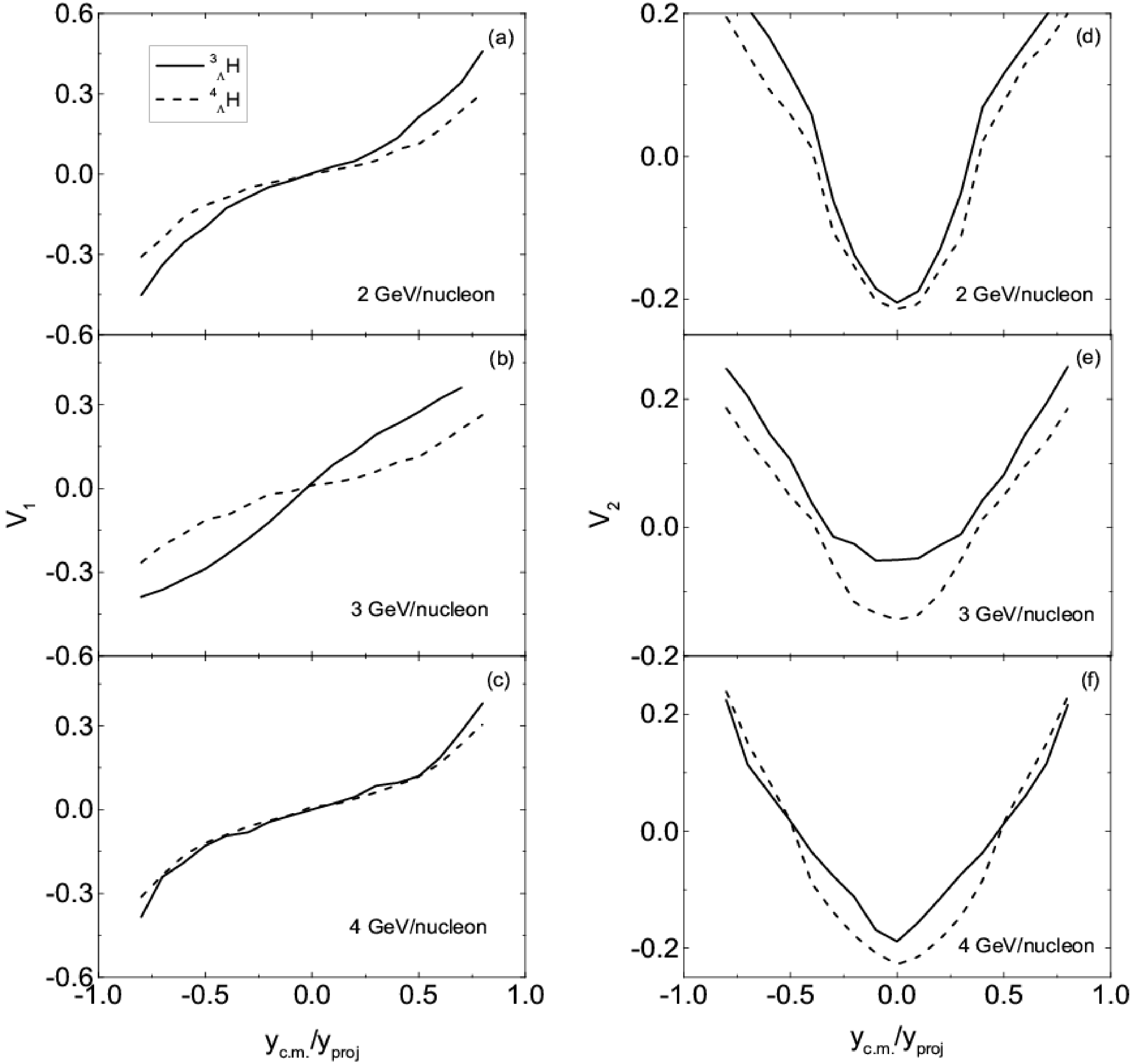

The STAR Collaboration, PRL130, 212301 (2023)

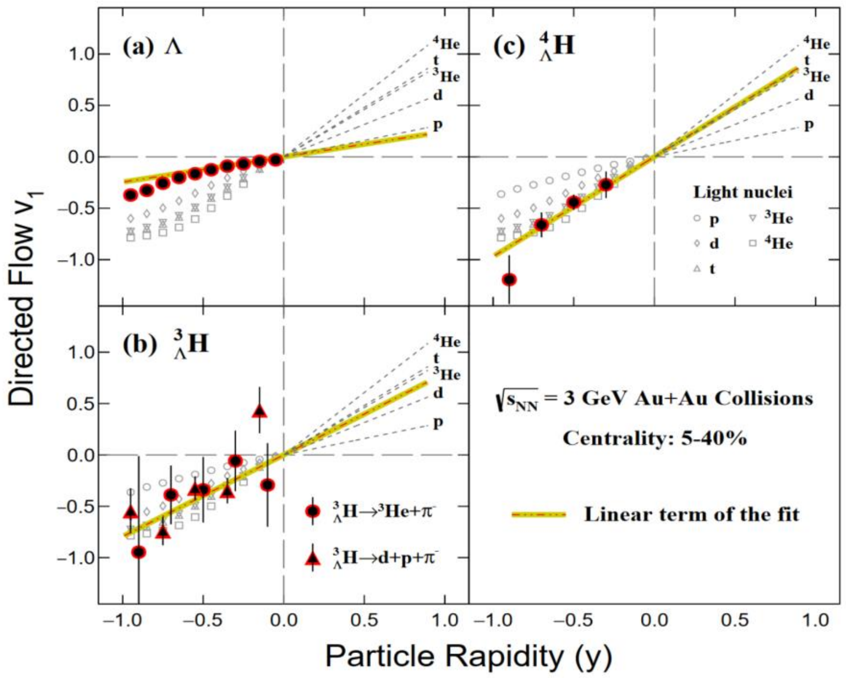

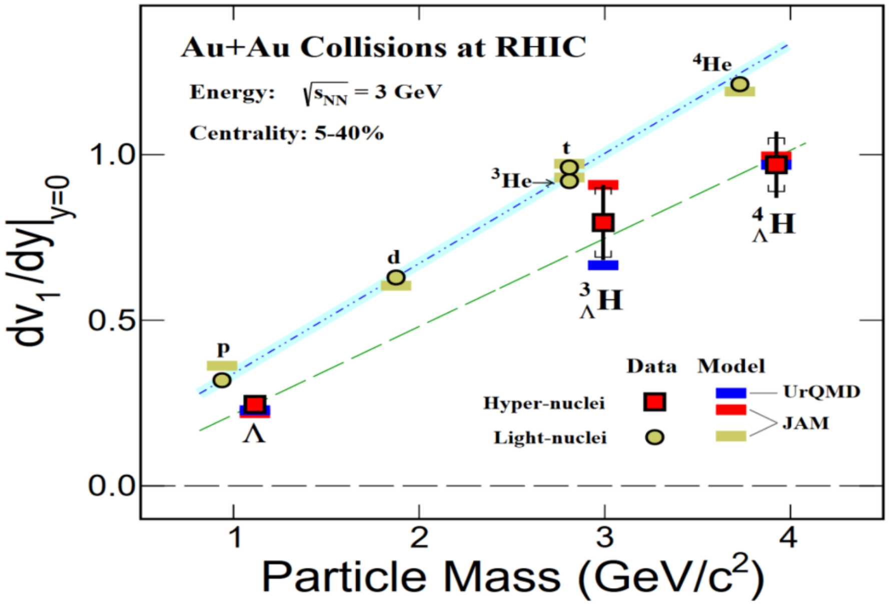

3) Surface coalescence for cluster construction

A. Boudard, J. Cugnon, S. Leray et al., Nucl. Phys. A 740, 195-210 (2004)
Hui-Gan Cheng, Zhao-Qing Feng, Chinese Physics C 45, 084107 (2021)

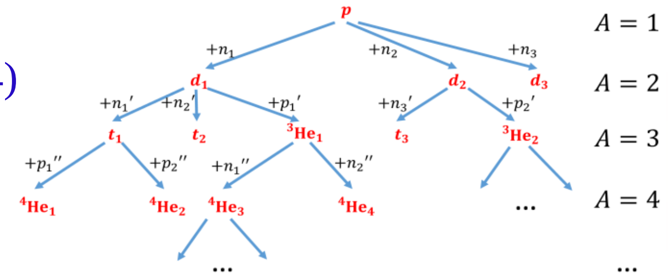

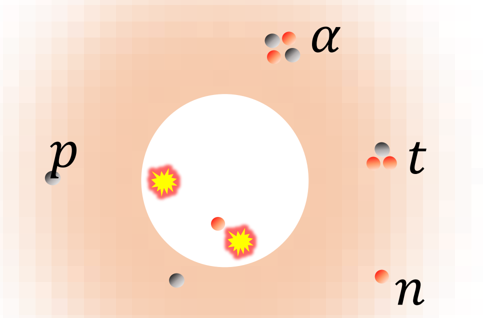

$$R_{Nj}P_{Nj} \leqslant h_0, \quad R_{Nj} \geqslant 1 \text{ fm},$$

$$R_{Nj} = \left|\boldsymbol{R}_N - \boldsymbol{r}_j\right|,$$

$$P_{Nj} = \left|\frac{m_j}{M_N + m_j}\boldsymbol{p}_N - \frac{M_N}{M_N + m_j}\boldsymbol{p}_j\right|.$$

Table 2. Suface coalescence parameters of Set 1 and Set 2.

Construction	h_0/ (fm MeV/c)	
	Set 1	Set 2
$p+n \rightarrow d$	387	336
$d+n \rightarrow t$	387	315
$d+p \rightarrow {}^3$ He	387	315
$t+p \rightarrow {}^4$ He	387	300
^{3}He $+n \rightarrow {}^4$ He	387	300

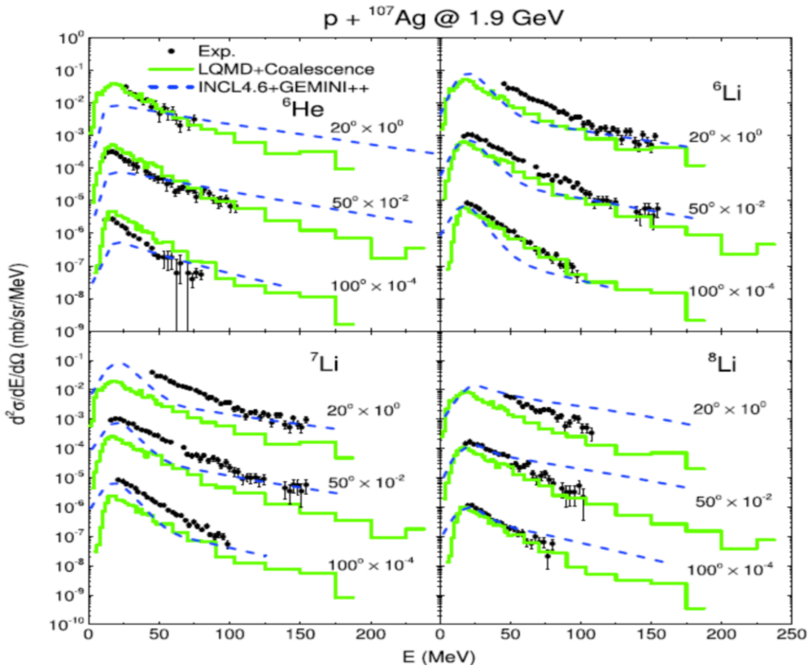

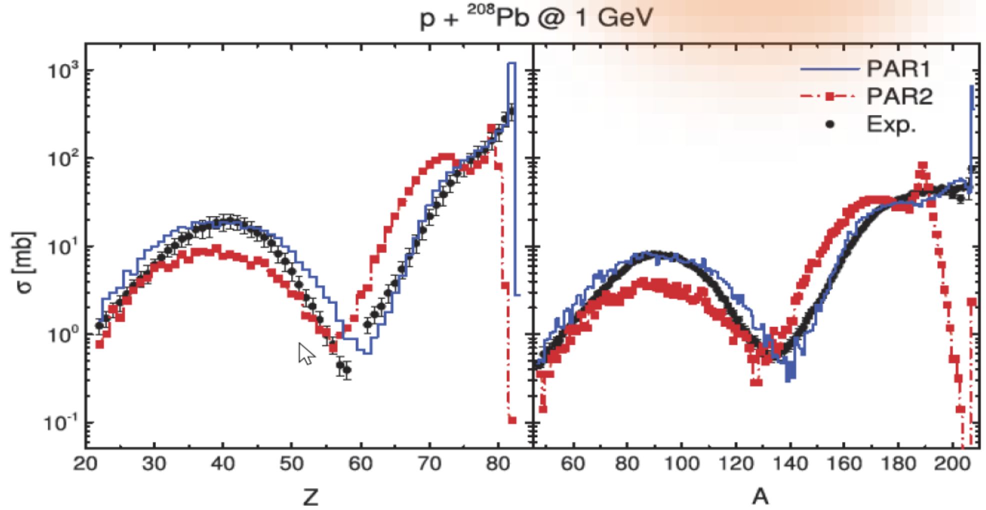

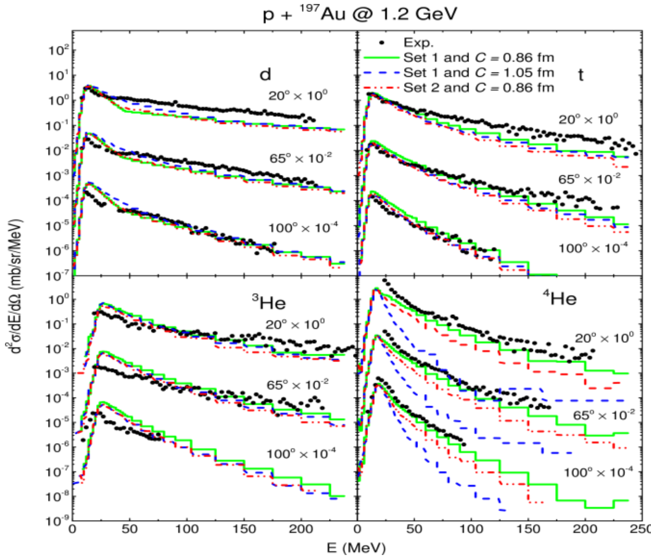

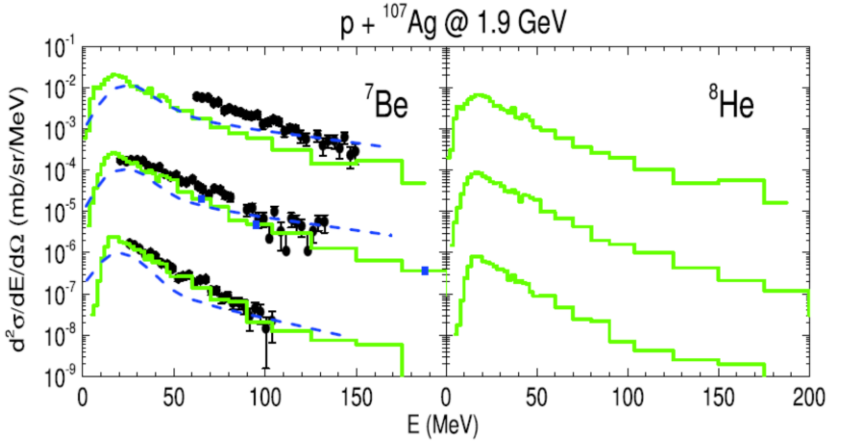

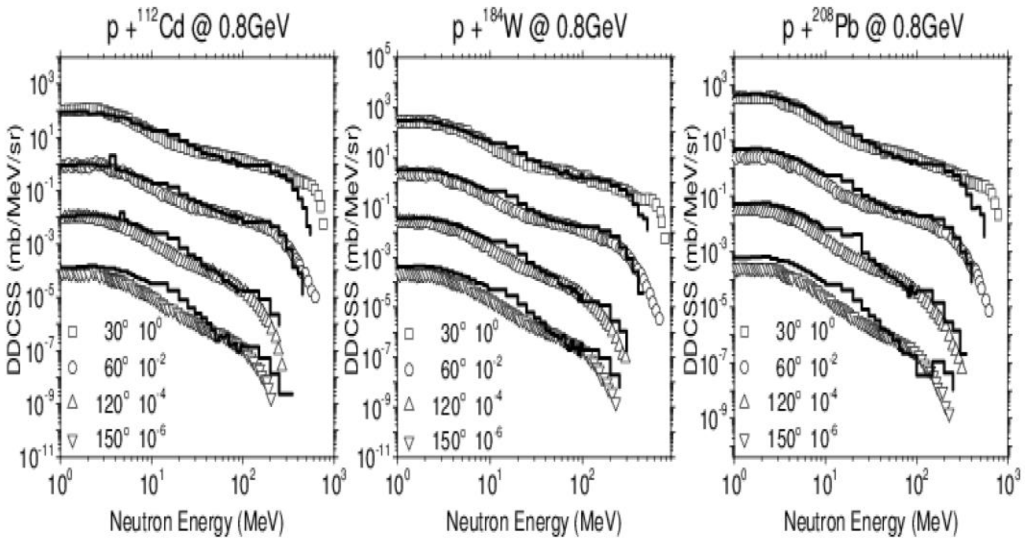

(Hyper) nuclear fragments with antiproton induced reactions

Zhao-Qing Feng, Physical Review C 101, 064601 (2020); 93, 041601(R) (2016)

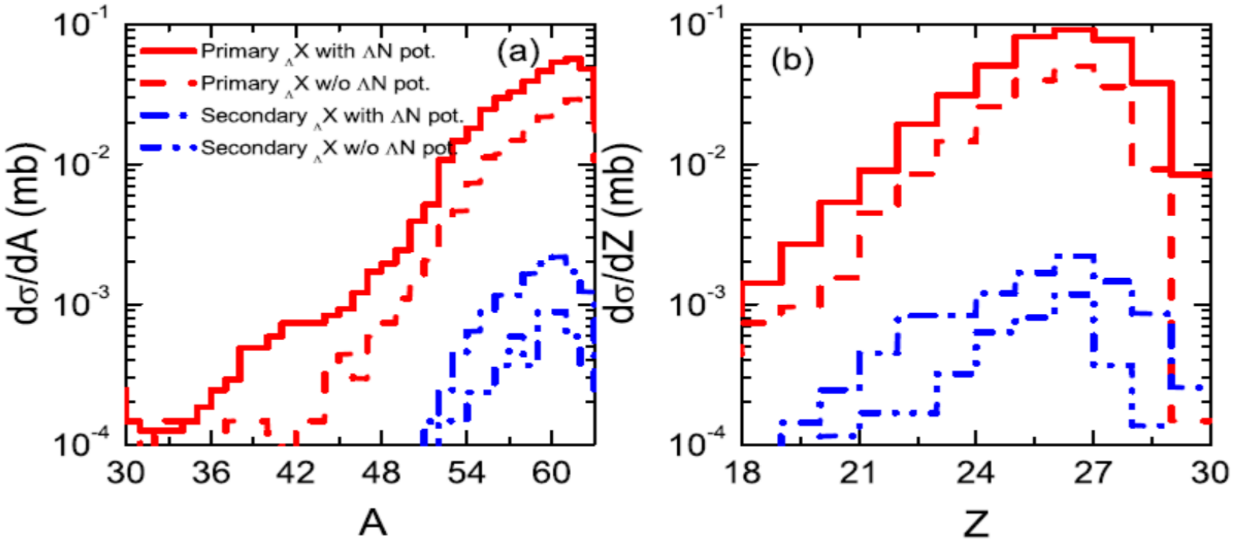

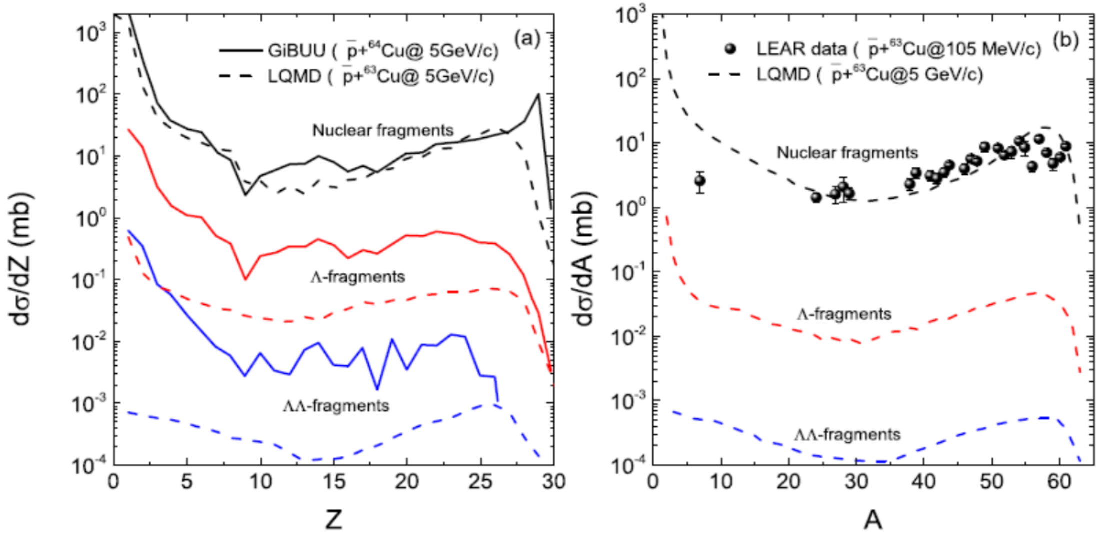

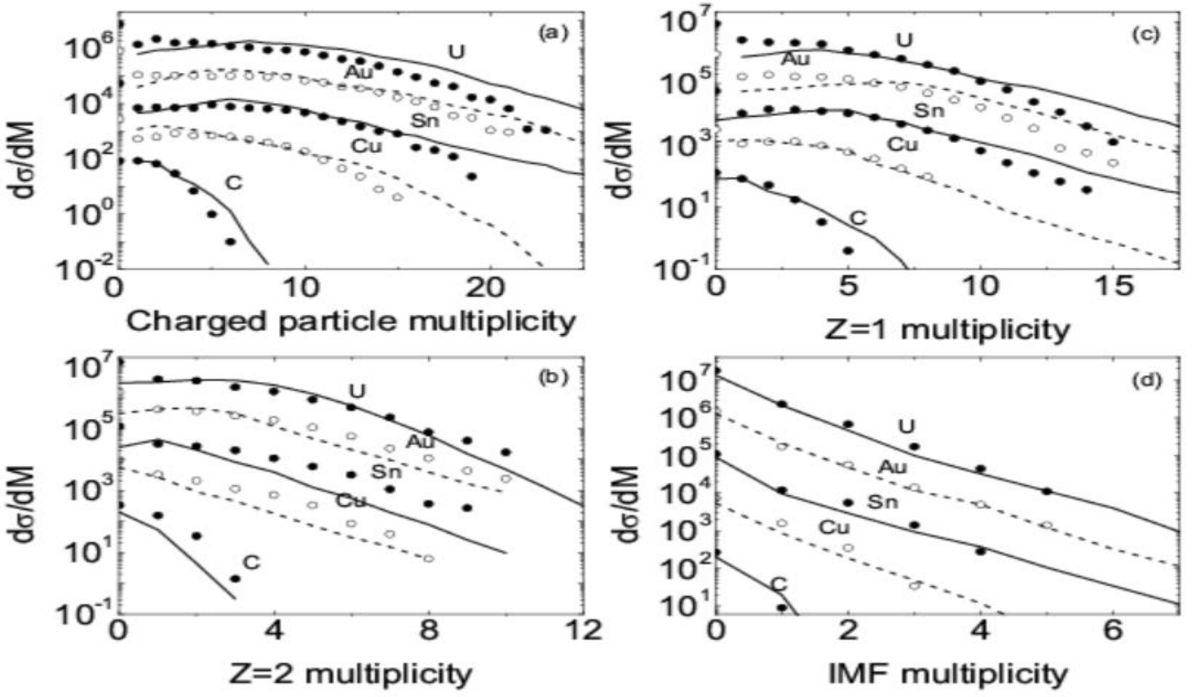

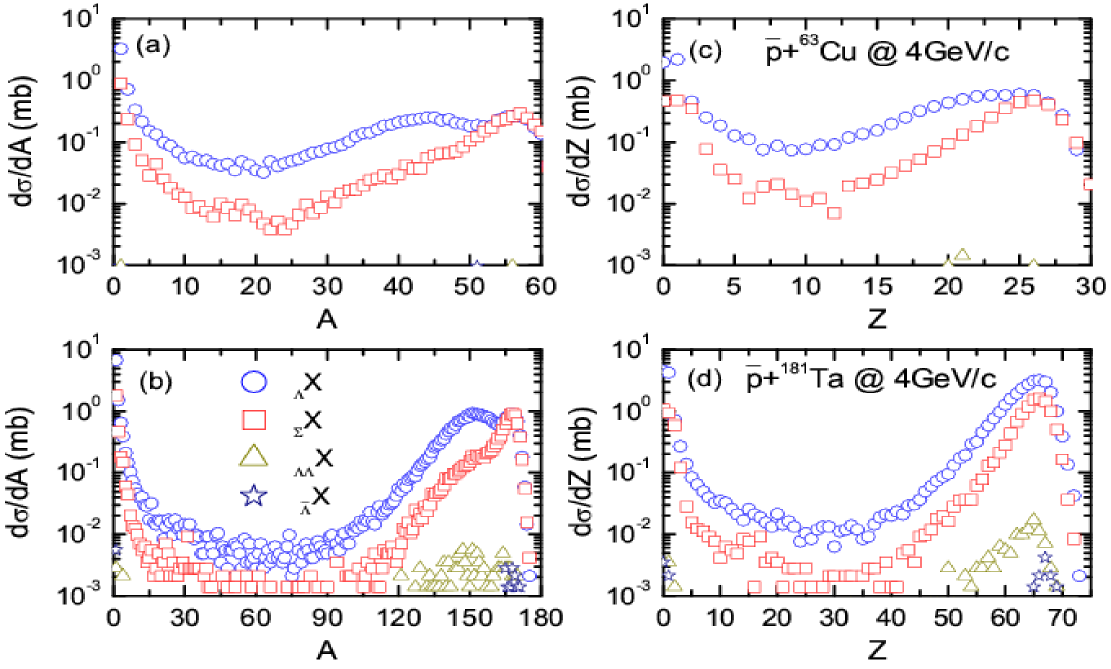

4) Kinetic approach for cluster production

P. Danielewicz, G. F. Bertsch, Nuclear Physics A 533 (1991) 712-748
Akira Ono, Prog. Part. Nucl. Phys. 105, 139-179 (2019)
R. Wang, Y. G. Ma, L. W. Chen et al., Phys. Rev. C 108, L031601 (2023)
Hui-Gan Cheng, Zhao-Qing Feng, Phys. Rev. C 109, L021602 (2024)

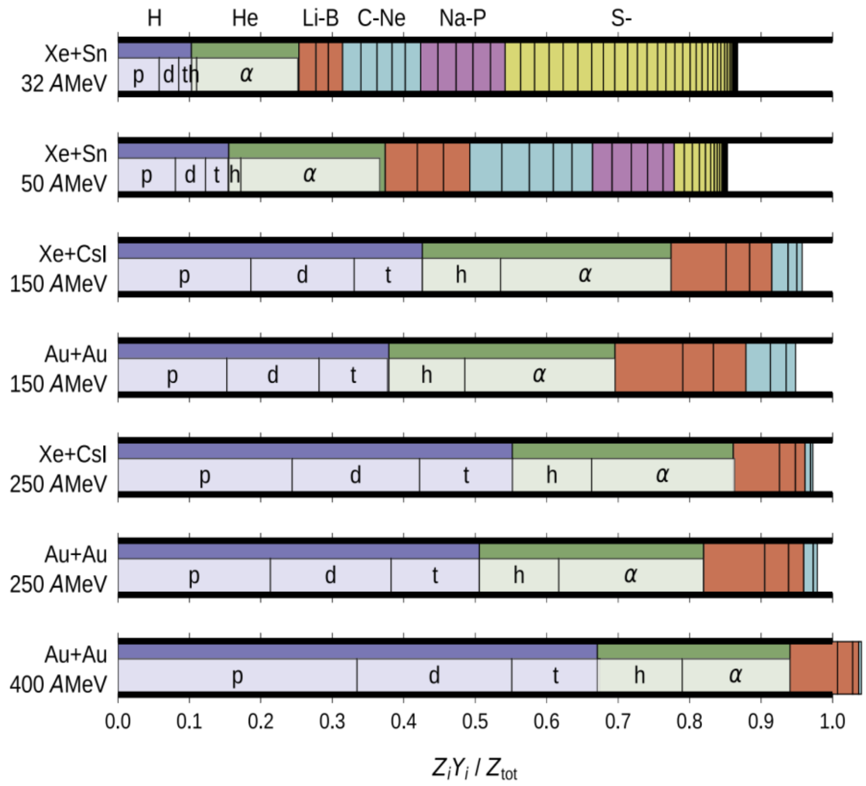

Year	models	Author(s)	Cluster(s)	Energy	Treatment(s)
1991	pBUU	P. Danielewicz et al.	d, t, h	fermi /intermediate energies	kinetic, Mott cut
2013	AMD-cluster	A. Ono	$2N, 3N, \alpha$	fermi /intermediate energies	kinetic, fermionic mean field
2021	SMASH	J. Staudenmaier et al.	d	GeV and higher	kinetic
2022	PHQMD	G. Coci et al.	d	GeV and higher	kinetic
2023	IBUU	R. Wang et al.	d, t, h, α	intermediate energies	kinetic, Mott cut
2023	LQMD	H. G. Cheng and Z. Q. Feng	d, t, h, α	fermi /intermediate energies	Kinetic, binding energy, Pauli effects

Clusters are produced by multinucleon or nucleon-cluster collisions

$$\frac{d\sigma}{d\Omega} = P(C_1 + C_2 \to C_3 + C_4) \times \frac{v_{\tilde{p}_{\rm rel}}}{v} \frac{\left|[\partial e(k)/\partial k]_{k=\tilde{p}_{\rm rel}}\right|}{\left|[\partial H(p_f)/\partial p_f]_{p_f=p_{\rm rel}}\right|} \frac{p_{\rm rel}^2}{\tilde{p}_{\rm rel}^2} \left[\frac{d\sigma_{\rm NN}}{d\Omega}\right]_{\tilde{p}_{\rm rel}}$$

$N_1+N_2 \leftrightarrow$ deuteron, $N_1+N_2+D_1 \to$ deuteron$+N'_1$, $N_1+N_2+N_3 \leftrightarrow$ triton (helium-3),
$N_1+N_2+N_3+D_1 \to$ triton (helium-3)$+N'_1$, $N_1+N_2+N_3+N_4 \leftrightarrow$ alpha
$p+\Lambda \leftrightarrow {}_{\Lambda}^{2}H$, $p+\Lambda+n \leftrightarrow {}_{\Lambda}^{3}H$, $p+\Lambda+n+n \leftrightarrow {}_{\Lambda}^{4}H$, $p+\Lambda+\Lambda \leftrightarrow {}_{\Lambda\Lambda}^{3}H$, $p+n+\Lambda+\Lambda \leftrightarrow {}_{\Lambda\Lambda}^{4}H$

…

III. LQMD transport model

兰州量子分子动力学模型 (LQMD)

Heavy-ion collisions (5 MeV – 5 GeV/nucleon) and hadron induced reaction (p, $\bar{p}$, π, K, e, etc)

- **LQMD transport model** (Skyrme interaction, Walecka model with σ, ω, ρ, δ)
- **Neutron star equation of state** (nuclear symmetry energy at sub- and supra- saturation densities in HICs, isospin splitting of nucleon effective mass from HICs, particle production, 2-body and 3-body potential, multi-body correlation)
- **In-medium effects of hadrons** (optical potentials, energy conservation and in-medium effects, i.e., Δ(1232), N*(1440), N*(1535)), hyperons (Λ,Σ,Ξ) and mesons (π,K,η,ρ,ω,ϕ…))
- **Kinetic production of (hyper)clusters and nuclear fragmentation reactions** (production cross section, phase-space distribution, collective flows, cluster transportation, Mott effect, e.g., deuteron, triton, ^{3}He, α, $_{\Lambda(\Sigma)}X$, $_{\Lambda\Lambda}X$, $_{\Xi}X$, $_{\bar{\Lambda}}X$)
- **Nuclear fusion near Coulomb barrier energies** (barrier distribution, neck dynamics, fusion cross section etc)
- **Hadron induced nuclear reactions** (spallation reaction, physics at PANDA such as hypernuclear, neutron skin thickness etc)

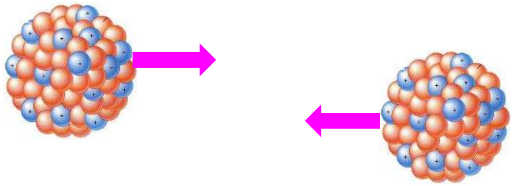

Transport models for heavy-ion collisions

Progress in Particle and Nuclear Physics 125 (2022) 103962

Contents lists available at ScienceDirect

Progress in Particle and Nuclear Physics

journal homepage: www.elsevier.com/locate/ppnp

Review

Transport model comparison studies of intermediate-energy heavy-ion collisions

Hermann Wolter [1,*], Maria Colonna [2], Dan Cozma [3], Pawel Danielewicz [4,5], Che Ming Ko [6], Rohit Kumar [4], Akira Ono [7], ManYee Betty Tsang [4,5], Jun Xu [8,9], Ying-Xun Zhang [10,11], Elena Bratkovskaya [12,13], Zhao-Qing Feng [14], Theodoros Gaitanos [15], Arnaud Le Fèvre [12], Natsumi Ikeno [16], Youngman Kim [17], Swagata Mallik [18], Paolo Napolitani [19], Dmytro Oliinychenko [20], Tatsuhiko Ogawa [21], Massimo Papa [2], Jun Su [22], Rui Wang [9,23], Yong-Jia Wang [24], Janus Weil [25], Feng-Shou Zhang [26,27], Guo-Qiang Zhang [9], Zhen Zhang [22], Joerg Aichelin [28], Wolfgang Cassing [25], Lie-Wen Chen [29], Hui-Gan Cheng [14], Hannah Elfner [12,13,20], K. Gallmeister [25], Christoph Hartnack [28], Shintaro Hashimoto [21], Sangyong Jeon [30], Kyungil Kim [17], Myungkuk Kim [31], Bao-An Li [32], Chang-Hwan Lee [33], Qing-Feng Li [24,34], Zhu-Xia Li [10], Ulrich Mosel [25], Yasushi Nara [35], Koji Niita [36], Akira Ohnishi [37], Tatsuhiko Sato [21], Taesoo Song [12], Agnieszka Sorensen [38,39], Ning Wang [11,40], Wen-Jie Xie [41], (TMEP collaboration)

Table 1
List of transport models that participated in the TMEP code comparisons discussed in this paper. The columns give the information on the name of the code, the main correspondents of the code, the energy range intended for the code, the treatment of effects of relativity (see Section 2.1), and the comparisons in which the code participated. The different comparisons are listed in the last column in the table by a numbers n, which refer to the subsections 3.n, where they are described in detail: n = 1 for Au+Au collisions around 1 AGeV, n = 2 for Au+Au collision at 100 and 400 AMeV, n = 3 for box-Vlasov, n = 4 for box-cascade with only nucleons, n = 5 for box-cascade with pion and Δ resonance production, and n = 6 for the prediction of pion ratios for Sn+Sn collisions.

BUU Type	Code Correspondents	Energy Range [A GeV]	Relativity	Comparisons
BLOB	P. Napolitani, M. Colonna	0.01–0.5	non-rel	2
BUU-VM	S. Mallik	0.02–1	rel	3,4,5
DJBUU	Y. Kim, S. Jeon, M. Kim, C.-H. Lee, K. Kim	0.05–2	cov	3
GiBUU	J. Weil, T. Gaitanos, K. Gallmeister, U. Mosel	0.05–40	rel/cov	1,2,3,4
IBL	W.J. Xie, F.S. Zhang	0.05–2	rel	2
IBUU	J. Xu, L.W. Chen, B.A. Li	0.05–2	rel	2,3,4,5
LBUU(LHV)	R. Wang, Z. Zhang, L.-W. Chen	0.01–1.5	rel	3
pBUU	P. Danielewicz	0.01–12	rel	1,2,3,4,5,6
PHSD	E. Bratkovskaya, W. Cassing	0.1–200	rel/cov	1,6
RBUU	T. Gaitanos	0.05–2	cov	1,2
RVUU	Z. Zhang, C.M. Ko, T. Song	0.05–2	cov	1,2,3,4,5
SMASH	D. Oliinychenko, H. Elfner, A. Sorensen	0.5–200	cov	3,4,5,6
SMF	M. Colonna, P. Napolitani	0.01–0.5	non-rel	2,3,4
χBUU	Z. Zhang, C.M. Ko	0.01–0.5	non-rel	6

QMD Type	Code Corespondents	Energy Range [AGeV]	Relativity	Comparisons
AMD	A. Ono	0.01–0.3	non-rel	2
AMD+JAM	N. Ikeno, A. Ono	0.01–0.3	non-rel+rel	6
BQMD/IQMD	A. Le Fèvre, J. Aichelin, C. Hartnack, R. Kumar	0.05–2	rel	1,2,6
CoMD	M. Papa	0.01–0.3	non-rel	2,4
ImQMD	Y.X. Zhang, N. Wang, Z.X. Li	0.02–0.4	rel	2,3,4
IQMD-BNU	J. Su, F.S. Zhang	0.05–2	rel	2,3,4,5,6
IQMD-SINAP	G.Q. Zhang	0.05–2	rel	2
JAM	A. Ono, N. Ikeno, Y. Nara, A. Ohnishi	1–158	rel	4,5
JQMD 2.0	T. Ogawa, K. Niita, S. Hashimoto, T. Sato	0.01–3	rel	4,5
LQMD(IQMD-IMP)	Z.Q. Feng, H.G. Cheng	0.01–10	rel	2,3,4,5
TuQMD/dcQMD	D. Cozma	0.1–2	rel	1,2,3,4,5,6
UrQMD	Y. J. Wang, Q. F. Li, Y. X. Zhang	0.05–200	rel	1,2,3,4,6

1. Lanzhou quantum molecular dynamics transport model (LQMD-Skyrme)

PHYSICAL REVIEW C 84, 024610 (2011)

Momentum dependence of the symmetry potential and its influence on nuclear reactions

Zhao-Qing Feng*
Institute of Modern Physics, Chinese Academy of Sciences, Lanzhou 730000, People's Republic of China

(Received 11 July 2011; published 19 August 2011)

$$H_B = \sum_i \sqrt{\mathbf{p}_i^2 + \mathbf{m}_i^2} + U_{\text{int}} + U_{\text{mom}}$$

$$U_{loc} = \int V_{loc}(\rho(\mathbf{r}))\, d\mathbf{r}$$

$$V_{loc}(\rho) = \frac{\alpha}{2}\frac{\rho^2}{\rho_0} + \frac{\beta}{1+\gamma}\frac{\rho^{1+\gamma}}{\rho_0^{\gamma}} + E_{sym}^{loc}(\rho)\rho\delta^2 + \frac{g_{sur}}{2\rho_0}(\nabla\rho)^2 + \frac{g_{sur}^{iso}}{2\rho_0}[\nabla(\rho_n - \rho_p)]^2,$$

$$U_{mom} = \frac{1}{2\rho_0}\sum_{i,j,j\neq i}\sum_{\tau,\tau'} C_{\tau,\tau'}\delta_{\tau,\tau_i}\delta_{\tau',\tau_j}\iiint d\mathbf{p}\,d\mathbf{p}'\,d\mathbf{r}\, f_i(\mathbf{r},\mathbf{p},t) \times [\ln(\epsilon(\mathbf{p}-\mathbf{p}')^2+1)]^2 f_j(\mathbf{r},\mathbf{p}',t).$$

Table 1: The parameters and properties of isospin symmetric EoS used in the LQMD model at the density of 0.16 fm^{-3}.

Parameters	α (MeV)	β (MeV)	γ	C_{mom} (MeV)	ϵ (c^2/MeV^2)	m^*_∞/m	K_∞ (MeV)
PAR1	-215.7	142.4	1.322	1.76	5×10^{-4}	0.75	230
PAR2	-226.5	173.7	1.309	0.	0.	1.	230

$$E_{sym}(\rho) = \frac{1}{3}\frac{\hbar^2}{2m}\left(\frac{3}{2}\pi^2\rho\right)^{2/3} + E_{sym}^{loc}(\rho) + E_{sym}^{mom}(\rho).$$

C_{sym}= 38 MeV
a_{sym}= 37.7 MeV
b_{sym}= -18.7 MeV

$$E_{sym}^{loc}(\rho) = \frac{1}{2}C_{sym}(\rho/\rho_0)^{\gamma_s} \qquad E_{sym}^{loc}(\rho) = a_{sym}(\rho/\rho_0) + b_{sym}(\rho/\rho_0)^2.$$

2. Covariant energy-density functional (LQMD.RMF)

Si-Na Wei, Zhao-Qing Feng,
Nuclear Science and Techniques 35, 15 (2024)
arXiv:2302.09984

$$
\begin{aligned}
L = &\bar{\psi}[i\gamma_\mu \partial^\mu - (M_N - g_\sigma \varphi - g_\delta \vec{\tau}\cdot\vec{\delta}) - g_\omega \gamma_\mu \omega^\mu - g_\rho \gamma_\mu \vec{\tau}\cdot\vec{b}^\mu]\psi \\
&+ \frac{1}{2}(\partial_\mu \varphi \partial^\mu \varphi - m_\sigma^2 \varphi^2) - U(\varphi) + \frac{1}{2}(\partial_\mu \vec{\delta}\partial^\mu \vec{\delta} - m_\sigma^2 \vec{\delta}^2) \\
&+ \frac{1}{2} m_\omega^2 \omega_\mu \omega^\mu - \frac{1}{4} F_{\mu\nu} F^{\mu\nu} + \frac{1}{2} m_\rho^2 \vec{b}_\mu \vec{b}^\mu - \frac{1}{4} \vec{G}_{\mu\nu} \vec{G}^{\mu\nu}
\end{aligned}
$$

$$
\begin{aligned}
F_{\mu\nu} &= \partial_\mu \omega_\nu - \partial_\nu \omega_\mu, \\
G_{\mu\nu} &= \partial_\mu \vec{b}_\nu - \partial_\nu \vec{b}_\mu, \\
U(\varphi) &= \frac{g_2}{3}\varphi^3 + \frac{g_3}{4}\varphi^4
\end{aligned}
$$

Energy density functional

$$
\varepsilon = \sum_{i=n,p} 2\int \frac{d^3k}{(2\pi)^3}\sqrt{k^2 + M_i^{*2}} + \frac{1}{2} m_\sigma^2 \varphi^2 + U(\varphi) + \frac{1}{2} m_\omega^2 \omega_0^2 + \frac{1}{2} m_\rho^2 b_0^2 + \frac{1}{2} m_\delta^2 \delta_3^2
$$

Temporal evolution in phase space

$$
\begin{aligned}
\dot{\mathbf{x}} = &\frac{\mathbf{p}_i^*}{p_0^*} + \sum_{i\neq j}^{N}\Big\{\frac{g_v^2}{2m_v^2} z_j^{*\mu} u_{i,\mu} B_i B_j \frac{\partial \rho_{ij}}{\partial \mathbf{p}_i} + \frac{g_v^2}{2m_v^2} z_i^{*\mu} u_{j,\mu} B_i B_j \frac{\partial \rho_{ji}}{\partial \mathbf{p}_i} + \frac{g_v^2}{2m_v^2} z_j^{*\mu} \rho_{ji} B_i B_j \frac{\partial u_{i,\mu}}{\partial \mathbf{p}_i} \\
&+ z_j^{*\mu}\frac{B_i B_j \bar{g}_v^2}{2m_v^2}\Big[\frac{\rho_{ij}}{1-p_{T,ij}^2/\Lambda_v^2}\frac{\partial u_{i,\mu}}{\partial \mathbf{p}_i} + \frac{u_{i,\mu}}{1-p_{T,ij}^2/\Lambda_v^2}\frac{\partial \rho_{ij}}{\partial \mathbf{p}_i} + u_{i,\mu}\rho_{ij}\frac{\partial[1/(1-p_{T,ij}^2/\Lambda_v^2)]}{\partial \mathbf{p}_i}\Big] \\
&+ z_i^{*\mu}\frac{B_i B_j \bar{g}_v^2}{2m_v^2}\Big[\frac{u_{j,\mu}}{1-p_{T,ji}^2/\Lambda_v^2}\frac{\partial \rho_{ji}}{\partial \mathbf{p}_i} + u_{j,\mu}\rho_{ji}\frac{\partial[1/(1-p_{T,ji}^2/\Lambda_v^2)]}{\partial \mathbf{p}_i}\Big] \\
&- \frac{m_j^*}{p_j^{*0}}\frac{\partial S_j}{\partial \mathbf{p}_i} - \frac{m_i^*}{p_i^{*0}}\frac{\partial S_i}{\partial \mathbf{p}_i}\Big\},
\end{aligned}
$$

$$
\begin{aligned}
\dot{\mathbf{p}} = &-\sum_{i\neq j}^{N}\Big\{\frac{g_v^2}{2m_v^2} z_j^{*\mu} u_{i,\mu} B_i B_j \frac{\partial \rho_{ij}}{\partial \mathbf{r}_i} + \frac{g_v^2}{2m_v^2} z_i^{*\mu} u_{j,\mu} B_i B_j \frac{\partial \rho_{ji}}{\partial \mathbf{r}_i} \\
&+ z_j^{*\mu}\frac{B_i B_j \bar{g}_v^2}{2m_v^2}\frac{u_{i,\mu}}{1-p_{T,ij}^2/\Lambda_v^2}\frac{\partial \rho_{ij}}{\partial \mathbf{r}_i} \\
&+ z_i^{*\mu}\frac{B_i B_j \bar{g}_v^2}{2m_v^2}\frac{u_{j,\mu}}{1-p_{T,ji}^2/\Lambda_v^2}\frac{\partial \rho_{ji}}{\partial \mathbf{r}_i} \\
&- \frac{m_j^*}{p_j^{*0}}\frac{\partial S_j}{\partial \mathbf{r}_i} - \frac{m_i^*}{p_i^{*0}}\frac{\partial S_i}{\partial \mathbf{r}_i}\Big\},
\end{aligned}
$$

TABLE I: Parameter sets for RMF. The saturation density ρ_0 is set to be 0.16 fm^{-3}. The binding energy of saturation density is $E/A - M_N = -16$ MeV. The isoscalar-vector ω and isovector-vector ρ masses are fixed to their physical values, $m_\omega = 783$ MeV and $m_\rho = 763$ MeV. The remaining meson mass m_σ is set to be 550 MeV.

model	g_σ	g_ω	g_2 (fm^{-1})	g_3	g_ρ	g_δ	K (MeV)	$E_{sym}(\rho_0)$ (MeV)	L (ρ_0)(MeV)
set1	8.145	7.570	31.820	28.100	4.049	-	230	31.6	85.3
set2	8.145	7.570	31.820	28.100	8.673	5.347	230	31.6	109.3
set3	8.145	7.570	31.820	28.100	11.768	7.752	230	31.6	145.0

Symmetry energy in LQMD.RMF

$$E_{sym} = \frac{1}{6}\frac{k_F^2}{E_F^*} + \frac{1}{2}\left[f_\rho - f_\delta\left(\frac{M^*}{E_F^*}\right)\right]\rho$$

$$f_{\rho,\delta} = g_{\rho,\delta}/m_{\rho,\delta}$$

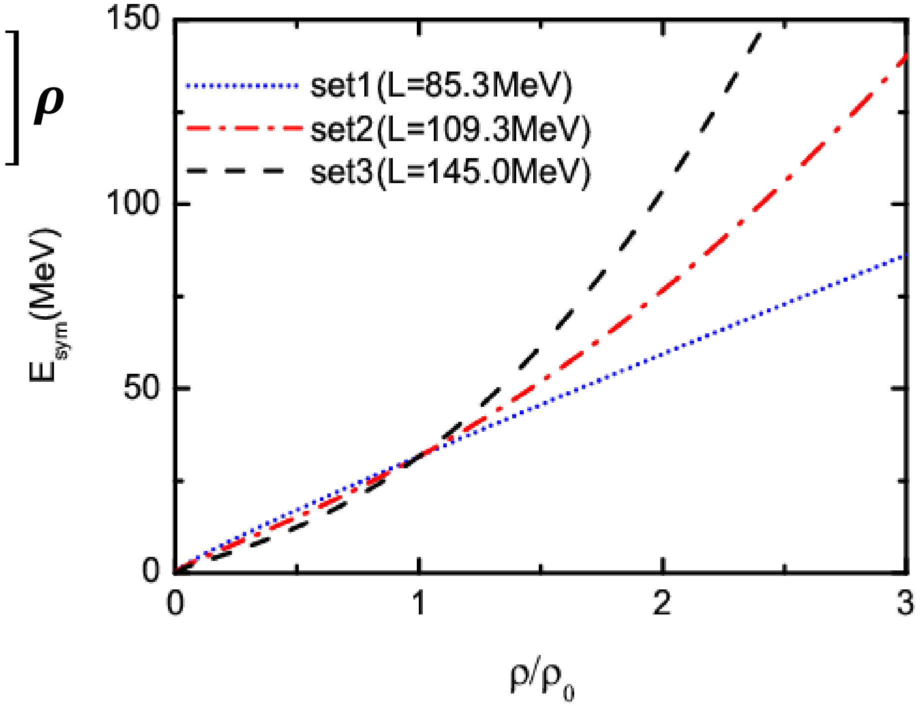

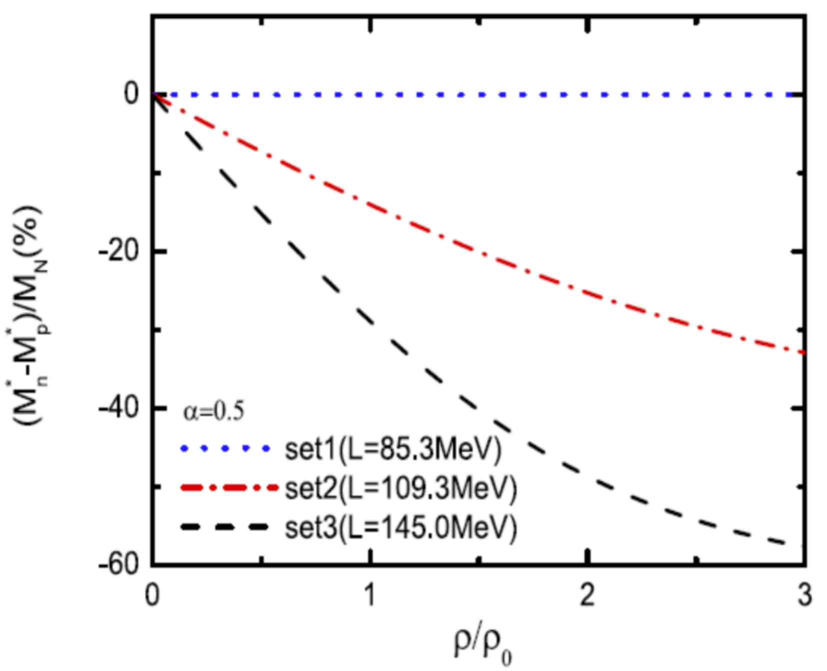

Results from LQMD.RMF calculation: collective flows for free protons

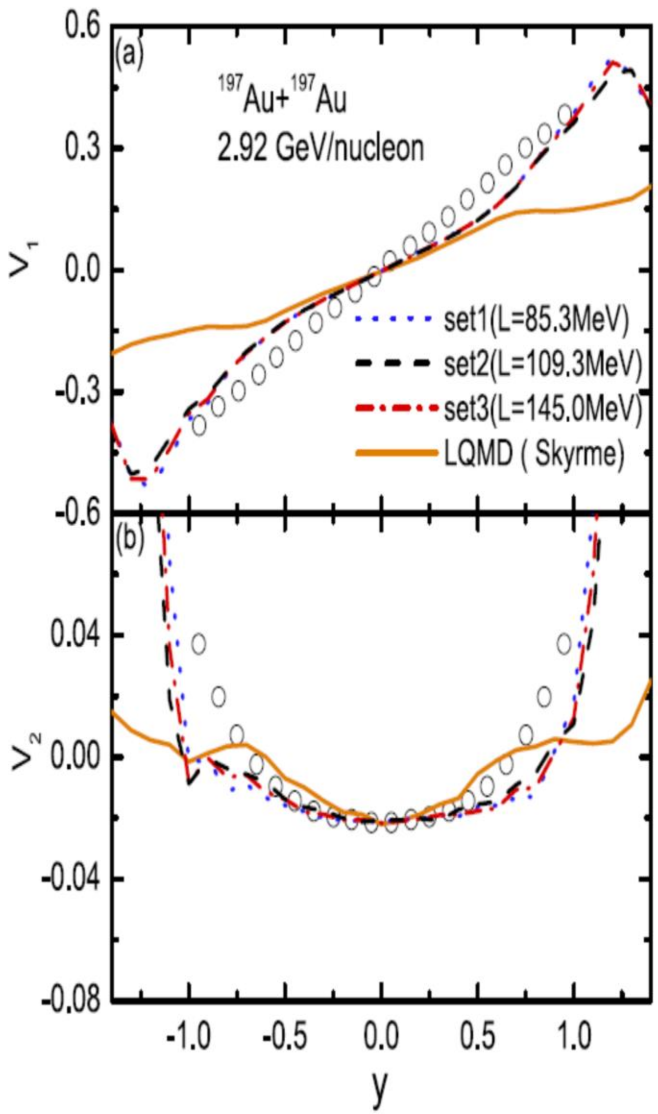

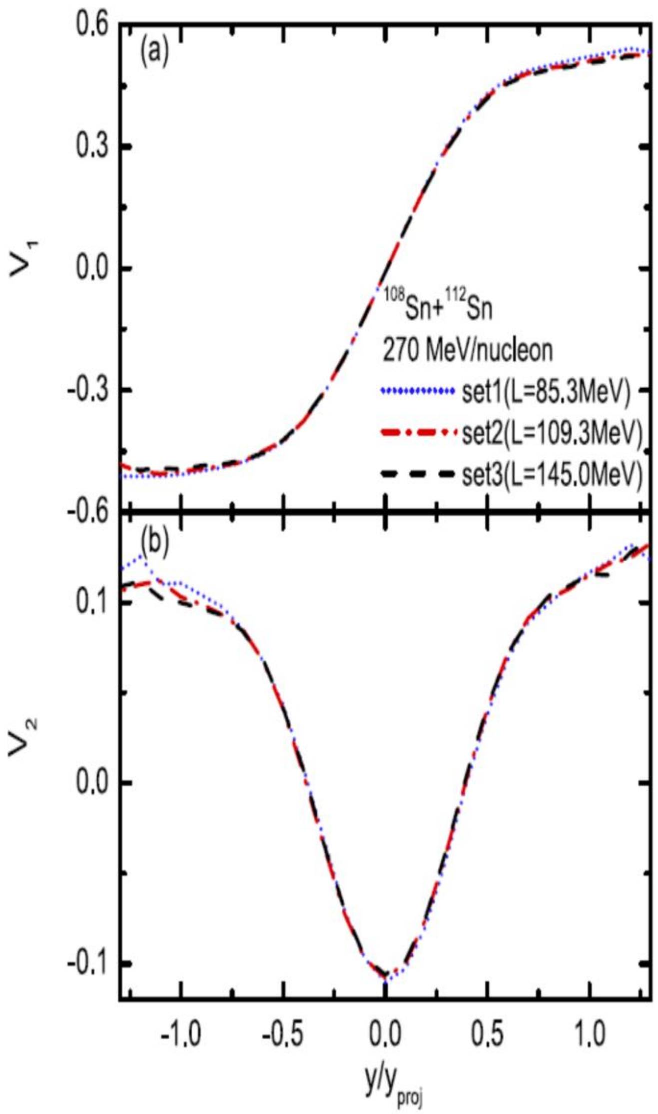

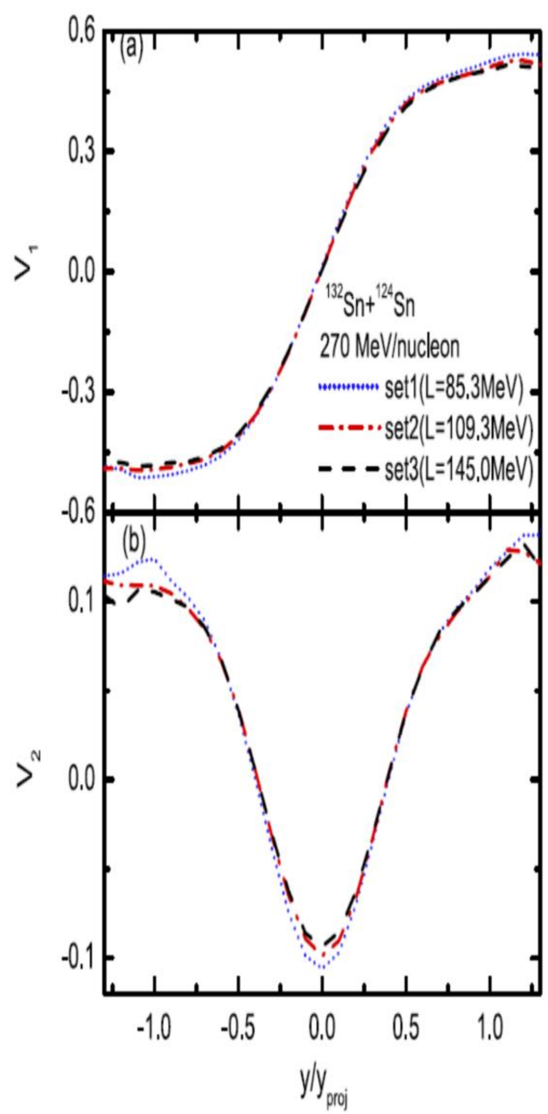

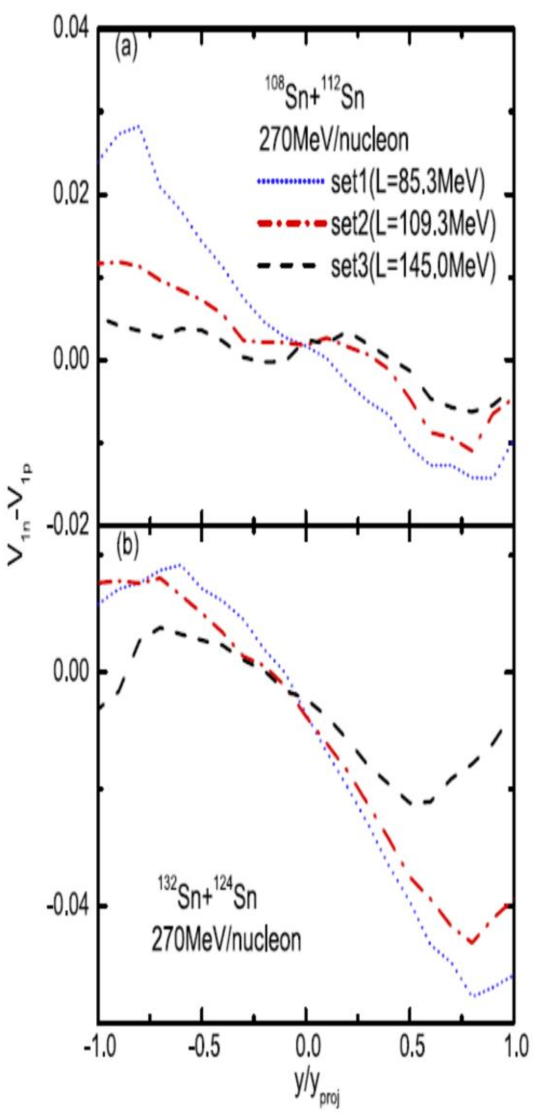

3. Particle production

π and resonances (Δ(1232), N*(1440), N*(1535), …) production:

$$NN \leftrightarrow N\Delta, \quad NN \leftrightarrow NN^*, \quad NN \leftrightarrow \Delta\Delta, \quad \Delta \leftrightarrow N\pi,$$
$$N^* \leftrightarrow N\pi, \quad NN \leftrightarrow NN\pi(s-state), \quad N^*(1535) \leftrightarrow N\eta$$

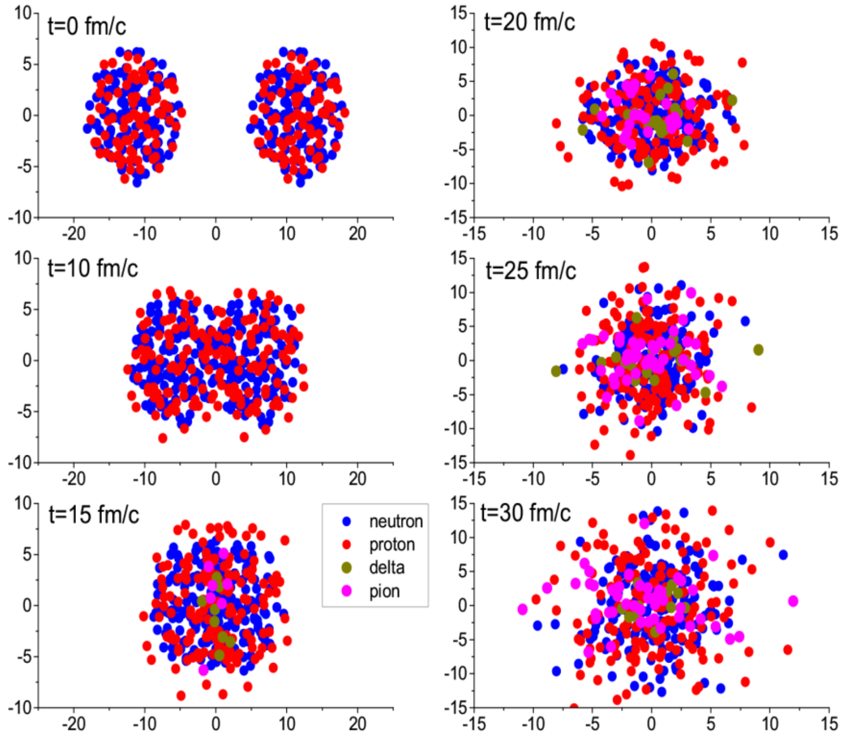

Collisions between resonances, NN*↔NΔ, NN*↔NN*

Strangeness channels:

$$BB \rightarrow BYK, BB \rightarrow BBK\overline{K}, B\pi(\eta) \rightarrow YK, YK \rightarrow B\pi,$$
$$B\pi \rightarrow NK\overline{K}, Y\pi \rightarrow B\overline{K}, \quad B\overline{K} \rightarrow Y\pi, \quad YN \rightarrow \overline{K}NN,$$
$$BB \rightarrow B\Xi KK, \overline{K}B \leftrightarrow K\Xi, YY \leftrightarrow N\Xi, \overline{K}Y \leftrightarrow \pi\Xi.$$

Reaction channels with antiproton:

$$\bar{p}N \rightarrow \overline{N}N, \quad \overline{N}N \rightarrow \overline{N}N, \overline{N}N \rightarrow \overline{B}B, \overline{N}N \rightarrow \overline{Y}Y$$
$$\overline{N}N \rightarrow \mathtt{annihilation}(\pi, \eta, \rho, \omega, K, \overline{K}, K^*, \overline{K}^*, \phi)$$

Statistical model with SU(3) symmetry for annihilation
(E.S. Golubeva et al., Nucl. Phys. A 537, 393 (1992))

The **PYTHIA** and **FRITIOF** code are used for baryon(meson)-baryon and antibaryon-baryon collisions at high invariant energies

4. hyperon-nucleon interaction in dense nuclear matter

$$H_Y = \sum_{i=1}^{N_Y} V_i^{Coul} + V_{opt}^Y(\boldsymbol{p}_i, \rho_i) + \sqrt{\boldsymbol{p}_i^2 + m_Y^2}$$

$$V_{opt}^Y(\boldsymbol{p}_i, \rho_i) = \omega_Y(\boldsymbol{p}_i, \rho_i) - \sqrt{\boldsymbol{p}_i^2 + m_Y^2}$$

$$\omega_Y(\boldsymbol{p}_i, \rho_i) = \sqrt{(m_Y + \Sigma_S^Y)^2 + \mathbf{p}_i^2} + \Sigma_V^Y,$$

Phenomenological potential by fitting
the results of chiral effective field theory

$$V_{opt}^{\Lambda}(\boldsymbol{p}_i, \rho_i) = V_a(\rho_i/\rho_0) + V_b(\rho_i/\rho_0)^2 + C_{mom}(\rho_i/\rho_0)\ln(\epsilon \boldsymbol{p}_i^2 + 1)$$

$$V_{opt}^{\Sigma}(\boldsymbol{p}_i, \rho_i) = V_0(\rho_i/\rho_0)^{\gamma_s} + V_1(\rho_n - \rho_p)t_{\Sigma}\rho_i^{\gamma_s -} + C_{mom}(\rho_i/\rho_0)\ln(\epsilon \boldsymbol{p}_i^2 + 1).$$

Phys. Lett. B 851 (2024) 138580

Contents lists available at ScienceDirect

Physics Letters B

journal homepage: www.elsevier.com/locate/physletb

Letter

Extracting the hyperon-nucleon interaction via collective flows in heavy-ion collisions

Zhao-Qing Feng

School of Physics and Optoelectronics, South China University of Technology, Guangzhou 510640, China

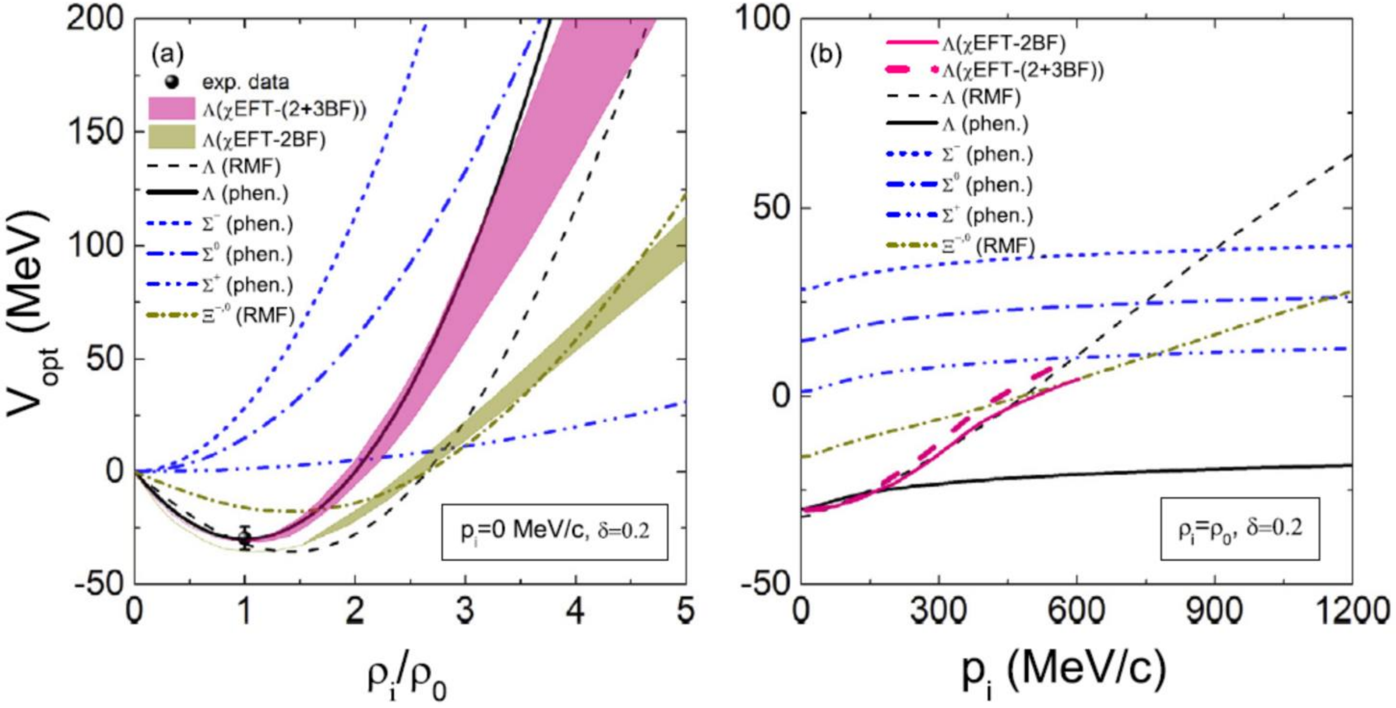

Extracting the hyperon-nucleon interaction via collective flows in heavy-ion collisions

Phys. Lett. B 851 (2024) 138580

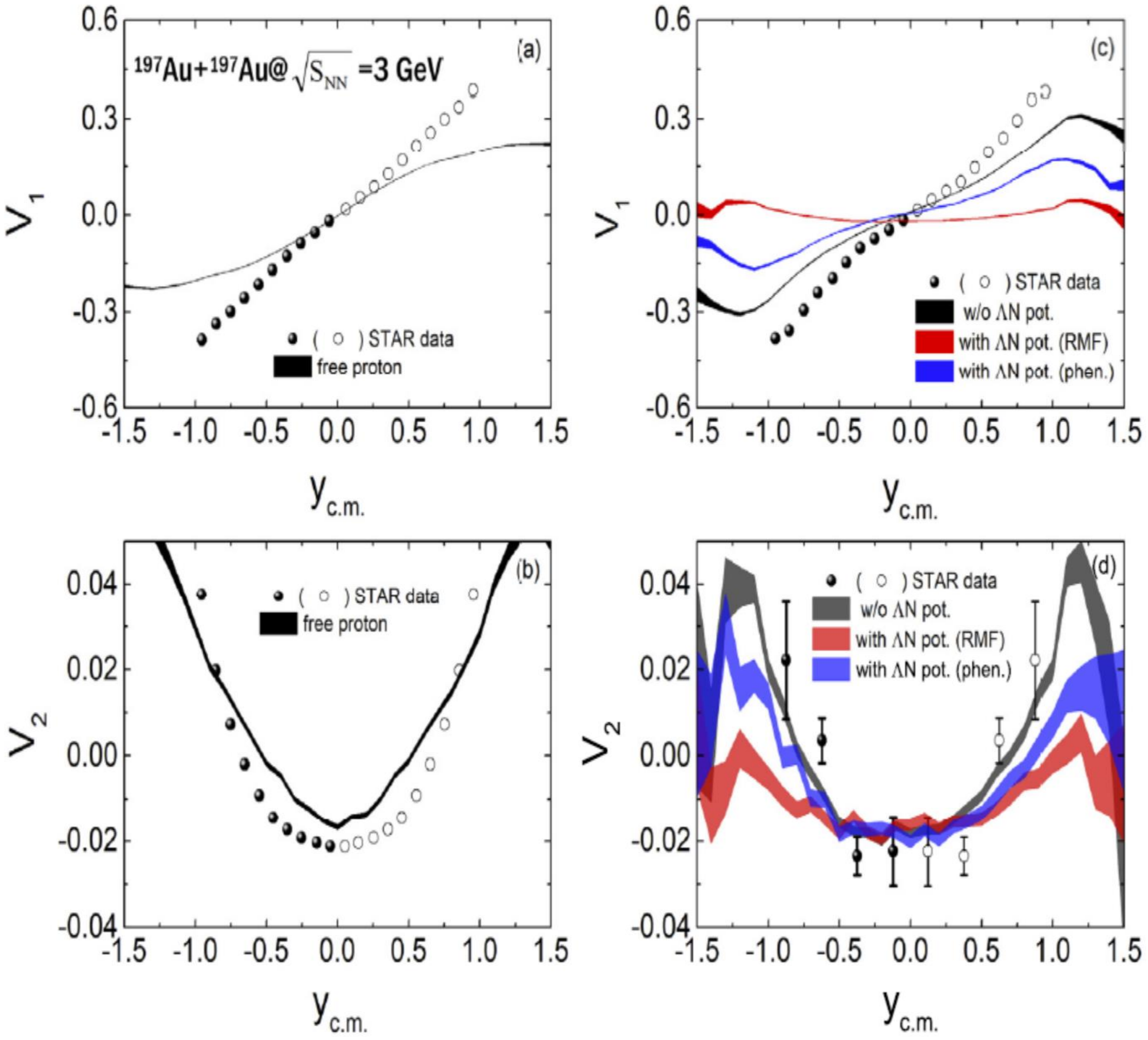

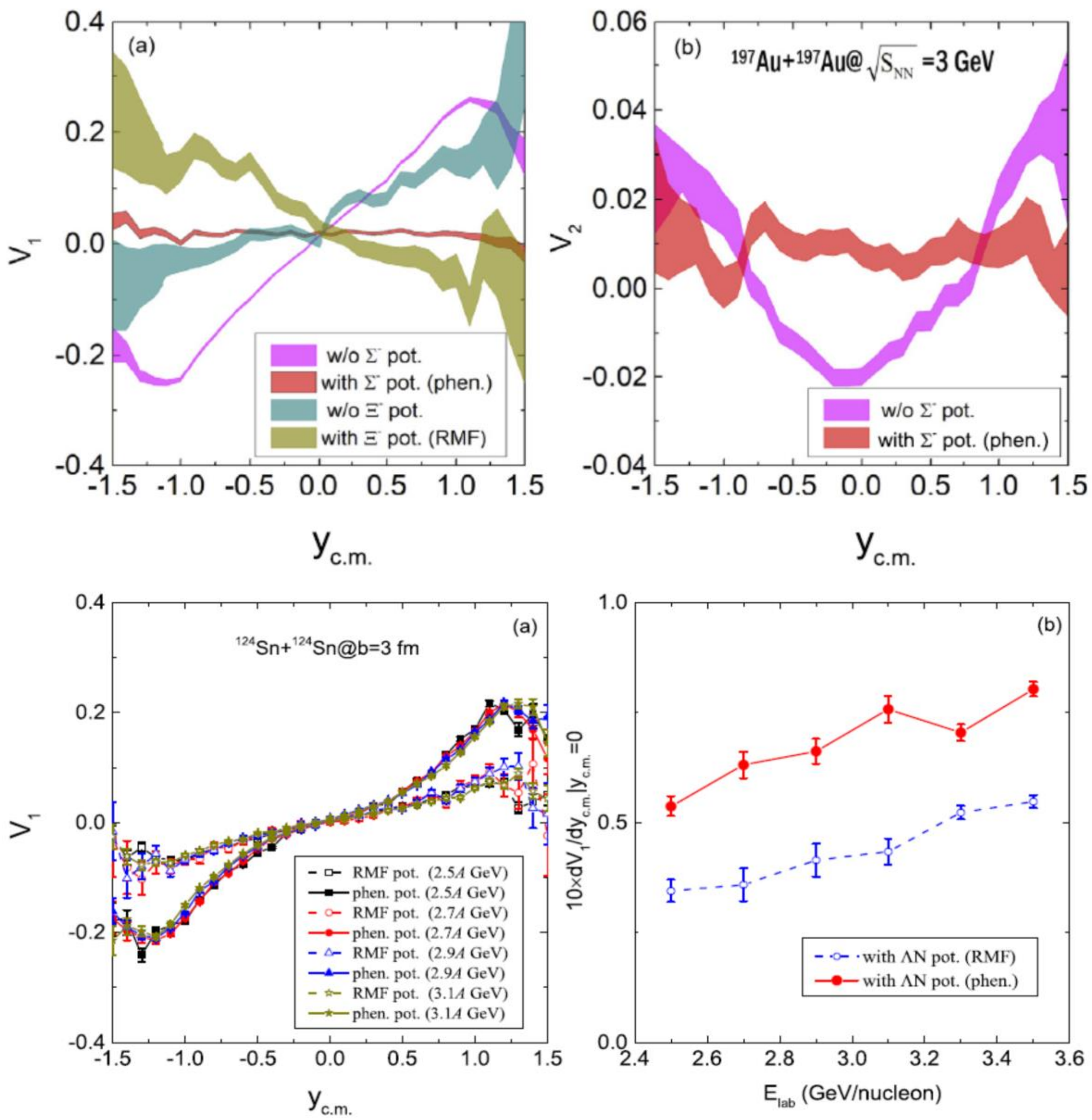

Correlation of the hyperon potential stiffness with hyperon constituents in neutron stars and heavy-ion collisions

Si-Na Wei, Zhao-Qing Feng, Wei-Zhou Jiang, PLB (accepted)

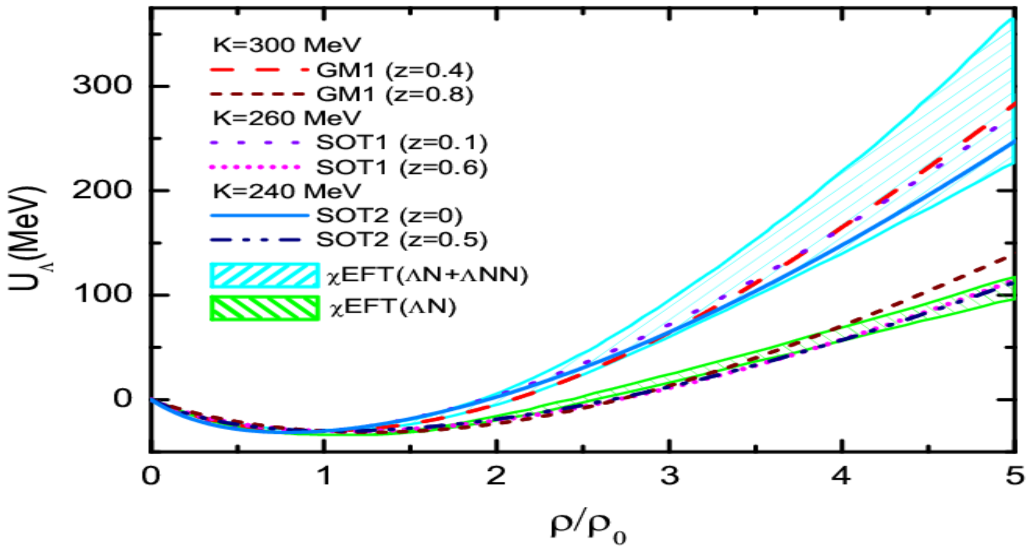

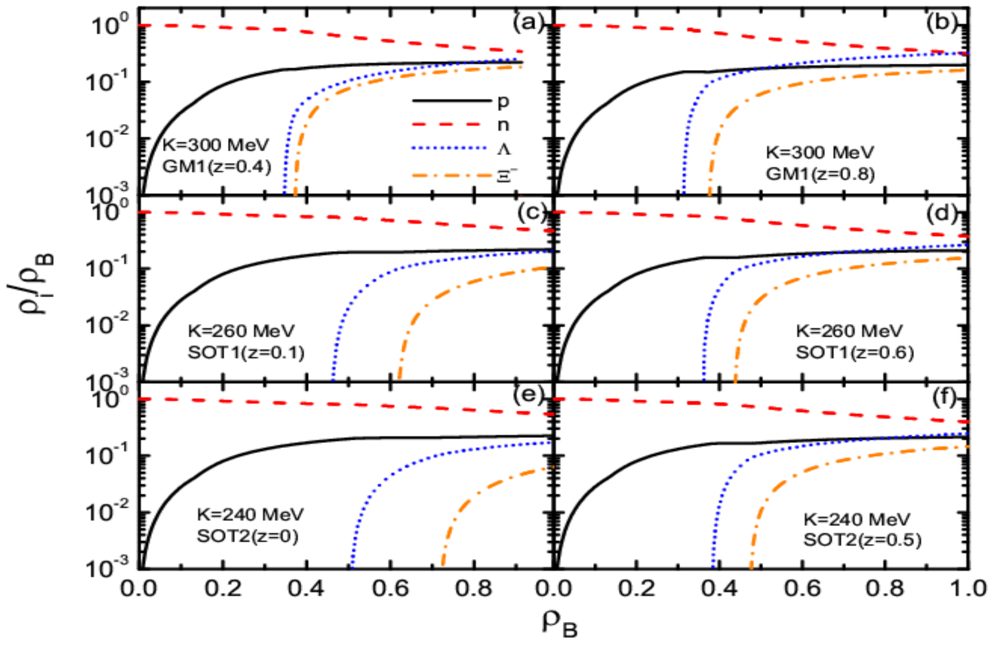

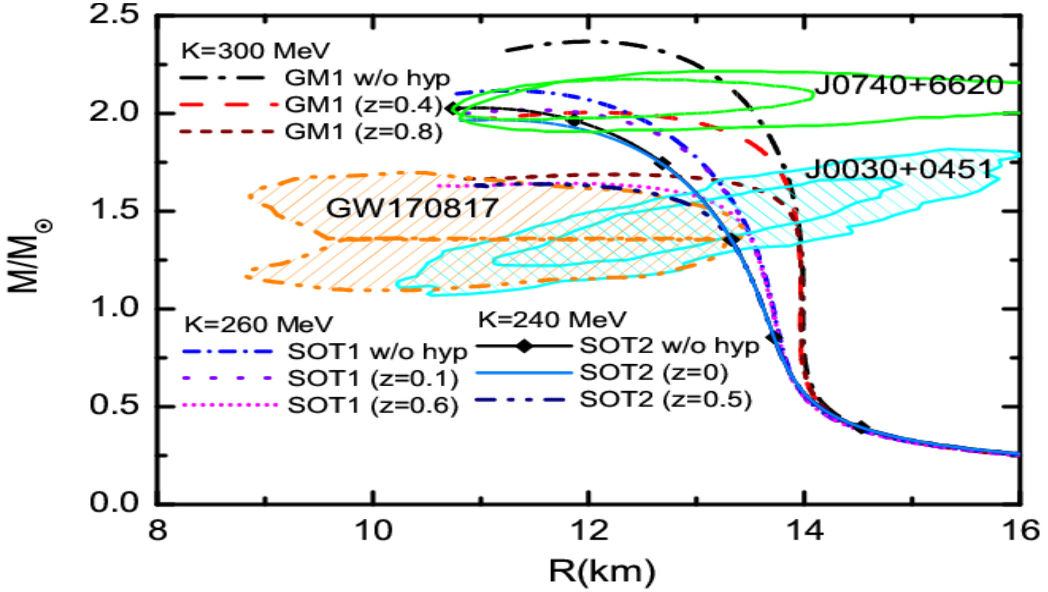

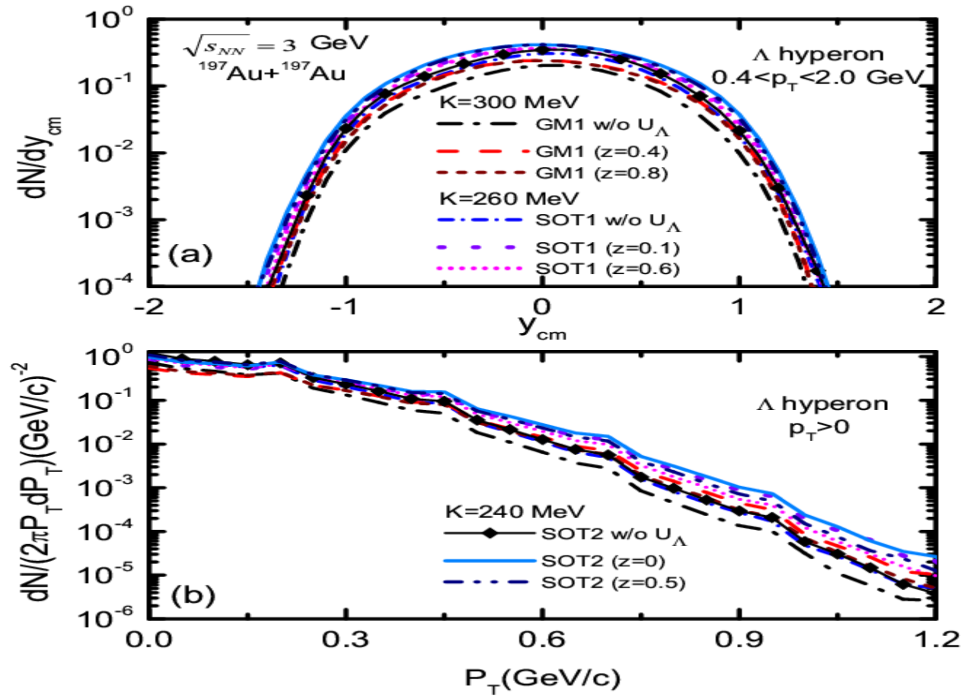

High-density symmetry energy from hyperon production in heavy-ion collisions, Physics Letters B 846 (2023) 138180

Contents lists available at ScienceDirect
Physics Letters B
journal homepage: www.elsevier.com/locate/physletb

Probing the high-density symmetry energy from subthreshold hyperon production in heavy-ion collisions

Zhao-Qing Feng
School of Physics and Optoelectronics, South China University of Technology, Guangzhou 510640, China

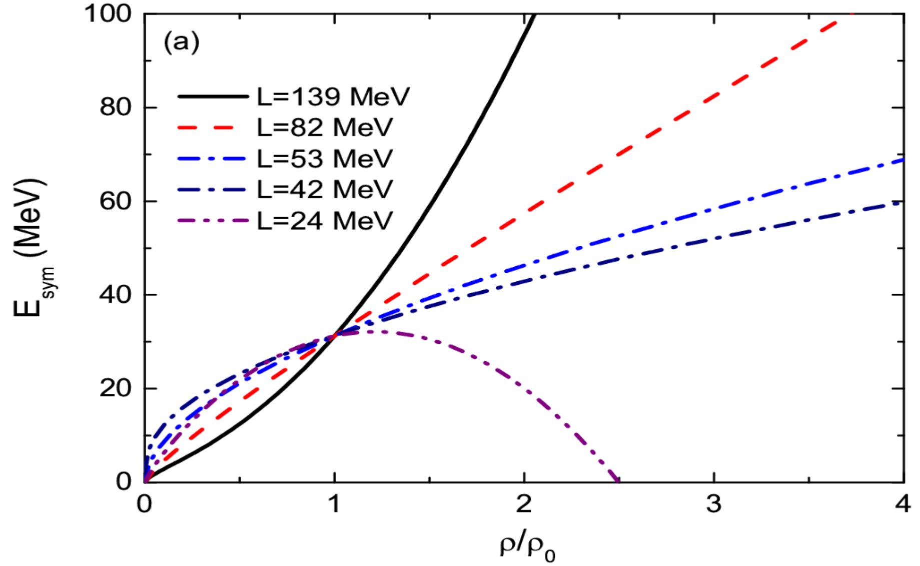

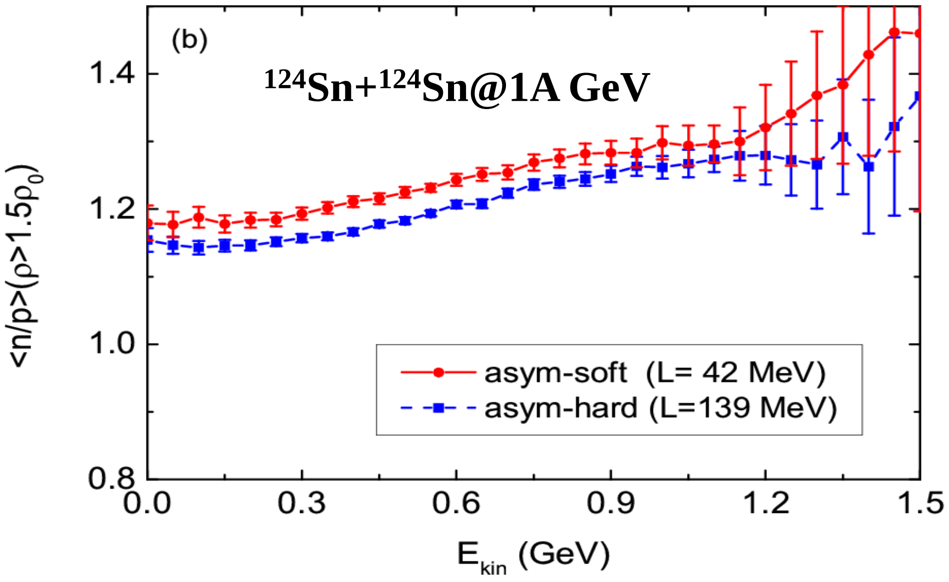

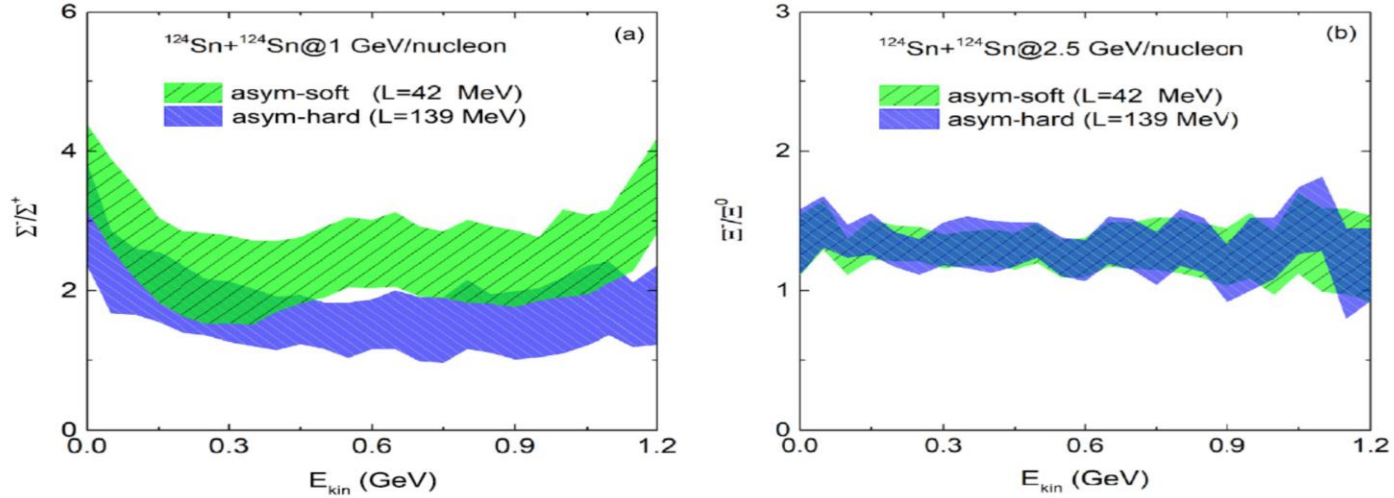

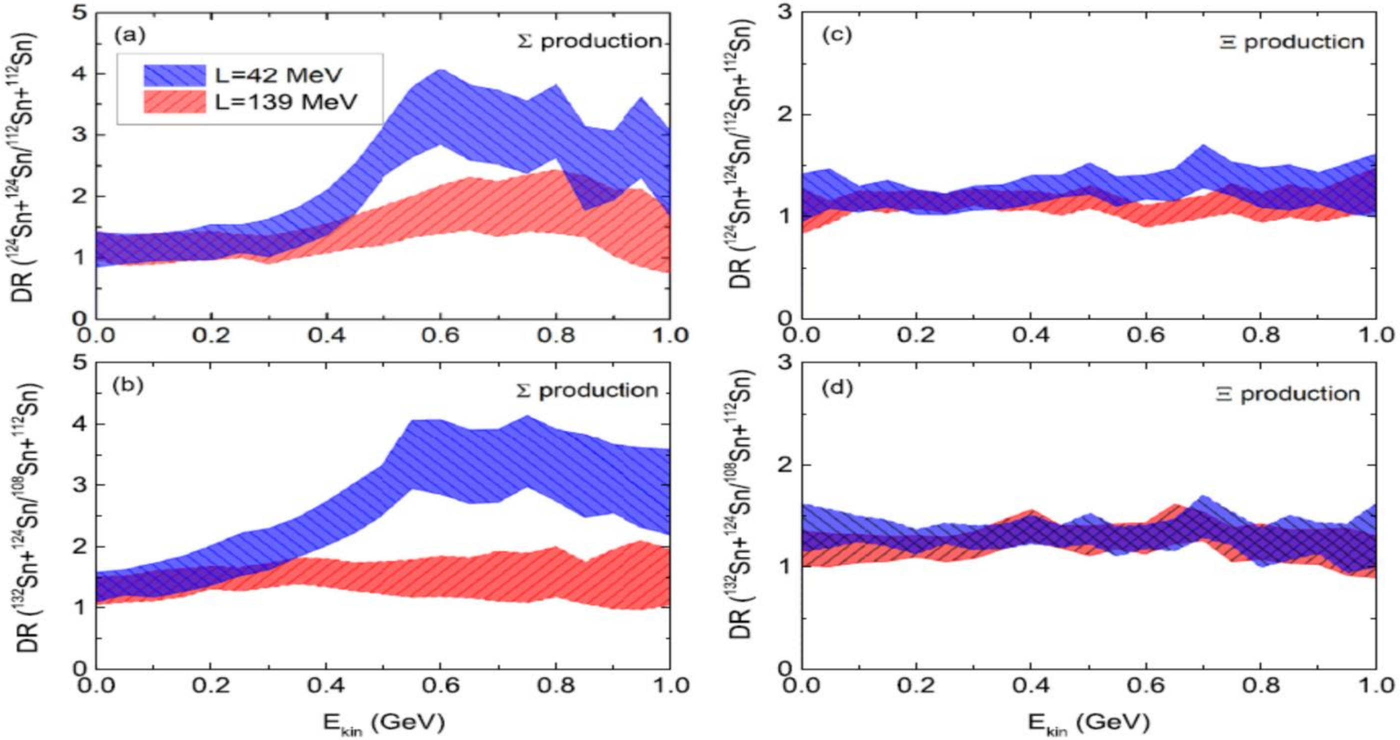

IV. Nuclear cluster and hypercluster production in HICs

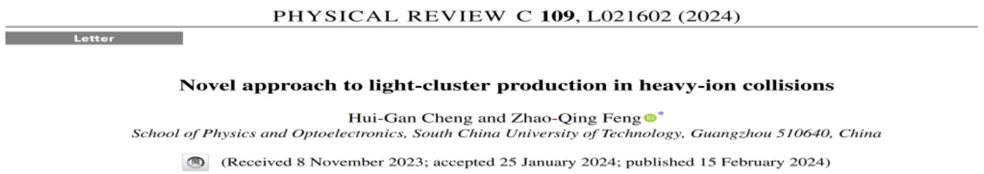
PHYSICAL REVIEW C **109**, L021602 (2024)

Letter

Novel approach to light-cluster production in heavy-ion collisions

Hui-Gan Cheng and Zhao-Qing Feng

School of Physics and Optoelectronics, South China University of Technology, Guangzhou 510640, China

(Received 8 November 2023; accepted 25 January 2024; published 15 February 2024)

Kinetic approach for cluster production

$$
\begin{aligned}
H &= \sum_i \frac{\mathbf{p}_i^{\,2}}{2m} + \frac{\alpha}{2}\sum_{\substack{i,j\\ j\neq i}} \frac{\rho_{ij}}{\rho_0} + \frac{\beta}{1+\gamma}\sum_i\left(\sum_{j,j\neq i}\frac{\rho_{ij}}{\rho_0}\right)^{\gamma} \\
&+ \frac{C_{sym}}{2}\sum_{\substack{i,j\\ j\neq i}} t_{z_i} t_{z_j}\frac{\rho_{ij}}{\rho_0} + \frac{g_{sur}}{2}\sum_{\substack{i,j\\ j\neq i}}{}' \left[\frac{3}{2L} - \left(\frac{\mathbf{r}_i-\mathbf{r}_j}{2L}\right)^2\right]\frac{\rho_{ij}}{\rho_0} \\
&+ \sum_i^{N_C} E^i_{\mathrm{z.p.}} + \sum_i^{N_d} V_{\mathrm{corr}} e^{-r_i^{\,2}/4L}
\end{aligned}
$$

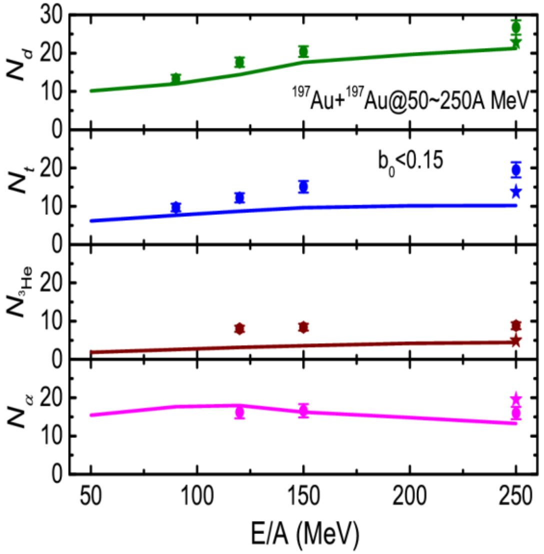

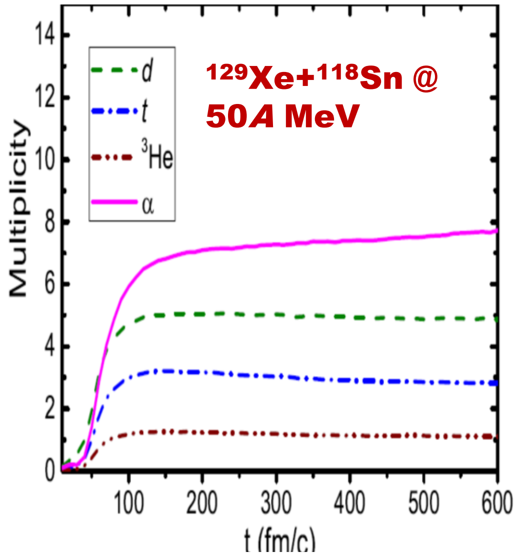


华南理工大学
South China University of Technology

博士学位论文

中高能区重离子碰撞中结团产生机制研究

作者姓名	程辉淦
学科专业	物理学
指导教师	冯兆庆教授
所在学院	物理与光电学院
论文提交日期	2023 年 10 月 16 日

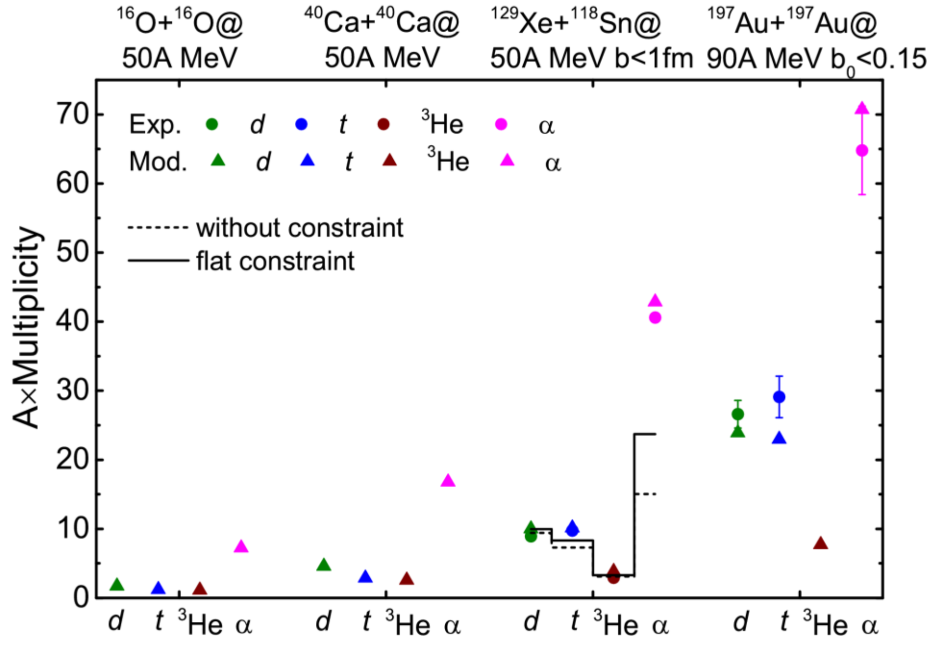

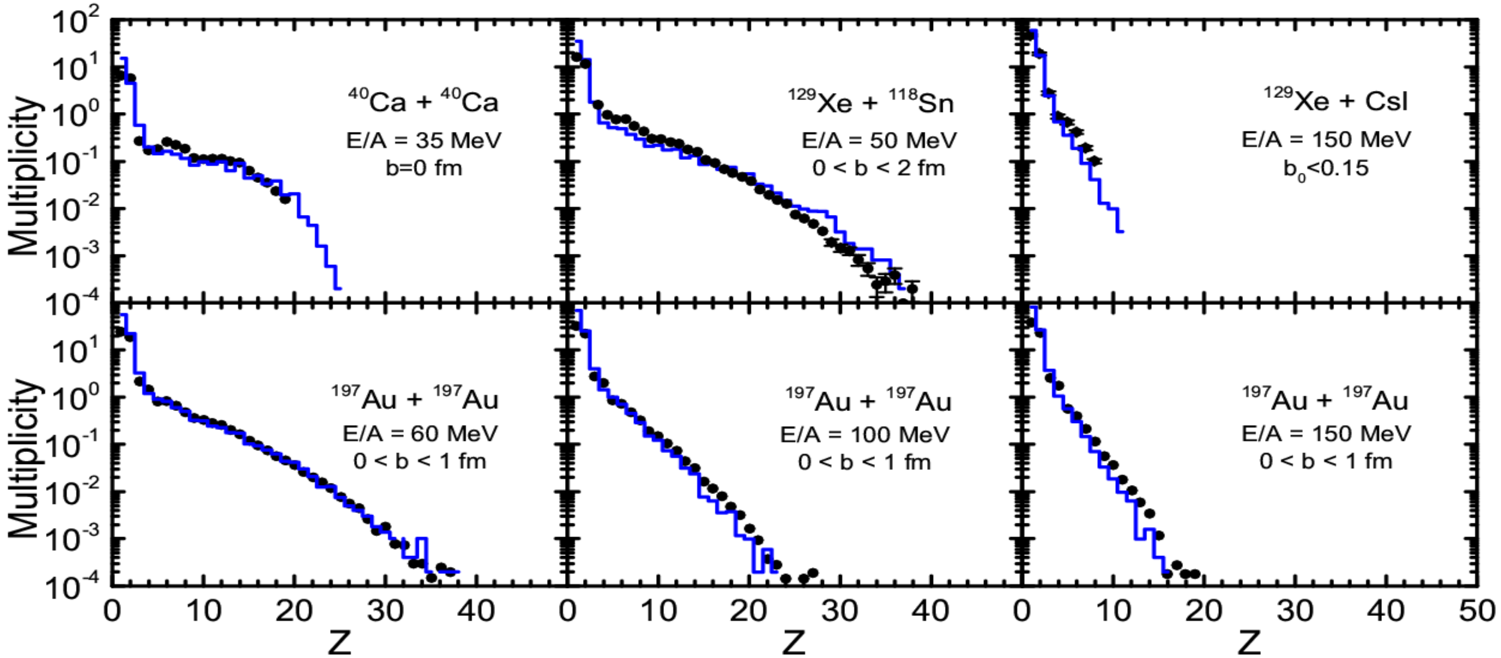

Collective flows (d, t, ^{3}He, α) *(Wigner density approach)*

Heng-Jin Liu, Hui-Gan Cheng, ZQF, Physical Review C 108, 024614 (2023)

HADES Collaboration, Phys. Rev. Lett. 125, 262301 (2020)

$$\frac{dN}{N_0 d\phi}(y, p_t) = 1 + 2v_1(y, p_t)\cos(\phi) + 2v_2(y, p_t)\cos(2\phi) + 2v_3(y, p_t)\cos(3\phi) + 2v_4(y, p_t)\cos(4\phi)$$

$$p_t = \sqrt{p_x^2 + p_y^2} \qquad y = \frac{1}{2}\ln\frac{E+p_z}{E-p_z}$$

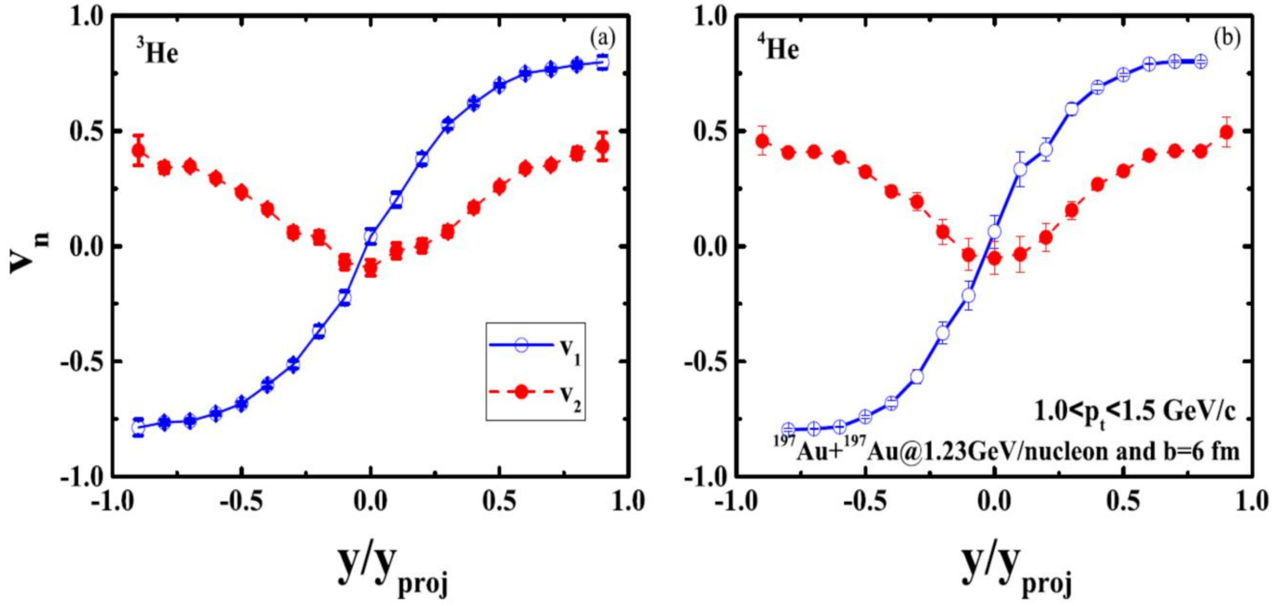

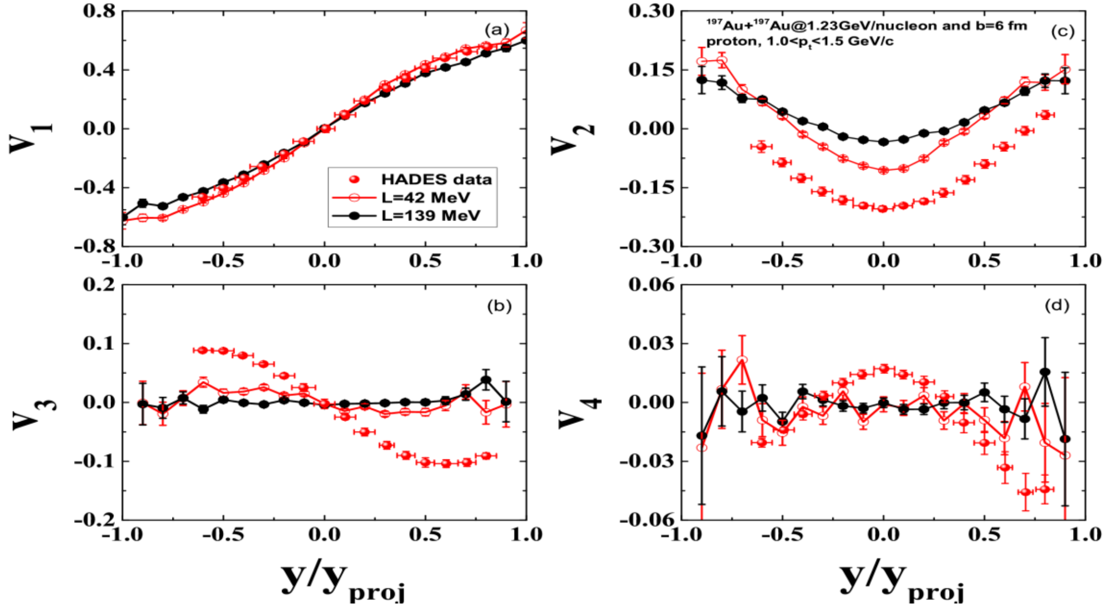

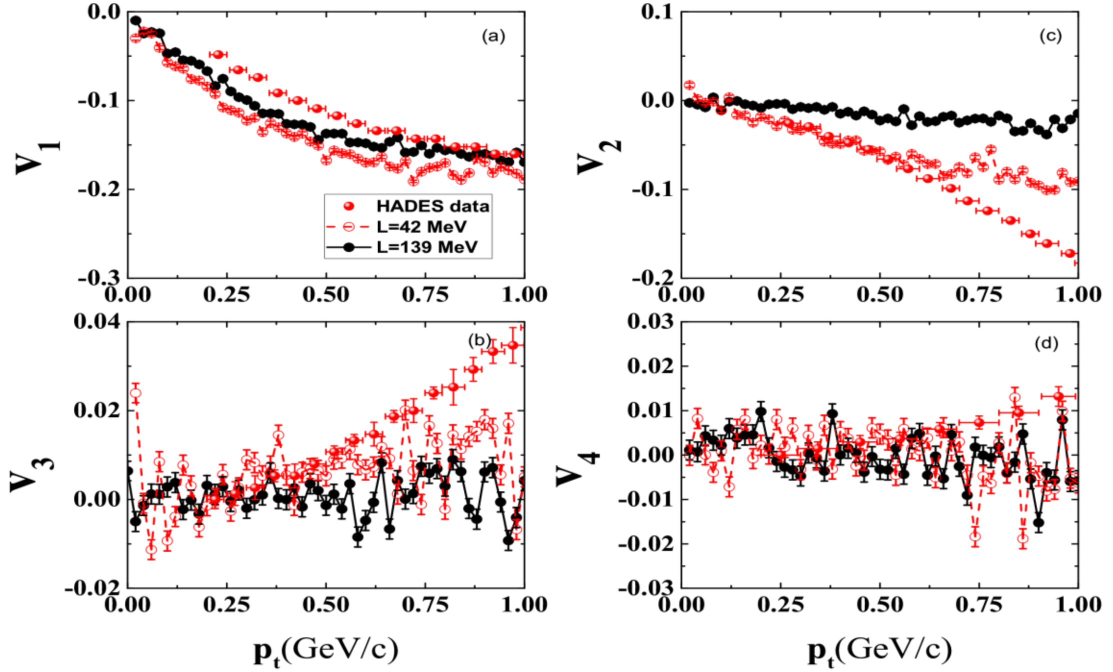

Hypernuclide production via HICs *(Wigner density approach)*

$^{124}Sn+^{124}Sn@2A$ GeV

Z. Q. Feng, Phys. Rev. C 102, 044604 (2020)

Data: C. Rappold et al., (HypHI collaboration)

Phys. Lett. B 747, 129 (2015)

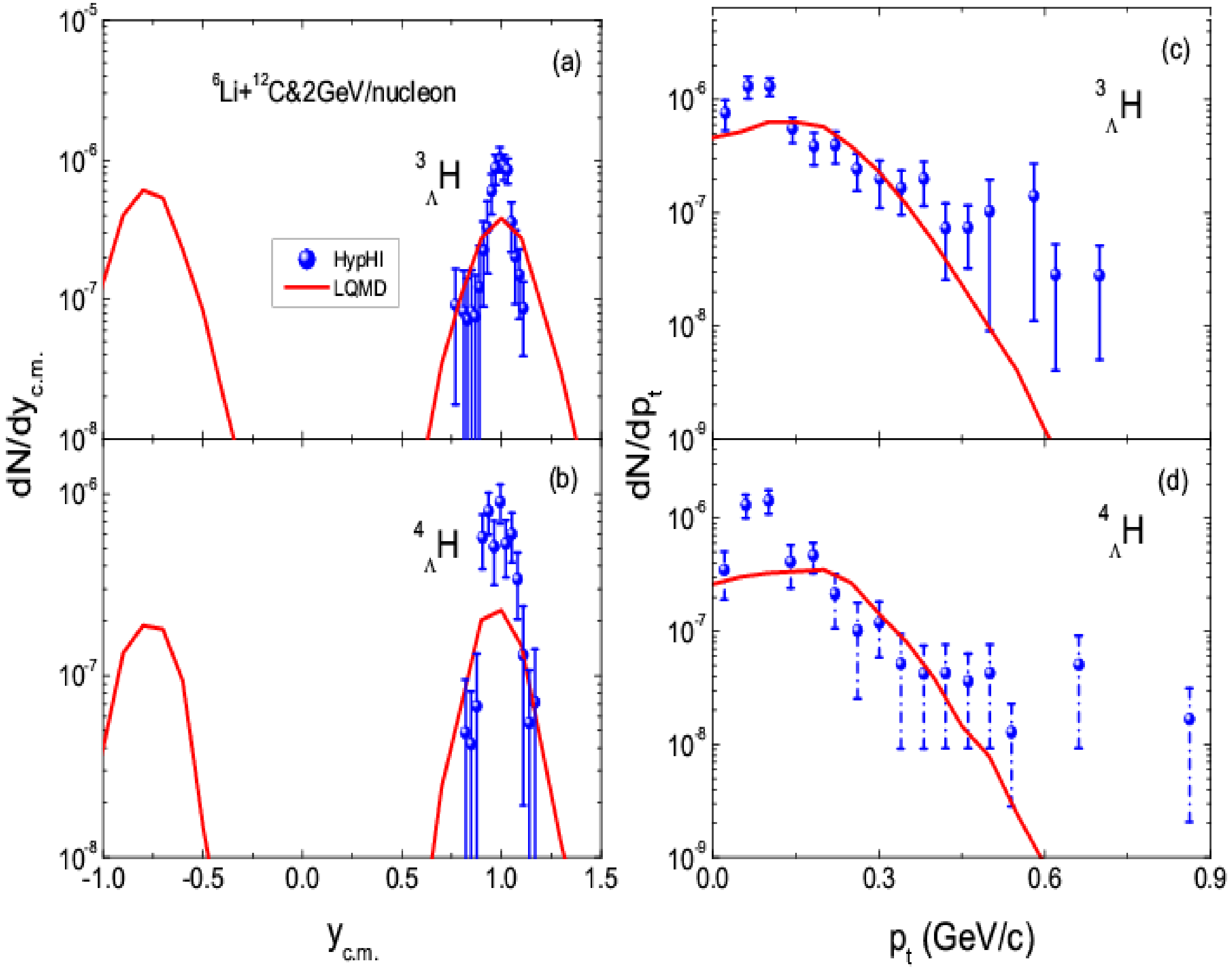

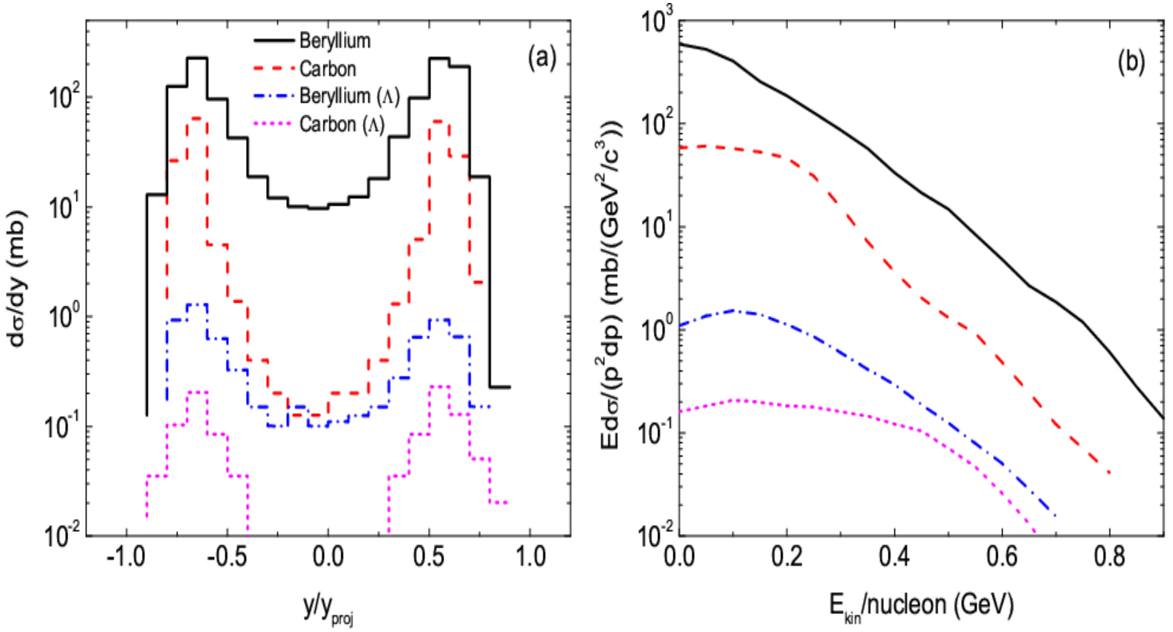

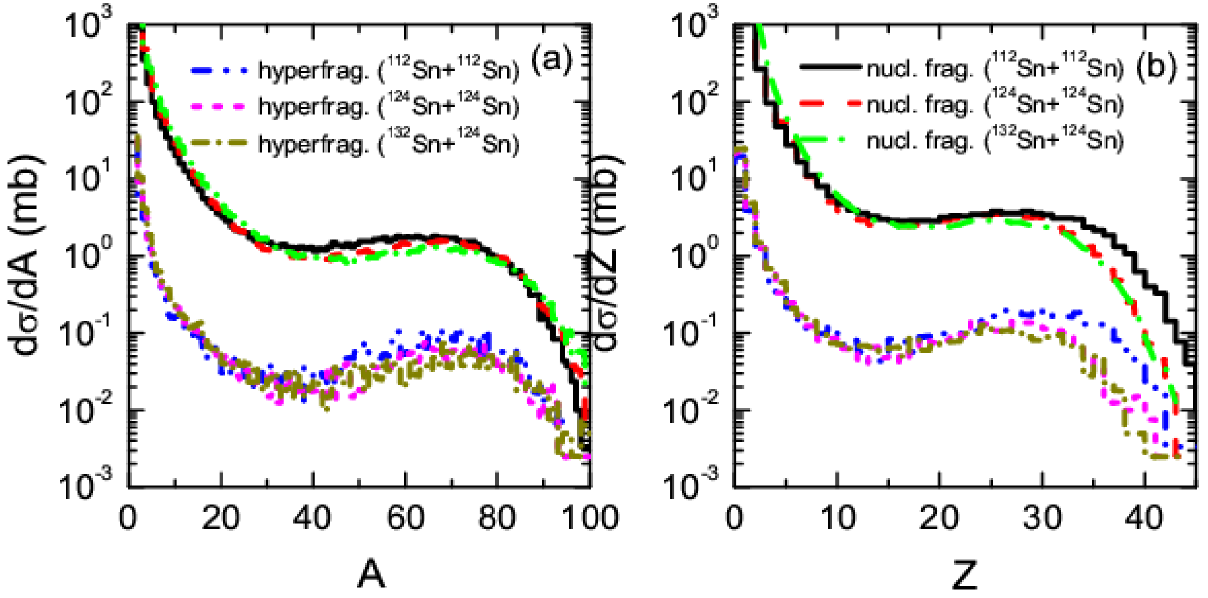

Multi-strangeness hypernuclide production

H.G. Cheng, Z. Q. Feng, Phys. Lett. B 824 (2022) 136849

^{197}Au+^{197}Au@3A GeV

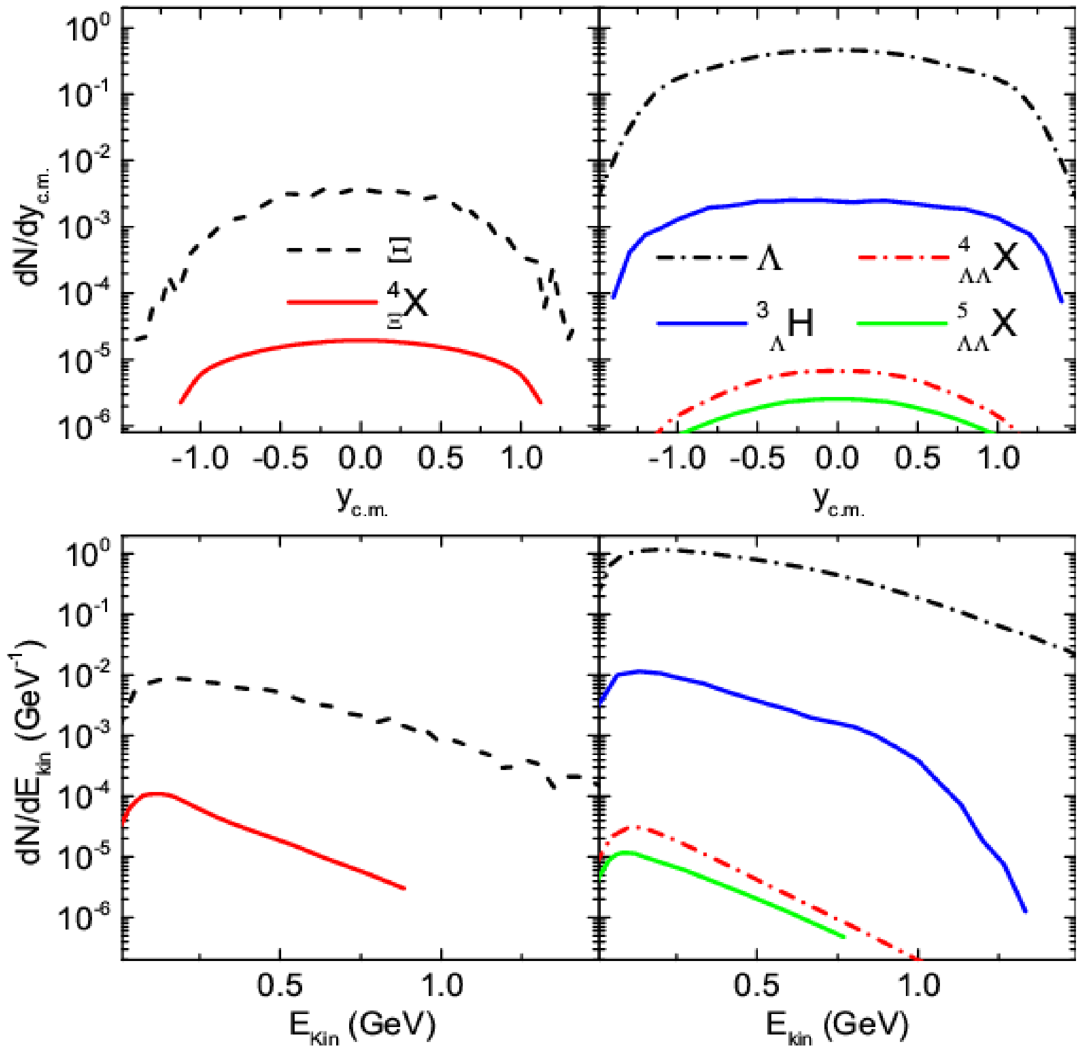

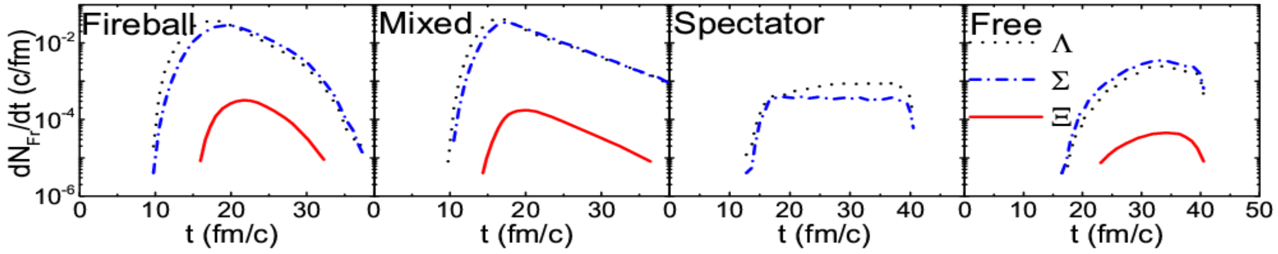

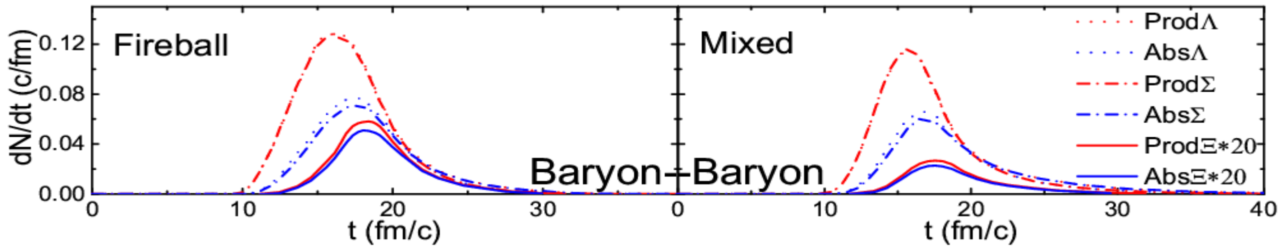

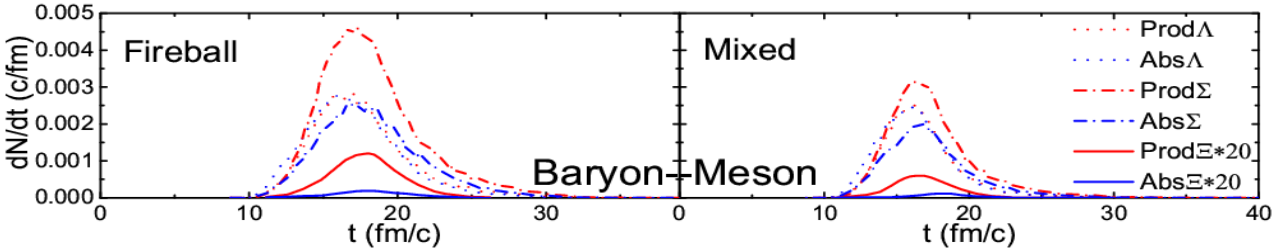

TABLE I. Comparison between cross sections of double lamda hypernuclei calculated with $r_0 = 3.5$ fm for Λ in ^{197}Au + ^{197}Au and ^{40}Ca + ^{40}Ca collisions at 3A GeV

Hypernuclei	Cross sections (mb)	
	^{197}Au + ^{197}Au	^{40}Ca + ^{40}Ca
$^{4}_{\Lambda\Lambda}$H	2.6×10^{-2}	1.0×10^{-4}
$^{4}_{\Lambda\Lambda}$He	1.0×10^{-2}	$\sim 10^{-5}$
$^{5}_{\Lambda\Lambda}$H	5.9×10^{-3}	$\sim 10^{-5}$
$^{5}_{\Lambda\Lambda}$He	5.1×10^{-3}	$\sim 10^{-5}$
$^{5}_{\Lambda\Lambda}$Li	1.4×10^{-3}	$\sim 10^{-6}$
$^{6}_{\Lambda\Lambda}$He	2.2×10^{-3}	$\sim 10^{-6}$
$^{7}_{\Lambda\Lambda}$He	6.8×10^{-4}	$\lesssim 10^{-6}$

V. Summary

- The Extremely proton-rich/neutron-rich hypernuclides might be created via heavy-ion collisions at HIAF energies, e.g., ${}^{3}_{\Lambda}H$ and ${}^{4}_{\Lambda}H$ production in the reaction of ${}^{20}Ne+{}^{12}C$ at HIAF.
- The high-density symmetry probes single and double ratios of Σ^-/Σ^+(double ratio) via the isotopic reactions ${}^{112}Sn+{}^{112}Sn$ and ${}^{124}Sn+{}^{124}Sn$, in particular above 0.4 GeV.
- The 3-body interaction potentials, e.g., ΛNN,ΣNN,ΞNN etc, might be constrained via heavy-ion collisions at HIAF.

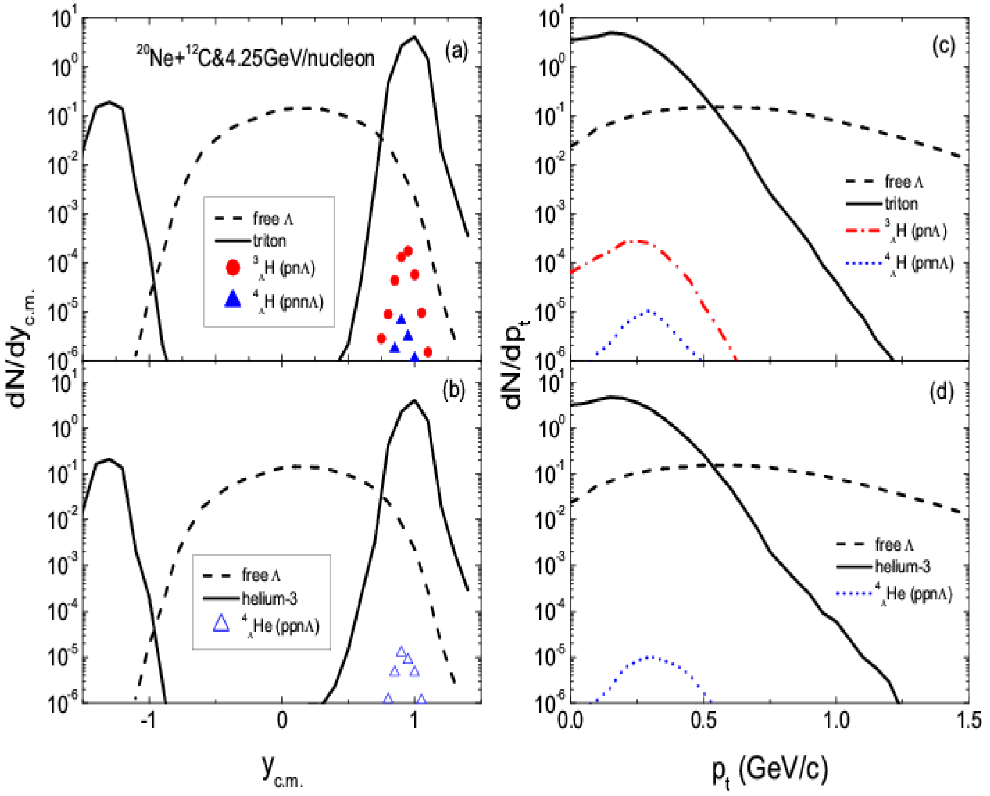

- Kinetic approach is implemented in the LQMD transport model for the nuclear cluster production in Fermi energy heavy-ion collisions, hypercluster in the near future, in which the binding energy, multinucleon (cluster) collisions, Pauli principle, Mott effect etc are taken into account.

Thanks for your attention！